Université d'Ottawa · University of Ottawa

Studies on Steady State and post-Steady State Ultrafiltration of different solutes

By

Syed Khateeb Zaidi

A Thesis submitted to the faculty of Graduated and Postdoctoral Studies in partial fulfillment of the requirements for the degree of
MASTER OF APPLIED SCIENCE
In the department of Chemical Engineering
University of Ottawa

2002

Dedicated to my beloved father.....

ABSTRACT

Concentration polarization in ultrafiltration with fully retentive membrane under unstirred conditions has been studied using three different types of solutes: (a) solute which exerts osmotic pressure and also forms a gel (polyethylene glycol), (b) solute which exerts osmotic pressure but does not form a gel (dextran) and (c) solute which does not exert osmotic pressure but forms a gel (silica). An unequivocal determination of whether pressure independent flux regime is osmotically controlled or gel layer dominated, is still open for discussion in the membrane literature. The present work reports a method that could be used to address this issue. It is shown that analysis of post steady state transient filtration data leads to clear demarcation of osmotically limited and gel layer controlled filtration. A method for determining additional filtration resistance offered by the polarization layer to permeate flow in macromolecular ultrafiltration has been proposed and verified experimentally. It has also been shown that the polarization layer thickness is not sensitive to the feed pressure but varies as a function of the bulk solute concentration; higher the bulk concentration thicker is the polarization layer. A fundamental analysis of deposited gel layer has been presented based on constant pressure filtration theory for the solute, which only forms a gel layer (silica). This was used to calculate specific resistance of the solute particles. The concentration and pressure dependence of specific resistance was also reported while silica gel porosity was determined by the Kozeny-Carman equation.

RESUMÉ

La polarization de la membrane entièrement rétentive employant trois genres différents de corps dissous communs dans l'ultrafiltration de membrane (UF) a été étudiée dans des conditions calmes: (a) Le corps dissous qui exerce la pression osmotique et forme également un gel (PEG), (b) le corps dissous qui exerce la pression osmotique mais pas des formes un gel (dextran), (c) le corps dissous qui n'exerce pas la pression osmotique mais forme un gel (silica). Une détermination claire de si le régime indépendant de flux de pression est osmotiquement commandé ou la couche de gel dominée, est encore ouverte pour la discussion dans la littérature de membrane. Le travail actuel indique une méthode qui pourrait être employée pour aborder cette question. On lui montre que l'analyse des données passagères de filtration d'état d'équilibre de poteau mène à la délimitation claire de la filtration commandée par couche osmotiquement limitée et de gel. La méthode proposée dans ce travail peut également être employée pour estimer la résistance additionnelle de filtration offerte par la couche de polarisation à l'écoulement perméable dans l'ultrafiltration macromoléculaire qui a été vérifiée expérimentalement. On lui a également montré que l'épaisseur de couche de polarisation n'est pas sensible à la pression d'alimentation mais change en fonction de la concentration en bloc de corps dissous; plus haut la concentration en bloc, est plus profondément la couche de polarisation. Une analyse fondamentale d'une couche déposée de gel a été présentée basée sur la théorie constante de filtration pour le corps dissous qui forme seulement une couche de gel (silica). Ceci a été employé pour calculer la résistance spécifique de la particule de corps dissous. La dépendance de concentration et de pression de la résistance spécifique a été également étudiée. La porosité de gel de silice a été déterminée par équation de Kozeny-Carman.

ACKNOWLEDGEMENTS

I would like to express my sincere appreciation to my supervisor, Dr. Ashwani Kumar, for his exemplary supervision and able guidance. He introduced me to the challenging and interesting field of ultrafiltration. He has been a constant source of encouragement, always providing me with stimulating inputs and suggestions during both the course of the research work and writing of this thesis.

I would like to express my gratitude to several others without whose contribution to this task is invaluable. I am especially thankful Dr. Sandeep Karode for his valuable suggestions that helped me prepare the initial framework and focus for the research topic. I am also grateful to Mr. Deepak Kirpalani for his assistance in LabVIEW programming and to all my colleagues and friends for their ready cooperation and support. Acknowledgements also go out to National Research Council of Canada for extending its excellent facilities.

I also would like to thank Dr. Jules Thibault, Chairman, Department of Chemical Engineering, faculty staff and fellow students for their cooperation and constant support.

My special thanks go out to my wife Gulreena whose patience, love and understanding enabled me to complete this work.

Last but not least, I pay special tribute to my parents, and in particular to my beloved father who encouraged me to pursue the MS degree and who has been a source of inspiration and moral support for me throughout all the ups and downs of my life.

Table of Contents

LIST OF TABLES

LIST OF FIGURES

Nomenclature

Symbols

a = Specific resistance (kg/m)

A = Membrane area, (m^2)

C = Solute concentration, (kg/m^3)

D = Diffusivity, (m^2/s)

d_h = Hydraulic diameter, (m)

d_p = Particle diameter, (m)

J_w = Water Flux, ($m^3/m^2.s$)

J_s = Solute flux, ($m^3/m^2.s$)

K = Boltzmann's constant.

k = Overall mass transfer coefficient, (m/s)

m_p = Mass of deposited particles, (kg)

M = Molecular weight of polymer, (Da)

n = Number of monomer subunits in polymer chain

ΔP = Trans-membrane pressure, (kPa)

R = Universal gas constant, ($J/mol\ K$)

R_f = Filtration resistance, (m^{-1})

Re = Reynolds number.

Sc = Schmidt number.

Sh = Sherwood number

T = Temperature, (K)

t = Time, *(s)*

V = Filtered volume (m^3)

V_1 = Molar volume of solvent, *(m^3/mol)*

x = Distance from membrane or gel surface, *(m)*

Greek letters

γ_p = Volume fraction of polymer

χ_{12} = Flory-Huggins interaction parameter

π = Osmotic pressure of solute, *(kPa)*

ρ = Density of polymer or solution, *(kg/m^3)*

δ = Thickness of polarization layer, *(m)*

ε_g = porosity of gel layer.

μ = Solvent viscosity, *(kg/m.s)*

Subscript and superscript

b = Bulk

f = Filtration

g = Gel layer

i = Intrinsic

p = Permeate

p = Polymer (In Florry-Huggins equation)

par = Particle

pol = Polarization

m = Membrane

s = Solution

sp = Specific

w = Wall

Abbreviations

MWCO = Molecular Weight Cut-Off

PEG = Poly Ethylene Glycol

PWP = Pure Water Permeation

TOC = Total Organic Carbon

UF = Ultrafiltration

NTU = Naphelometric Turbidity Unit

Publications

A New Method for Identifying Osmotically Limited and Gel layer Controlled Pressure Independent Flux in Ultrafiltration
S.K. Zaidi, S.K. Karode and A. Kumar
Accepted for publication in Canadian Journal of Chemical Engineering

Experimental Studies in dead-end ultrafiltration of dextran: Analysis of concentration polarization
S.K. Zaidi and A. Kumar
Submitted for publication in Journal of Separation and Purification Technology

Experimental Investigations of gel Layer in Dead End Ultrafiltration of Silica Suspensions.
S.K. Zaidi and A. Kumar
To be submitted for publication in Journal of Colloid and Interface Science

Application of Unsteady State Flux Response Method to Membrane Filtration Experiments
S.K. Zaidi, S.K. Karode and A. Kumar
Presented in 51st Canadian Chemical engineering Conference, Halifax, NS, Canada at Oct. 14-17, 2001

CHAPTER 1

1. Introduction

1.1 Definition of membrane process

Over the last 40 years membrane processes have been widely adopted by different industries. Membrane processes require two bulk phases that could be homogeneous or heterogeneous and physically separated by a third phase i.e. membrane. The membrane is the interphase between these two bulk phases. In separation processes, the feed is a mixture of different components such as liquid-liquid, liquid-solid, liquid-gas or gas-gas. The selection of membrane for the separation of components is such that it is preferentially selective to one or more species in feed mixture. The result will be two new streams, one is enriched with the desired species and the other is depleted; this enriched stream is called retentate or concentrate and depleted stream is called permeate. (Ho and Sirkar, 1992)

1.2 Classification of membranes

Membrane separation processes can be classified according to the driving force that causes the permeant to pass through the membrane (Matsuura, 1994). The driving force for separation could be pressure, concentration, temperature and electrical potential differences. Membrane separation process is a novel and highly innovative process

engineering operation. Membrane-based filtration is now used as an alternative to conventional industrial separation methods such as distillation, centrifugation and extraction. Membrane-based separation schemes potentially offer the advantages of highly selective separation, separation without auxiliary materials, ambient temperature, usually no phase changes, continuous and automatic operation and moreover highly economical in terms of low capital and running costs (Bowen, 1995). Technically and commercially most relevant membrane processes are pressure driven processes, such as reverse osmosis, ultrafiltration, microfiltration, or gas separation (Strathmann, 2001). A classification of membrane processes that is based on driving force is given in Table 1.1. Pressure driven membrane separation processes can be further classified by size range of species separated and applied driving force. As shown in Figure 1.1 (Mulder, 1996) ultrafiltration and microfiltration separate solute and colloidal particles of the size of approximately 1 to 100 *nm* and 0.1 to 10 μm using a pressure difference of usually 0.1-1 *MPa* and 10 –100 *kPa*, respectively.

1.3 Chronology of Development of membranes

La Hire (Cheryan 1986) was first to report the phenomenon of separation by membrane. He showed that the pork bladder is more permeable to water than to alcohol. In 1748, Abbe Nollet reported the discovery of Osmosis, when he observed that water diffused from dilute solution to a more concentrated one when separated by a semi permeable membrane. In 1865, Fick developed the first synthetic membrane, made of nitrocellulose (Glater 1998). Traube reported the development of artificial inorganic semi permeable membrane in 1867. In 1961, Loeb and Sourirajan reported the invention of the first

integrally skinned membrane. This invention was considered the key to the emergence of the current worldwide interest in membrane separation. This type of membrane is known as Loeb-Sourirajan membrane (Kesting, 1985). Additional information related to membrane development and inventions is given Table 1.2.

Table 1.1 Membrane processes and their applications (Franken and Fane, 1990)

Process	**Driving Force**	**Applications**
Electrodialysis **(ED)**	Electrical Potential difference	Desalination of brackish water removal of materials in wastewater.
Microfiltration **(MF)**	Pressure difference (10-100 kPa)	Removal of colloids from waste streams. Removal of dust particles from air.
Ultrafiltration **(UF)**	Pressure difference (0.1-1 MPa)	Separation of oil/water emulsions Recovery of proteins Recovery of electrophoretic paints.
Nanofiltration **(NF)**	Pressure difference (0.5-2 MPa)	Treatment of electroplating rinse.
Reverse Osmosis **(RO)**	Pressure difference (2-10 MPa)	Desalination of sea water Removal of nitrate from ground water.
Liquid Membranes **(LM)**	Concentration difference	Recovery of plating chemicals.
Gas Separation **(GS)**	Partial pressure difference (2-10 MPa)	Air separation Removal CO_2 from methane, H_2 recovery
Vapor Permeation **(VP)**	Partial pressure difference	Removal of non-condensable solvents/hydrocarbons from air.
Pervaporation **(PV)**	Partial pressure difference	Dehydration of solvents Removal of organics from wastewater.
Membrane Distillation **(MD)**	Temperature difference	Desalination of brine.

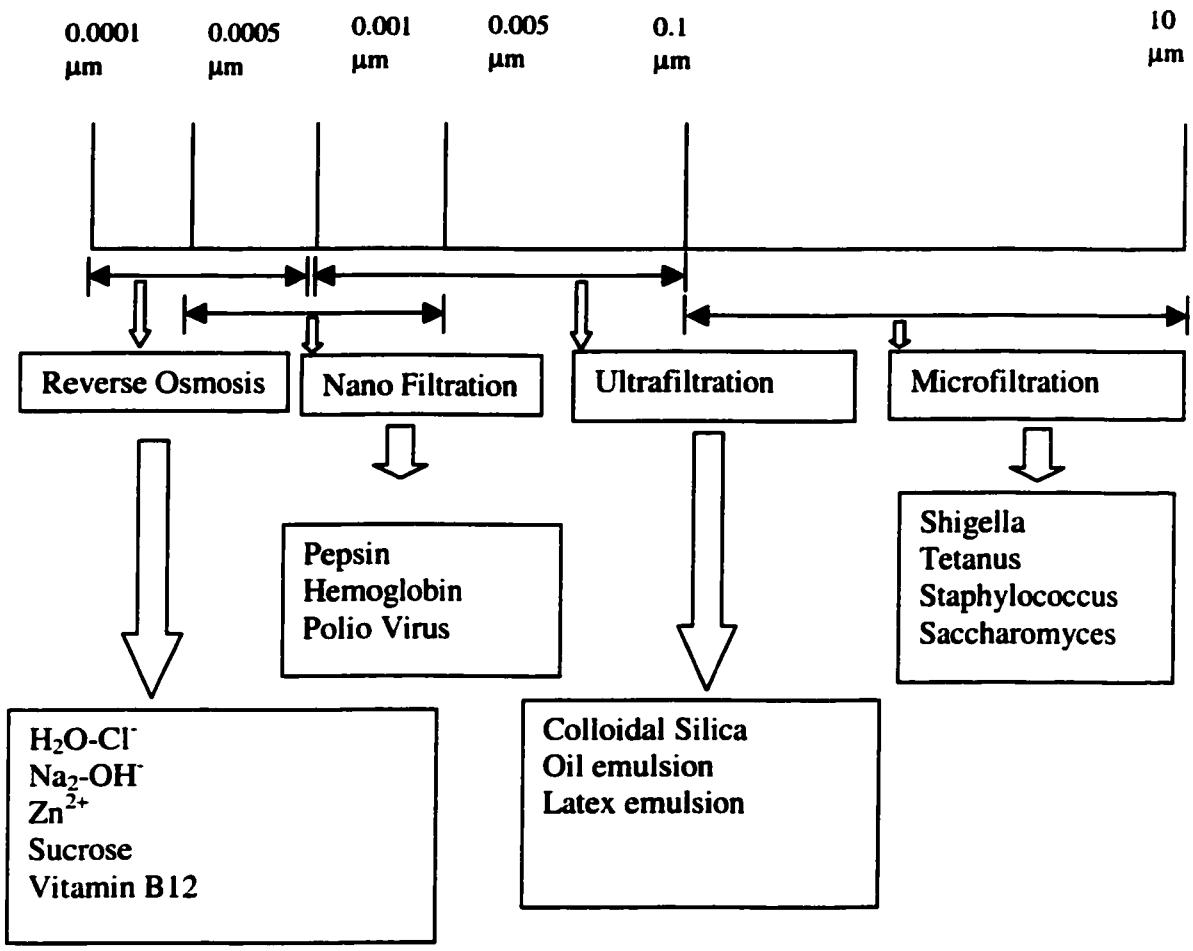

Figure 1.1.Application range of microfiltration, ultrafiltration, nanofiltration and reverse Osmosis, modified from (Mulder, 1996)

Table 1.2 Early membrane milestones (Lonsdale, 1822)

Event	Scientist	Year
Osmosis	Abbe Nollet	1748
Law of diffusion	Fick	1855
Dialysis, gas separation	Graham	1861-1866
Osmotic pressure	Traube, Pfeiffer, Van't Hoff	1860-1887
Microporous membranes	Zsigmondy	1907-1918
Distribution law	Donnan	1911
Membrane potential	Toerell, Meyer, Seiver	1930s
Hemodialysis	Kolff	1944

1.4 Ultrafiltration

Ultrafiltration is a pressure-driven membrane separation of chemical species from a solvent, usually water, using semi permeable membrane as shown in Figure 1.2 (modified from Peppin, 2001). Ultrafiltration membranes are porous filters with pore size in the range of 1 to 200 nm and are most commonly made of polymeric materials such as polyamide, polysulphone, cellulose acetate, polycarbonate and number of other advanced polymers. Various configurations exist to support and contain the membranes, such as hollow fibre, tubular, plate and frame or spiral-wounds modules. Selection of the module type depends on solution to be filtered and other operating conditions. In general stirred and unstirred, dead-end and cross flow filtration are recognised as different types

of filtration modes. In the unstirred dead-end filtration solution is put under pressure without any agitation in the liquid whereas in stirred dead-end filtration agitation is done with a stirring bar. In cross flow filtration the solution is pumped to flow tangentially over membrane surface. Membrane ultrafiltration separation processes have found wide applications in food processing industries, downstream separation in biotechnology, wastewater treatment and pharmaceutical industry (Shen, 1977 and Jackson, 1982). Other important applications include recovery of protein from cheese whey, concentration of eggs for the use of bakery industry, purification of fruit juices, recovery of beer from yeast suspension, recovery of raw material from wastewater in the cornstarch production, recovery of paint from waste water in the textile industry, purification of waste water in the production of PVC, treatment of oil/water wastes, and concentration of blood plasma for the plasma powder (Lonsdale, 1982).

A layer of solution on the membrane surface with substantially higher solute concentration than that of the bulk solution is formed as the ultrafiltration of solute progresses. This is usually termed as "concentration polarization" and boundary layer is called 'polarization layer'. The extent of polarization is determined by the convective transport towards the membrane and the diffusion away from membrane back into the bulk solution. The latter is a function of the mass transfer coefficient in the boundary layer. Concentration polarization has received considerable theoretical and experimental attention over last 25 years. It has been observed that as feed pressure increases, the permeate flux first increases and then becomes more or less pressure independent. Concentration polarization may cause lowering of flux due to an increase in osmotic

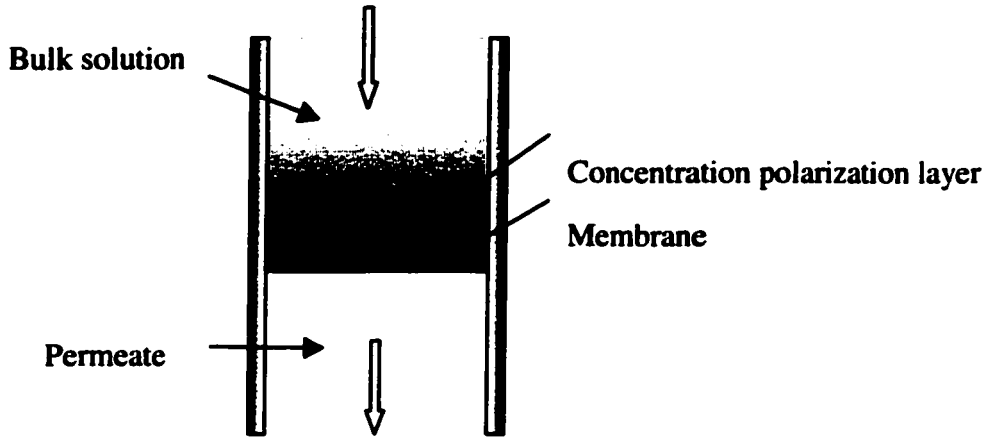

Figure. 1.2 Dead end (batch) filtration system.

pressure difference across membrane (Kozinski, 1972; Goldsmith, 1971). In some cases the concentration at membrane surface can exceed the gel concentration, which results in the gel layer formation on the membrane surface (Blatt, 1970). The hydraulic resistance of the gel layer may considerably lower the flux. Another phenomenon, which may influence is the adsorption of species on the external membrane surface and/or internal pore surface (Fane, 1983a). Due to the pore constriction and/or pore blockage, the hydraulic resistance of membrane increases. For example the filtration of protein can be influenced considerably by this phenomenon depending on the type of protein and membrane used in filtration (Nilsson, 1990).

1.4.1 Early History of Ultrafiltration

Development of truly semi permeable synthetic membrane has attracted the attention of the 19th century scientists. The phenomenon of Osmotic pressure was of special interest and a variety of techniques for measurement of Osmotic Pressure were developed. Development of these techniques seem especially important since utilization of pressure as driving force was a forerunner of what is known today as RO (Glater, 1998). Bechold reported the most important and carefully documented use of pressure as a driving force in 1907. These Ultrafiltration studies were done by forcing solutions at pressures up to several atmospheres through membranes formed by impregnating filter paper with acetic acid collodion. Bechold was successful in developing membranes with graded porosities and designing the first ultrafilter. He is also credited with coining of the term "Ultrafiltration".

1.5 Ultrafiltration of Macromolecules

Membrane ultrafiltration of macromolecules is known to exhibit the phenomenon of limiting flux. The permeate flux is found to increase with increasing applied pressure till a critical value is reached where further increase in the applied pressure does not increase the permeate flux. This is usually explained either by the formation of gel layer or concentration polarization built up on membrane surface due to rejected particle or solutes. Some additional phenomenon suggested (Bhattacharjee and Bhattacharya, 1992) to account for this flux reduction, are listed below:

1. A decrease of the hydraulic driving force due to increasing osmotic pressure.

2. Resistance offered by pore plugging or an adsorption layer, when membrane shows almost perfect rejection of the solutes.

1.6 Previous Work

In this section we have presented a critical literature review and highlighted deficiencies in the approach of previous workers including identification of areas for further investigation. Based on this analysis, a rational for developing the objectives of current work is presented.

Polyethylene glycol (PEG)

In ultrafiltration of Polyethylene Glycol (PEG) solution, osmotic pressure and gel layer play an important role. Trettin and Doshi (1981) concluded that pressure independent filtration of PEG was gel layer controlled. However, these authors ignored the existence of the polarization layer and modeled the flux using Darcy's law by setting the filtration resistance in the pressure dependent filtration regime to membrane resistance for pure water. The filtration resistance for the pressure independent regime was set to the sum of membrane resistance for water and an additional resistance termed as resistance of the so called gel layer. Wijmans et al. (1984) and Nakao et al. (1986) interpreted flux data based on the osmotic pressure model and gel layer model (van Oers et al., 1992) and concluded that for macromolecules with molecular weight ranging from 10-100 kDa, osmotic pressure limitation was more likely than gel layer formation. These authors also assumed that filtration resistance was wholly comprised of the membrane resistance for pure water. Bhattacharjee and Bhattarcharya (1992) have developed a model for prediction of limiting flux. This model combines film, gel and filtration theories to

predict limiting flux as a function of time. Nicolas et al. (1994) studied concentration polarization phenomenon in unstirred dead end ultrafiltration of different solutes including PEG and concluded that flux decline can be predicted more accurately when concentration dependence of osmotic pressure and diffusivity are known. Bhattachrjee and Bhattachrya (1996) modified their previous model and developed a new unified model for flux prediction for batch UF. Using this model they have presented the flux decline analysis by considering effect of osmotic pressure as well as gel layer; their model predictions agreed well with the experimental results. Karode (2000) proposed a theoretical method for the prediction of gel concentration in macromolecular ultrafiltration using lattice fluid hydrogen bond theory (LFHB). Bhattacharjee and Datta (2001) have predicted flux and rejection during UF in stirred cell using variable diffusivity concept. Karode (2001) reported a theoretical study for an unsteady state flux response using different solutes, which form a gel as well as exert an osmotic pressure and concluded that with a step change in trans-membrane pressure, unsteady state flux is shown to result in unique flux-pressure profiles for different types of solutes common in ultrafiltration. It should be noted that in ultrafiltration of macromolecules using a retentive membrane, the polarization ratio (defined as the ratio of the solute concentration at the membrane surface to that in the bulk, i.e. C_w/C_b) is expected to be high due to the low diffusivity of the solute. In such a case, the polarization layer could offer an additional filtration resistance, which needs to be considered for determination of overall resistance.

Dextran

There is ample evidence in literature to show that ultrafiltration of dextran is osmotic pressure limited (Goldsmith 1971, Wijman, et al., 1985; Jonsson, 1984 and Pradanos et al. 1995). Goldsmith (1971) reported this earlier and suggested that a degree of osmotic limitation must be taken in to account whenever macromolecular solutes are ultrafiltered. Clifton et al. (1984) have used osmotic effects to explain ultrafiltration flux in hollow fiber modules. Nakao, et al. (1986), in their work on resistance to the permeate flux in unstirred ultrafiltration of dissolved macromolecular solution, have calculated the boundary layer concentration of dextran and concluded that this concentration was pressure dependent due to the compressibility of concentrated boundary layer. They further concluded that no gel layer was found during ultrafiltration of dextran even with a very high dextran concentration of 400 kg/m^3. van Oers et al. (1992) reported UF data for dextran for totally retentive membranes in an stirred cell. They measured permeate flux as a function of time for sudden variation of trans-membrane pressure and concluded that during filtration of dextran only polarization layer is build up which takes less than a minute and osmotic pressure model provides a good description of flux values for their experiments with dextran. Choe and Masse (1986) also studied the flux decline of dextran in UF and concluded that the change in driving force due to the increase in osmotic pressure at membrane surface could be accounted for this decline. Furthermore, they found that mass transfer coefficient variation with bulk concentration in the cell was insignificant during the batch concentration process.

Karode (2000) theoretically predicted the unsteady state flux behavior using dextran as a model solute, and showed that concentration at the surface of membrane is a function of

bulk feed concentration and applied pressure. He predicted the membrane wall concentration as a function of time. Further, theoretical studies (Karode, 2001) on unsteady state flux response to a step change in trans-membrane pressure showed that a solute which exert osmotic pressure but does not form a gel layer exhibits a gradual flux decline with time followed by a reversible steady state flux for a sudden increase followed by a decrease to the initial value of trans-membrane pressure. Chudacek and Fane (1984) also studied the dynamics of polarization in stirred and unstirred ultrafiltration of dextran and concluded that polarization time is a function of concentration and pressure. All these studies suggested that flux decline in ultrafiltration of dextran could be due to the osmotic pressure at the membrane surface. Considerable theoretical and experimental work has been dedicated over last 20 years where most of the authors have explained the cause of flux decline however, it appears that there are no reported data in literature where the contribution of resistance due to polarization to actual filtration resistance and growth of solute concentration at membrane surface due to increase in applied pressure have been shown experimentally.

Silica

The third solute for our studies was (Silica) which is known to form only a gel and does not exert an osmotic pressure. During ultrafiltration of colloidal suspensions, particles are convectively driven to the membrane surface where they accumulate and tend to form a cake or gel layer. This particle build-up near the membrane surface is known as concentration polarization, and results in an increase in hydraulic resistance against the permeate flux; this causes a decline in permeate flux with time. As a rule, treatment of solutes causes an instantaneous reduction in flux relative to the pure water flux of the

membrane. There are several phenomena, which are responsible for this flux reduction. Gel layer formation is usually the dominating flux inhibitor when treating colloidal suspensions specially silica. The unsteady nature of the permeate flux decline is caused by changes in the hydraulic boundary condition at the membrane surface due to the cake formation as filtration proceeds.

Numerous studies in the past have shown that UF of certain inorganic suspensions form gel layer on membrane surface. The osmotic pressure effect is negligible and hence flux is governed by gel polarization model. The gel polarization model is based on the assumption that the concentration of solute on the membrane cannot exceed a certain value termed as the gel concentration (C_g). Formation of polarization layer takes place after ultrafiltration has been started. Once gel concentration has been reached, the net solute flux does not lead to further increase of the concentration at the membrane surface, however the thickness of gel layer may change. Several studies have been conducted on colloids but only few of them have been devoted precisely to the study of ultrafiltration of colloidal silica. Blatt et al. (1970), Porter (1972a, b), Goldsmith (1971), Henry (1972) and Madsen (1977) are, amongst many others, who have studied macro solute and colloidal ultrafiltration and have reported experimental results for the limiting flux, which provided strong support to the gel polarization model.

Fane (1984) has investigated ultrafiltration of suspensions of various silica-based particulates (silica sol and diatomaceous earth). He reported that the effect of particle size on ultrafiltration of fine colloids is different for stirred and unstirred conditions and concluded that without stirring, flux is lower for the smaller particles as is common in filtration practice. He also found that specific gel resistance increases with feed

concentration, which is a well-known phenomenon for ultrafiltration of highly charged particles. Doshi and Trettin (1981) suggested that unflocculated charged particles will link together electrostatically in a favourable way if feed has low particle concentration. They stated that increase of particle concentration causes more particles to compete for these optimum positions, and as a result of this a more resistive cake will be formed. Chudacek and Fane (1984) studied dynamics of polarization in both stirred and unstirred conditions using totally retentive membrane for a silica solute with mean particle diameter of 16nm at trans-membrane pressures ranging between 30 and 200 *kPa*. They have interpreted their result based on constant pressure filtration theory and concluded that specific resistance provided by the solute is in accordance with their size and conformation, and are both pressure and concentration dependent. Static et al., (1988) studied filtration of laboratory made and commercial silica using Amicon cell. They studied the effects of silica particle size, stirring conditions, pressure and pH on ultrafiltration and concluded that under unstirred conditions flux increases with increase in particle size while under stirred conditions particle size does not influence flux value. Further, membrane resistance was found to be independent of experimental conditions of used in this investigation. They have also observed a decrease in specific resistance with increasing pH due to an increase in surface charge density of the silica particles.
The unsteady state flux behaviour of silica suspension and dextran solution has been studied by van Oers (1992). He concluded that under certain experimental conditions silica forms a gel layer and transient flux of silica was well predicted by gel polarization model. Vladisavljevic et al. (1992) studied the influence of temperature on the silica sol ultrafiltration and concluded that temperature has considerable influence on flux but does

not affect gel concentration and boundary layer thickness. Finally Choe et al., (1986) and Himachi et al., (1999) studied the filtration of colloidal suspension using bentonite; they have investigated cake characteristics and studied membrane surface fouling through the measurement of deposit thickness in crossflow microfiltration. Many experimental and theoretical studies have been conducted on ultrafiltration of colloidal suspensions in general including few that have been dedicated to ultrafiltration of silica. It appears that additional experimental investigations dealing with solute deposit structure such as solute concentration, deposit porosities and thickness are required.

1.7 Outline of thesis

Objectives of this research were determined based on review of literature and limitations of reported work. Solutes including macromolecules are usually characterized by their propensities for exerting osmotic pressure at the membrane surface. Three different types of solutes that are known to exhibit different characteristics in ultrafiltration were selected for experimental studies as described below:

1. Solute, which exert an osmotic pressure and also forms a gel (Polyethylene Glycol)
2. Solute, which exert an osmotic pressure but does not form a gel (Dextran)
3. Solute, which do not exert an osmotic pressure but forms a gel (Silica).

General objective of this research is to fabricate laboratory scale experimental set up with proper controls to investigate flux decline phenomena, which occur during the ultrafiltration of macromolecules in general and post steady state ultrafiltration in particular.

The specific objectives of this thesis are as follows:

- To develop a method for analysis of unsteady state filtration data to differentiate between osmotically limited and gel layer controlled pressure independent filtration regimes for those solutes (e.g. PEG), which exert osmotic pressure and also form gel. Further extend the proposed method to estimate the additional filtration resistance offered by the polarization layer in macromolecular UF.
- To apply the above method to solutes (e.g. dextran), which only exert osmotic pressure. Additional aim was to determine flux and variation of flux with sudden change in applied pressure (pressure cycling) along with determination of concentration profile of solute adjacent to the membrane surface.
- To apply the above analysis with required modifications to ultrafiltration of the solutes (e.g. silica) which only form a gel and do not exert osmotic pressure. To study deposited gel layer formation including the application of gel layer model and constant pressure filtration theory for determining the resistance under different experimental conditions.

This thesis is organized in 6 Chapters. Current Chapter deals with Introduction and Background. Chapter 2 presents Theoretical Background followed by Chapter 3, which describes Experimental Methods and Analysis Techniques. A detailed discussion of results is presented in Chapter 4. The Conclusions of present study along with Recommendations for future work are given in Chapter 5 while References are listed in Chapter 6. A typical set of sample calculations is given in Appendix.

CHAPTER 2

2. Theory

2.1 Theory of Ultrafiltration

Ultrafiltration is a pressure driven membrane separation process by which macromolecular solutes and/or colloidal particles are separated from a solvent usually water. The relationship between applied pressure and the rate of permeation (flux) for a pure solvent usually water flowing under laminar conditions in tortuous membrane channels is modeled using modified Darcy's law where solvent flux is directly proportional to the effective pressure difference and inversely proportional to the filtration resistance. The constant of proportionality is the inverse of solvent viscosity (Ward, 1987). Mathematically, this can be written as:

$$J_w = \frac{\Delta P}{\mu R_m} \tag{2.1}$$

Where, J_w is the flux of pure solvent, ΔP is pressure difference, R_m is the membrane resistance and μ the solvent viscosity.

In the case of UF with a solute that is retained by the membrane, the driving force and the flow resistance would be modified due to the occurrence of concentration polarization or Gel layer formation. Permeate flux for such cases can be obtained using the model reported by Wijmans et al. (1984)

$$J_s = \frac{\Delta P - \Delta \pi}{\mu R_f} \tag{2.2}$$

Where, J_s is the solute flux, ΔP is the applied pressure, R_f is the total filtration resistance, which is comprised of membrane resistance (R_m), resistance offered by polarization layer (R_{pol}) and $\Delta \pi$ the osmotic pressure difference across the membrane.

2.2. Concentration Polarization

The separation of solute and solvent takes place at the membrane surface where solvent passes through the membrane and retained solutes cause the concentration at membrane surface to increase, this effect is known as concentration polarization. Concentration polarization may lead to gel layer as well as concentration layer at the membrane surface. The concentration profile is established within a boundary film generated by hydrodynamic conditions (Figure 2.1,van Oers et al., 1992). In the presence of higher concentration at the membrane surface, there will be a tendency of solute to diffuse back in to the bulk solution according to Fick's law of diffusion.

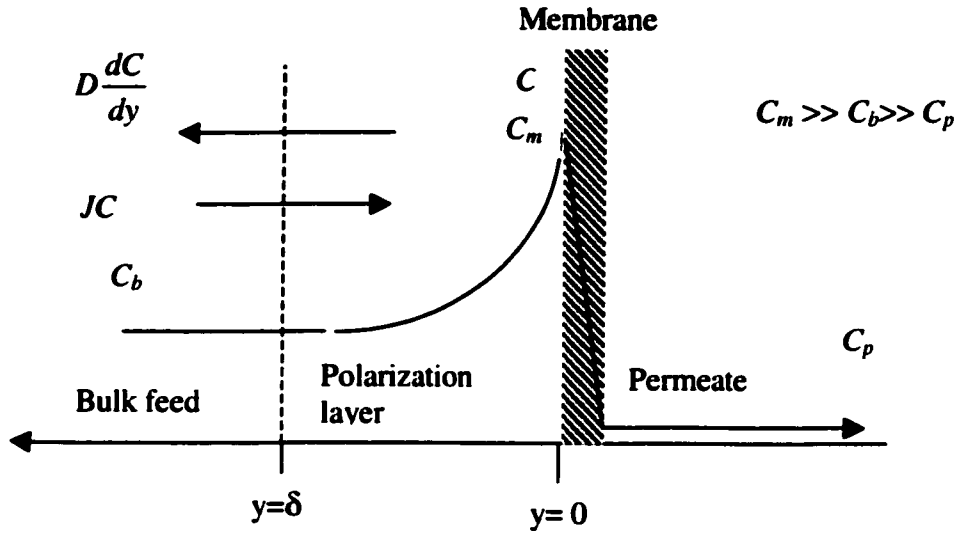

Figure 2.1: Concentration profile at membrane surface

A solute mass balance was applied above the membrane surface (Bowen, 1995) that equates the rate of convective transport of solutes towards the membrane surface to the rate of solute leakage through the membrane plus the rate of solute due to back diffusion. It was assumed that the diffusion coefficient and both solvent and solute densities are constant. Also the concentration gradient parallel to membrane surface is negligible as compared to that concentration gradient orthogonal to membrane surface. One gets following Equation for flux (Zydney, 1997)

$$-JC - D\frac{dC}{dy} = -JC_p \tag{2.3}$$

Where D is the diffusion coefficient of the solute in the solvent, C and C_p are solute concentration in boundary layer and in permeate, respectively. An integral of Eq. (2.3)

over boundary layer thickness δ with boundary conditions of $C\ (y = \delta) = C_b$ and $C\ (y = 0) = C_m$, gives the well known film model relationship:

$$J = k \ln\left[\frac{C_m - C_p}{C_b - C_p}\right] \tag{2.4}$$

Where $k = D/\delta$, the overall mass transfer coefficient of the solute in the boundary layer, and C_m is the concentration of membrane surface.

Flux is very sensitive to operational parameter that may affect the mass transfer coefficient. The overall mass transfer coefficient (k) is usually obtained from the following correlation (Gekas et.al. 1987).

$$Sh = k\ \frac{d_h}{D} = K'\ \mathrm{Re}^{a'}\ Sc^{b'}\left(\frac{d_h}{L}\right)^{c'} \tag{2.5}$$

Where K′, a′, b′, c′ are constants, which vary with flow regimes. Sh, Re and Sc are Sherwood, Reynolds and Schmidt numbers, respectively. The mass transfer coefficient has been shown to have slight tendency to decrease with increasing pressure and bulk concentration (Jonsson, 1984)

2.3 Gel Polarization Model

Based on filtration experiments with macromolecular solution and colloidal dispersion, several authors (Blett et al., 1970, Porter, 1972, Kozinski and Lightfoot, 1972, Fane et at., 1981) have reported that steady state flux reaches asymptotically a limiting value where further increase in applied pressure results in minimal increase in permeate flux.

Michaels (1968) and Blatt et al. (1970) advanced the hypothesis that as the concentration in polarization layer at the membrane surface increases, macromolecule reaches its solubility limit and precipitates on the membrane surface to form solid or thioxotropic gels. For colloidal dispersion the gel layer is expected to resemble a layer of close pack spheres (Porter, 1972a). As a consequence, a constant gel layer concentration is rapidly reached, which is expected to be virtually independent of bulk solution concentration, applied pressure, fluid flow conditions or membrane characteristics. According to Michael's model, an increase in applied pressure produces a temporary increase in flux which brings more solutes to gel layer which increase its thickness and resistance to solvent flow, thereby reducing the flux to its original level.

For 100% solute rejection ($C_p = 0$) Equation (2.4) can be written in the following form

$$J = k_s \ln\left[\frac{C_m}{C_b}\right] \tag{2.6}$$

Where C_m is concentration at membrane surface and J is the limiting flux, which is independent of the applied pressure. In case of gel formation C_m has been replaced by the constant gel layer concentration C_g

2.4 Osmotic Pressure Model

In a typical feed concentration in ultrafiltration of macromolecules, the osmotic pressure is almost negligible and consequently osmotic effects are frequently ignored (Blett et al., 1970, Porter, 1972a). However, the membrane concentration C_m is significantly higher

than bulk concentration and therefore the osmotic pressure of the solution is no longer negligible. The permeate flux in this case is governed by:

$$J_s = \frac{\Delta P - \Delta \pi}{\mu R_f} \tag{2.7}$$

Where R_f is total filtration resistance, μ the solvent viscosity and $\Delta \pi = \pi (C_m) - \pi (C_p)$ with the concentration C_m and C_p at the membrane surface and in the permeate, respectively. Again a rejection of 100% is assumed and in that case the osmotic pressure difference is determined by using the concentration at membrane surface. The osmotic pressure π is often represented in terms of a polynomial as follows:

$$\pi = a_1 + a_2 c^2 + a_3 c^3 \tag{2.8}$$

Where a_1 is the coefficient in van't Hoff's law for infinitely dilute solutions and constants a_2 and a_3 represent the non-ideality of the solution.

2.5 Resistance Model

In Ultrafiltration of macromolecules, the resistance of membrane might be calculated using Equation (2.1). However this equation is not valid for estimating total filtration resistance for those solutes that exert osmotic. In order to estimate actual filtration resistance, Equation (2.7) is differentiated with respect to time to give the following equation:

$$\frac{dJ_s}{dt} = \frac{1}{\mu R_f}\left[\frac{d\Delta P}{dt} - \frac{d\Delta \pi}{dt}\right] - \frac{\Delta P - \Delta \pi}{\mu R_f^2}\left(\frac{dR_f}{dt}\right) \tag{2.9}$$

By analyzing post steady state transient filtration data obtained by reducing the driving pressure as a function of time, the actual filtration resistance can be calculated from the slope of the graph obtained by plotting dJ_v/dt v/s dP/dt. For those solutes that form a gel layer, which is considered as a packed bed of solute particle or molecules, the hydrodynamic resistance of the gel layer can be calculated using the Kozeny-Carman equation provided that the layer of silica gel formed on surface of membrane, is considered as a small particle porous layer through which the filtrate flows linearly (Stakic et al., 1988, Karode, 2000 and van Oers, 1992)

$$\frac{\Delta P}{\delta_g} = \frac{180\mu(1-\varepsilon_g)^2 J}{d_p{}^2 \varepsilon_g{}^3} \tag{2.10}$$

Re-arranging above equation and substituting R_g from Darcy's law (Equation 2.1) we get

$$R_g = \frac{180(1-\varepsilon_g)^2}{d_p{}^2 \varepsilon_g{}^3}\delta_g \tag{2.10a}$$

Where d_p is the diameter of the particle and δ_g is the thickness of gel layer with the porosity of ε_g.

$$\delta_g = \frac{m_p}{A_m(1-\varepsilon)\rho} \tag{2.11}$$

Where A_m, m_p is area of membrane and mass of particle in gel layer respectively.

2.6 Filtration Theory

For dead end (unstirred) filtration under constant pressure conditions and in the absence of particle back-transport, the resistance R_f increases with time, as

$$m_p = VC_b \tag{2.12}$$

Where V is the total volume filtered and C_b the bulk concentration.

Furthermore, According to the filtration theory the resistance of polarized solids can be written as (Stakic et al., 1988)

$$R_{pol} = a\frac{m_p}{A_m} \tag{2.13}$$

Here R_{pol} is resistance due to polarization, in case of gel formation $R_{pol} = R_g$

Substituting m_{pol} from Eq. (2.12) to Eq. (2.13) we get

$$R_{pol} = a\frac{VC_b}{A_m} \tag{2.14}$$

Here 'a' is specific resistance and can be approximately related to particle properties by

$$a = \frac{180(1-\varepsilon_g)}{d_p{}^2\varepsilon_g{}^3\rho} \tag{2.15}$$

Equation (2.1) can also be expressed in the following form

$$J(t) = \frac{1}{A}\frac{dV}{dt} = \frac{\Delta P}{R_m\mu + aVC_b\mu/A} \tag{2.16}$$

To obtain flux as a function of time, we must integrate Equation (2.16), solve for V and re- substitute in Eq. (2.16), as described by Chudacek and Fane (1984).

$$\frac{1}{J^2} = \frac{(R_m \mu)^2}{(\Delta P)^2} + \frac{2C_b a \mu}{\Delta P} t \qquad (2.17)$$

Thus a plot of $1/J^2$ vs. t should produce a straight line. The slope and intercept values of this line could be used to calculate ' a' and R_m respectively.

2.7 Influence of operating conditions on ultrafiltration flux

In ultrafiltration, flux is very sensitive to the actual operating conditions such as pressure, temperature and material interactions. Flux is directly proportional to applied pressure, according to well-known Darcy's Equation. The influence of pressure is further defined by osmotic pressure, gel layer model and resistance model. The viscosity of the solution decreases when the temperature is increased. The result is an increase in fluid flow through membrane. According to the Darcy's Eq. 2.1, the fluid flow is inversely proportional to the viscosity. A general trend is that flux decreases as the bulk concentration increases. The film model Eq. (2.6) predicts that flux J varies proportionally with the logarithm of the bulk concentration C_b. Filtration theory predicts that flux decrease is proportional to $t^{-1/2}$ under unstirred condition (Reihanian et al., 1983 and Karode, 2000). This decrease is also predicted by gel layer and osmotic pressure models (Jonsson, 1989). The film theory predicts that there is sharp drop in flux as the boundary layer is build up, after initial polarization the flux more or less remains constant with time. However, a gradual, long-term decay in flux is noted in many applications.

CHAPTER 3

3. Experimental Methods and Analysis

3.1 Materials

Membrane

The UF membrane used in this work had a nominal MWCO of 6 kDa and was prepared in the laboratory on a 1079 backing (Tyvek, Du-Pont, USA). Membrane casting formulation contained 25% of polysulfone, (Radel-R Amoco, U.S.A) and 21% polyvinylpyrrolidone (PVP)(Sigma, USA) in N-methyl-2-pyrrolidinone (NMP) (Anachemia, USA). The membrane was prepared by the phase inversion method as described elsewhere (Dal-Cin et al., 1994). Same membrane was used for all of the experiments.

Solutes:

Polyethylene Glycol (PEG) of 35 kDa molecular weight was supplied by Fluka chemie AG, Switzerland. Dextran T40 was supplied by Polysciences, INC., USA and had a Molecular weight of 39 kDa whereas Fumed Silica (silica content: 99.8%, Aerosil 200, primary particle diameter of 12 nm) was purchased from Sigma Chemical, Canada.

3.2 Solution preparation and feed concentration

Feed concentration was varied between 0.2 and 5 kg/m^3 for PEG and Dextran whereas for silica feed concentration was varied between 14 and 28 kg/m^3. These values were arrived at on the basis of reported literature values. The solutions of PEG and Dextran were prepared by weighing and mixing the required amounts of solute in water followed by stirring for 15 to 20 minutes. Silica suspensions were prepared by adding required amount of silica in water and placing the mixture in ultrasonic bath for two hours. (Mettler Electronic Corp. USA, Model No. ME 4.6). Ultrasonic treatment helped to make a suspension without any large size aggregates.

Concentrations of PEG and Dextran in the feed as well as permeate stream were measured on the basis of Total Organic Carbon (TOC) content. TOC content was estimated using a TOC Analyser (Shimadzu Corporation, Japan), while concentration of silica were measure - using Naphelometric turbidimeter (Model-DRT 100 HF Scientific, Inc. Canada).

3.3 Determination of solute concentration using TOC analysis

Solute concentration in feed and permeate was determined using well-established TOC technique. In this method the solution concentration can be determined by reacting the solute with oxygen to give CO_2. An automated system from Shimadzu Corporation, Japan, was used throughout this investigation.

3.3.1 Measuring Procedure

The total carbon (TC) combustion tube is filled with oxidation catalyst and heated to 680 °C. Carrier gas (high purity air) is supplied into this tube at a flow rate of 150 ml/min through mass flow controllers and moistened by a humidifier. After a sample was introduced in to the TC combustion tube via injector (100 µl at the maximum for the TC catalyst), the components in the sample are combusted to produce CO_2. The carrier gas that contains combustion product from the TC combustion tube is allowed to flow through Inorganic Carbon (IC) reaction vessel where it is cooled and dried on an adsorbent. It is subsequently allowed through a halogen scrubber in to a sample cell set in a nondispersive infrared gas analyser (NDIR) where CO_2 is detected. A data processing module calculated NDIR generated peak area. The peak area is proportional to the TC concentration of the sample therefore, if calibration equation expressing the relation between peak area and TC concentration has been obtained in advance using standard TC solution, the TC concentration of sample can be determined from the calculated peak area. Reference TC is composed of both TOC (total organic carbon) and IC (inorganic carbon) and TOC concentration can be obtained by subtracting the IC concentration from the TC concentration.

3.4 Determination of solute concentration by Nephelometry

Determination of concentrations of particles in cloudy solutions is done by measuring the loss in intensity of a beam of light passing through the solution. Solute concentration of silica in feed and permeate was determined based on the turbidity of solution. Turbidity of solution can be measured using Naphelometric turbidimeter. The DRT-100

Naphelometric turbidimeter is constructed of solid-state electronic components. This instrument measures reflected light from scattered particles in suspension and direct light passing through a liquid. The optical signal provides a linear readout of turbidity. The most commonly used turbidity units are NTU (Nephelometric Turbidity Unit) and FNU (Formazin Nephelometric Unit), as designated by the International Standards Organization (ISO) and United Sates Environmental Protection Agency (USEPA). These are based on using a detector placed at 90° from the incident beam to detect scattered light, and are interchangeable units.

3.5 Apparatus

Figure 3.1 shows a schematic diagram of the experimental set up. As shown in Figure 3.1, all experiments were performed using a commercial ultra-filtration stirred cell unit (Cell Model No: 8050; Amicon, USA). The specifications of the stirred cell unit are listed below:

Area of membrane:	3.1×10^{-3} m^2
Diameter of cell:	0.063 m
Operating pressure:	517 kPa (75 psi) gauge
Feed volume:	1.6×10^{-4} m^3 (160 ml)

For each experiment, the feed chamber was purged with nitrogen. The membrane was set up at the base of the feed chamber. The permeate samples were collected at the bottom of the cell unit through a 1.5 *mm* diameter silicone tube that stayed submerged in permeate during the experiment. Membrane flux was measured by recording the change in weight of a standard beaker with time. To determine the transient flux through the

membrane, mass of permeate collected in a beaker was recorded using a Standard weighing balance (SARTORIUS Model No: BP221S). A serial port communication program (RS-232) was developed using LabVIEW software for recording weights. A static pressure transducer (Ashcroft, USA Model No: K5) was installed on the feed side of the cell. The analog output of a static pressure transducer was digitized using a National Instruments PCI 4023E A/D card and a CB-68LP connecting block. A data acquisition system in LabVIEW was used to synchronize the pressure and weight (flux) measurements. The rate of change in flux and pressure were also plotted simultaneously in real-time with the developed software to monitor the transient responses. A program flow diagram of the data acquisition system is given in Figure 3.2.

3.6 Experimental Procedure

1) Initially Pure Water Permeation (PWP) was measured for new membrane.

   The weight of flux was recorded every two seconds through data acquisition software LabVIEW. An error of less than 0.1% in measuring this flux was observed. The filtration resistance for pure water was calculated using Equation 2.1.

2) For a given feed, flux versus time data were collected at constant feed pressure until steady state was reached, the steady state in our analysis has been assumed when the change in flux with respect to time is minimal i.e. less than 3 % for a filtration time of 100 seconds.

3) Once steady state was reached the pressure release valve (item 9 in Figure. 3.1) was opened a crack to let the feed pressure decay as a function of time.

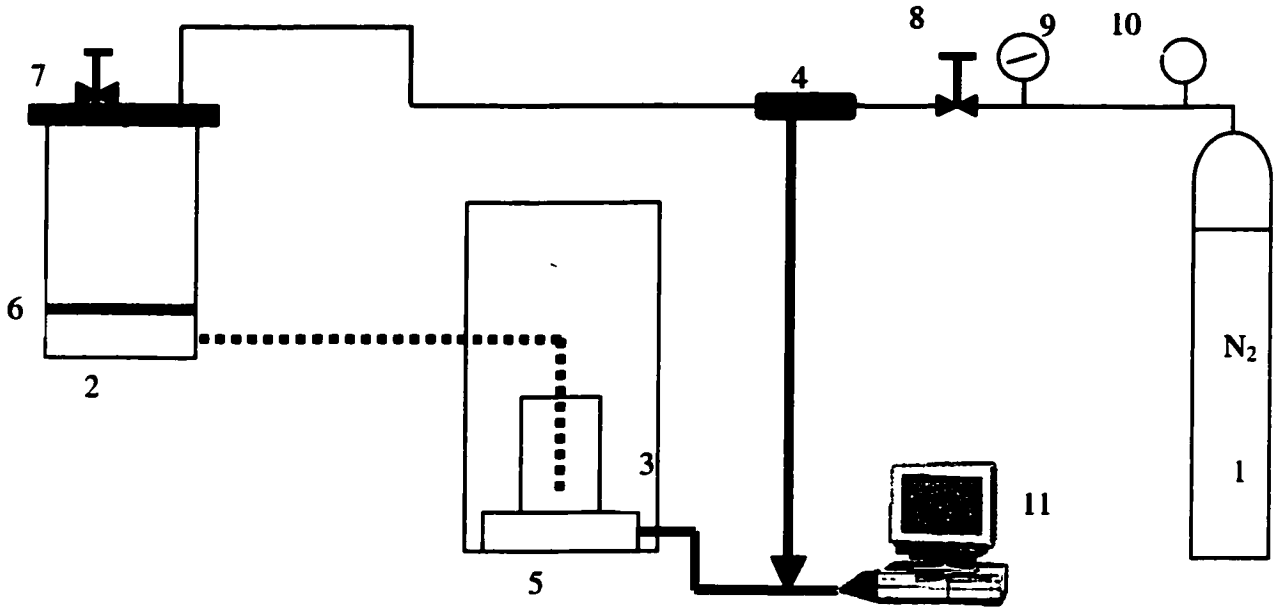

1. Gas cylinder 2. Stirred cell 3. Beaker 4. Pressure Transducer
5. Balance 6. Membrane 7. Pressure relief valve
8. Pressure release valve 9. Pressure gauge 10 Pressure Regulator
11. Computer (Data Acquisition)

Fig. 3.1 Experimental Set up

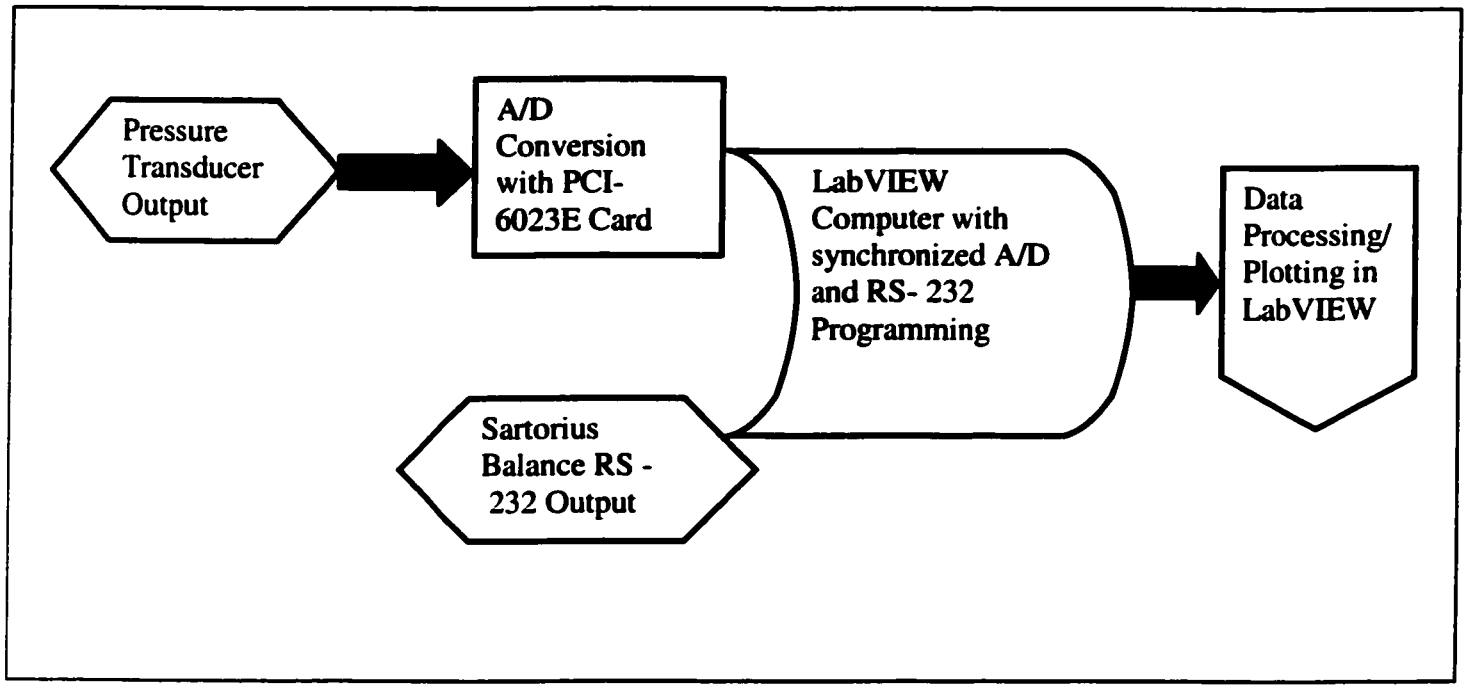

Figure 3.2: Program Flow Chart for Data Acquisition System

4) Unsteady state filtration data were continuously recorded using data acquisition system

Pure water permeation was measured at the start as well at the end of each ultrafiltration experiment to determine the membrane resistance and original flux. PWP values for all of the solutes used (PEG, dextran and silica) did not vary significantly for the membranes used in this study. Therefore, it can be assumed that flux measurements were not affected by adsorption of solute on the surface or in the matrix of membrane. All experiment in this study has been performed at room temperature.

3.7 Model Parameters and physical properties of solutes

In this section the values for the parameters used for the calculation are given for PEG, dextran and silica.

3.7.1 Polyethylene Glycol

Viscosity

The viscosity of PEG solution has been expressed by the following relationship (Thomas et al., 1960)

$$\frac{\mu_{sp}}{C} = [\mu_i] + k'[\mu_i]^2 C \tag{3.1}$$

Where

μ_{sp} = Specific viscosity of solution

C = Solute concentration (kg/m^3)

μ_i =Intrinsic viscosity (m^3/kg)

k' = Constant (a value of 0.33 is used in literature for most polymer)

The specific viscosity μ_{sp} is as follows:

$$\mu_{sp} = \frac{\mu - \mu_{water}}{\mu_{water}} \tag{3.2}$$

μ = Viscosity of solution ($Pa.s$)

μ_{water} = Viscosity of water ($Pa.s$)

Diffusivity

The diffusivity at infinite dilution is related to molecular weight of polymer in solution and has been expressed by the following correlation (Bhattacharjee and Dutta, 2001)

$$D = \frac{2.74 \times 10^{-9}}{M^{\frac{1}{3}}} \tag{3.3}$$

Where M is molecular weight of polymer (solute) in feed solution.

Osmotic Pressure

The osmotic pressure of PEG is related to concentration and is given by Flory's equation Such a correlation has been reported by Bhattacharjee et al. (1996) which demonstrates that Flory's equation for the change in chemical potential (the osmotic pressure) of PEG as a function of it's volume fraction was an accurate correlation for relating osmotic pressure and concentration of PEG.

Flory's equation relates the osmotic pressure with solute volume fraction as follows:

$$\pi = -\frac{RT}{V_1}\left[\ln(1-\gamma_p) + (1-\frac{1}{n})\gamma_p + \chi_{12}\gamma_p\right] \tag{3.4}$$

Where, $\gamma_p = c/\rho_p$ is volume fraction of polymer, c is the polymer concentration, ρ_p is polymer density and n is the number of monomer sub units in the polymer chain. The Flory-Huggins interaction parameter χ_{12} is a linear function of solute concentration for linear chain polymers and the concentration dependence is best expressed as

$$\ln|\chi_{12}| = p + qc \tag{3.5}$$

where p, and q are constants having values -0.604 and 1.7452 m^3/kg respectively.

3.7.2 Dextran

Viscosity

Dynamic viscosity of dextran solution is correlated with temperature and concentration according to the following relationship (Rene et al., 1991)

$$\ln \mu = a + b \ln(T - 273) \tag{3.6}$$

where

$$a = -5.078 + 3.428\times10^{-2} C - 1.133\times10^{-4} C^2 + 2.298\times10^{-7} C^3 \tag{3.7}$$

$$b = -0.5972 - 2.409\times10^{-3} C + 1.583\times10^{-5} C^2 - 4.279\times10^{-8} C^3 \tag{3.8}$$

Estimation of viscosity values of dextran T40 solution is done using the correlations reported by van Oers (1992).

Diffusivity

Literature values of diffusion coefficient of dextran in water at 20 deg. C (Granath et al., 1967) were corrected for temperature and solvent viscosity. Diffusivity for dextran T40 in our experiments was 6.0×10^{-11} m^2/s.

Osmotic Pressure

Many authors present osmotic pressure data for dextran of different molecular weights (Wijmans et al., 1985, de Balman et.al., 1989 and Ogsten et al., 1979). According to them, there was no significant influence of molecular weight on osmotic pressure. Figure 3.3 shows a plot of osmotic pressure vs. concentration for dextran and PEG.

For model calculation the osmotic pressure data of Wijmans for dextran is used.

$$\Delta\pi = 35.5C_m + 0.752C_m^{\ 2} + 76.4\times10^{-4}C_m^{\ 3} \tag{3.9}$$

3.7.3 Silica

Viscosity

Viscosity value of 1.1×10^{-3} Pa.s for silica suspension of 7-100 kg/m^3 concentration range was reported by van Oers, (1995)

Diffusivity

The diffusion coefficient of silica particles can be calculated by the Stokes-Einstein equation,
where K is Boltzmann's constant.

$$D = \frac{KT}{3\pi\mu_{water}d_{par}} \tag{3.10}$$

Osmotic Pressure

Since silica is expected to show very little interaction with water under our experimental conditions, therefore it is assumed silica suspension behaves almost ideally and hence osmotic pressure is negligible.

Table 3.1 Physical properties of solutes, van Oers, (1992) and Karode, (2000)

	PEG	DEXTRAN	SILICA
M.W, *Da*	35000	39000	
Diffusivity, m^2/s	8.7×10^{-11}	6.0×10^{-11}	3.6×10^{-11}
Density, kg/m^3	1200	1125	2250
Particle size, nm			12

3.8 Characterization of Ultrafiltration membrane

3.8.1 Molecular Weight Cut off (MWCO)

The characterization and performance of UF membrane is generally done by determining permeate flux with pure water and permeate flux and separations of test solutions containing solutes of varying molecular weights. The molecular weight cut-off (MWCO) of membrane was determined utilizing these sieving experiments. Dilute solutions of *0.2* kg/m^3 of polyethylene glycol (PEG) of various molecular weights (200-35,000 Da) were used to evaluate the membrane molecular weight cut off.

3.8.2 Procedure for determination of MWCO

- Pure water permeation (PWP) was measured initially at a selected trans-membrane pressure
- For a feed concentration of *0.2* kg/m^3 of PEG for different molecular weight,

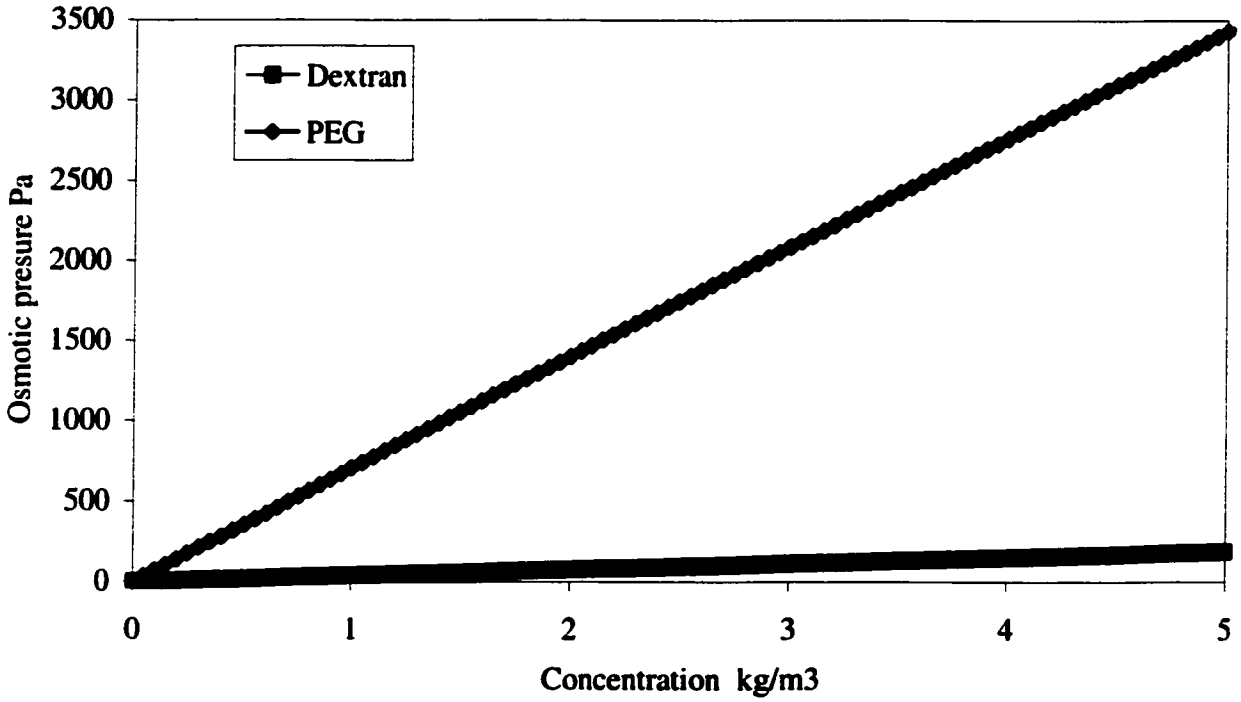

Figure 3.3 Osmotic pressure vs. concentration for Dextran and PEG

permeate samples were collected after a steady state has reached. A steady state was assumed when the recorded flux values were within ±0.2%. Concentration of PEG in the permeate stream was measured by determining Total Organic Carbon (TOC) content. This entire experimental procedure is repeated for a complete range of solutes, which were selected to cover the entire range of 0 to 100% separation of solutes.

- All experiments were conducted at constant pressure of 405 kPa, and the membrane was washed thoroughly in between each experimental run. A PWP recovery of within ± 5.0% of original was considered adequate.

The PWP, product rate (PR) and TOC data for all solutes are entered manually in a worksheet for further analysis and plotting using EXCEL spreadsheet. All experiments were performed using the experimental set up shown in Figure. 3.1 and described in section 3.3. The conventional testing and molecular cut off procedure of membrane is also shown in Figure.3.5.

3.8.3 Determination of retention curve

After the pure water experiment the same membrane was used for the determination of separation of PEG solutions. After a steady state has reached, PEG concentrations in permeate and concentrate were determined. The molecular weight cut off is based on the average of at least three different experimental runs and at least three meaningful separation values were included for generating MWCO curve. Meaningful values are those between 5% to 95% separations, from a curve fitting point of view. Zero and 100% separations are only marginally useful unless accompanied by value just above zero or

below 100%. Ideally the solutes would be selected so that the separation data is obtained over the complete range 0-100%. This allows better estimation of the actual MWCO of membrane.

Solute separation, f in percent was defined as follows

$$f = \frac{\text{TOC in feed} - \text{TOC in product}}{\text{TOC in feed}} \times 100\ \% \tag{3.11}$$

Where, f is % separation and TOC is total organic carbon content.

Separation versus molecular weight of solute was plotted as shown in Figure 3.4. Molecular weight cut off is defined as the molecular weight of a solute for which the membrane can retain greater than 90% of the solute and not necessarily 100% retention. The separation characteristics for these membranes are usually described by the percent retention of specific solutes.

3.9 Experimental plan and Data Analysis

As mentioned earlier that three different types of solutes were used throughout the investigation and the prime objective was to develop a technique to differentiate between osmotic limited and gel controlled pressure independent ultrafiltration.

The experiments were planned accordingly in three different stages in the following order.

1) Ultrafiltration using PEG as a solute. 2) Ultrafiltration using dextran as a solute
3) Ultrafiltration using silica as a solute

Concentration range was defined under section 3.1. A complete experimental plan and data analysis technique including the procedure used to evaluate the ultrafiltration membrane characterization and data analysis is presented in Figure. 3.6.

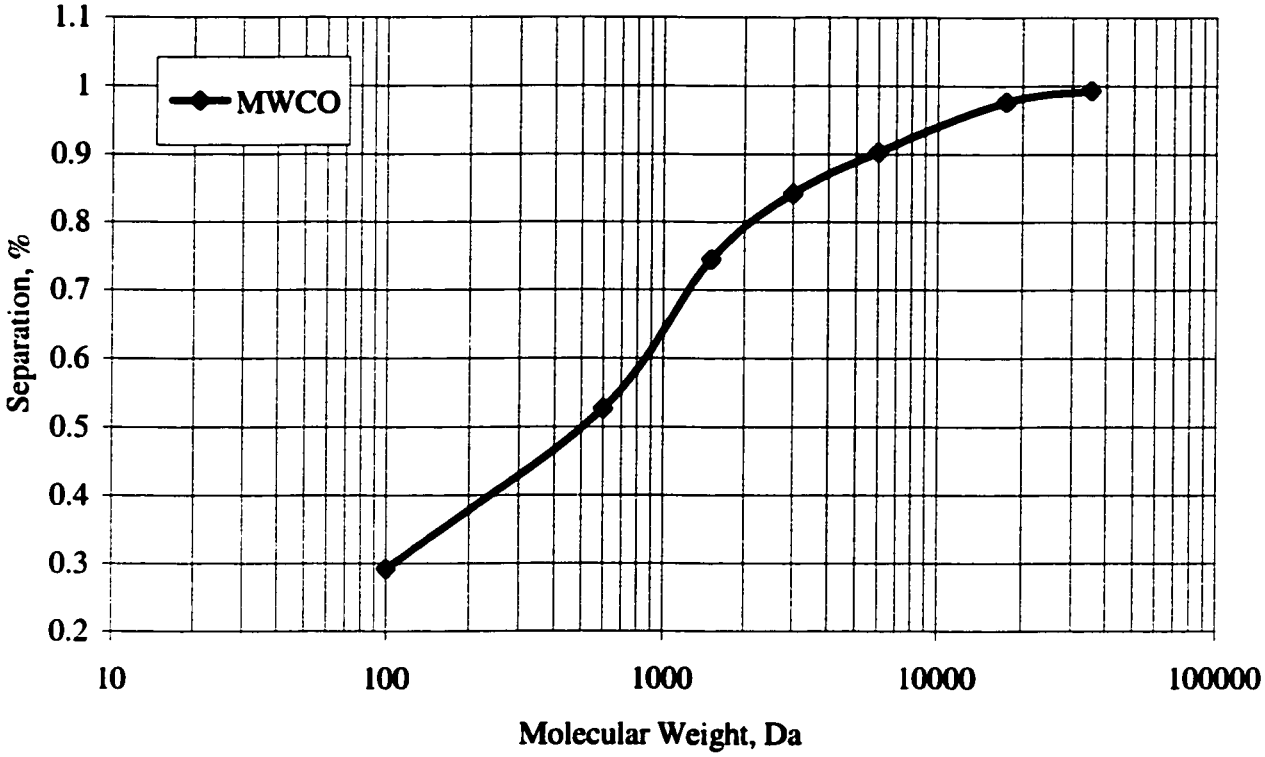

Fig. 3.4 Molecular weight cut off (MWCO)

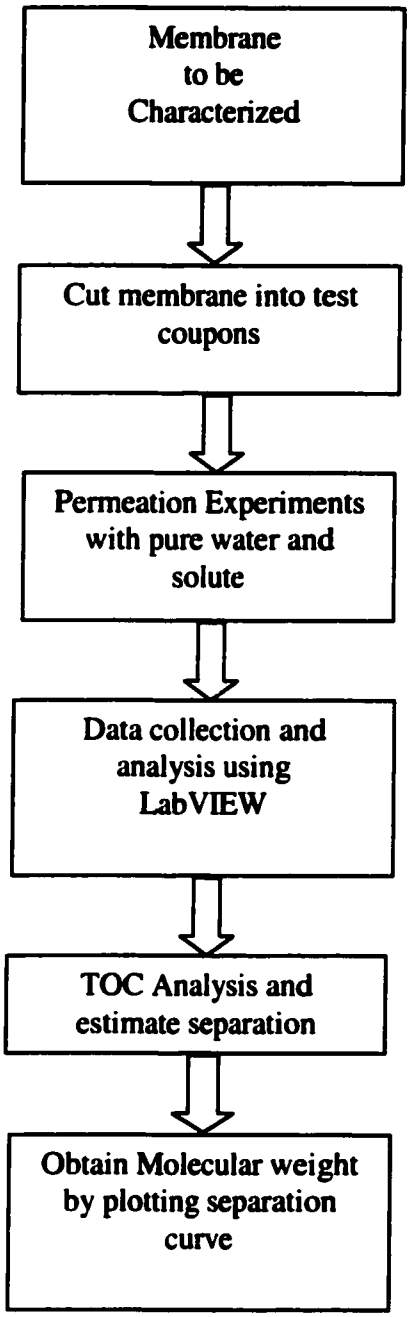

Fig. 3.5 Conventional testing and molecular cut off procedure of membrane

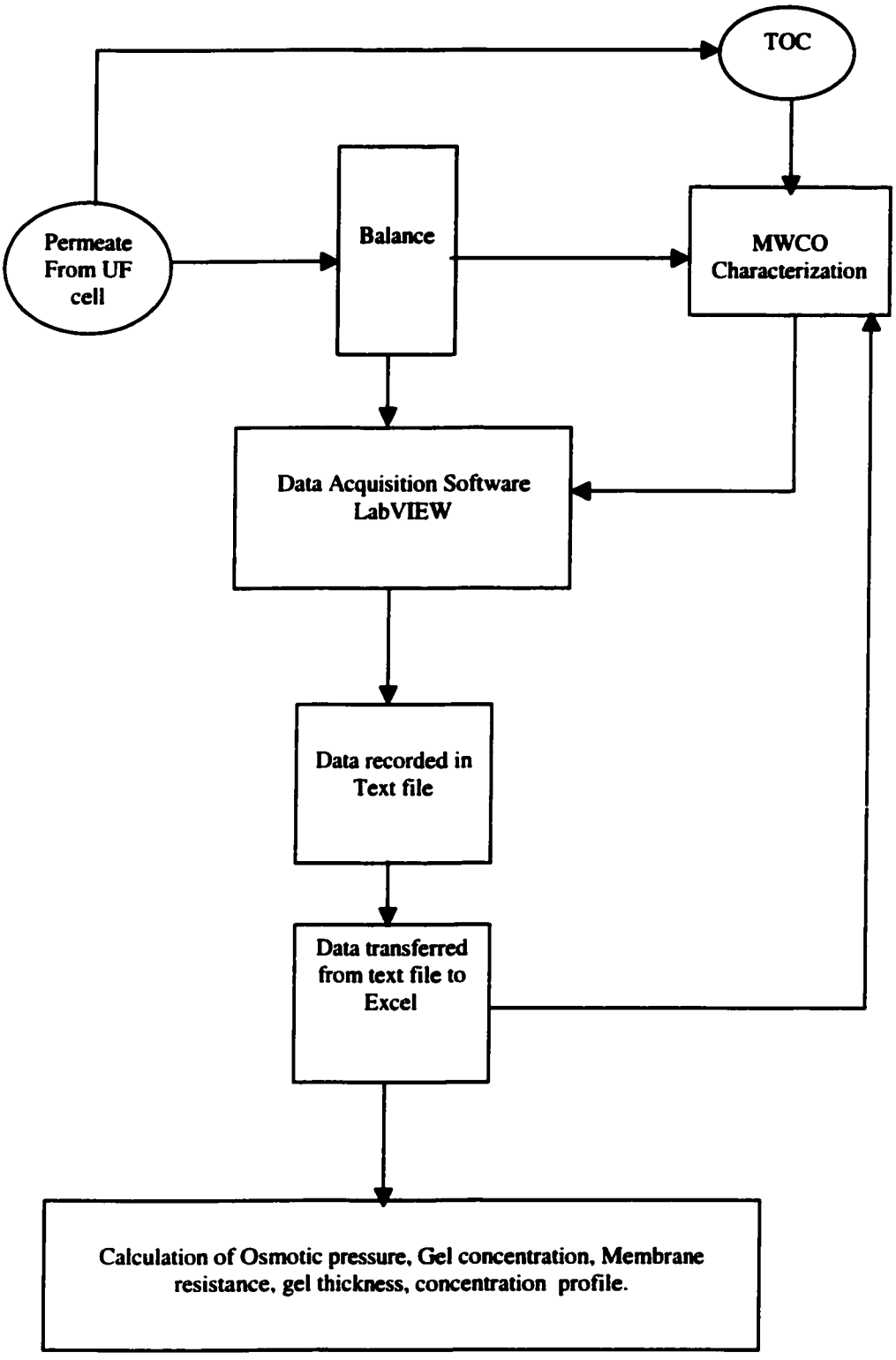

Fig. 3.6 Experimental plan and Data analysis procedure

3.9.1 Data analysis method

- Solute separation, f in percent was calculated using Equation 3.11.
- Solute permeation data was recorded using data acquisition software LabVIEW.
- An automatic data file was created in text by LabVIEW program on a selected drive.
- The file was transferred in Excel Spread Sheet for further calculation of fluxes, osmotic pressure, gel concentration, thickness, filtration resistance using different models. These parameters are defined in sections of Chapter 2 and Chapter 3 for different solutes.

3.9.1.1 Data analysis for PEG and dextran

Many researchers have reported Ultrafiltration of PEG and dextran; however, in their analysis for calculating filtration resistance they have ignored osmotic pressure terms and have modeled flux using Darcy's law. The novelty of this research is the development of a new method for the analysis of unsteady state data that includes osmotic pressure term in order to calculate the filtration resistance. A brief description of various steps in this analysis is given below:

- Using unsteady state permeation data, the actual filtration resistance can be calculated as described in Chapter 2 (Section 2.5). Second term on right hand side of Equation 2.9 was neglected as it was found to be very small to make any significant contributions to the calculations e.g. on right hand side second term was less than 0.01 % of the first term in the present study. For subsequent calculations following Equation was used.

$$\frac{dJ_s}{dt} = \frac{1}{\mu R_f}\left[\frac{d\Delta P}{dt} - \frac{d\Delta \pi}{dt}\right] \tag{3.12}$$

By analyzing post steady state transient filtration data obtained by reducing the driving pressure as a function of time, the actual filtration resistance can be calculated from the slope of the graph obtained by plotting dJ_s/dt v/s $d\Delta P/dt$. The slope of the resulting graph would be linear if $d\Delta\pi/dt$ was equal to zero or the difference between $d\Delta P/dt$ and $d\Delta\pi/dt$ was constant. Moreover, since the shape of the flux versus pressure curve is non-linear (linear at low pressure and tapering off at high pressure) the only case where the variation of dJ_s/dt and $d\Delta P/dt$ would yield a linear slope would be at a $d\Delta\pi/dt$ value of zero. In the case of gel layer controlled filtration, the solute concentration at the surface of the membrane remains constant (time independent) at the gel concentration. This would produce a linear slope for the dJ_s/dt v/s dP/dt graph. In the case of osmotically limited pressure independent filtration, the solute concentration at the surface of the membrane would be a function of the applied pressure. Therefore, after achieving a steady state in the experiment, a reduction in the driving pressure with time would cause a change in the solute concentration at the surface of the membrane with time, resulting in a non-linear graph between dJ_s/dt v/s dP/dt. Using the simple technique described above, it is possible to unequivocally determine whether the pressure independent filtration regime is a result of a gel layer controlled filtration or an osmotically limited filtration. Once the actual filtration resistance was calculated, these resistance values at each feed pressure and the osmotic pressure of the solute at the membrane surface (or π_w) can be calculated using Equation 2.7 described in Chapter 2.

- Using osmotic pressure, concentration at membrane surface C_w, can be calculated using Flory's equation (described in Section 3.7.1), which relates osmotic pressure and concentration. Utilizing this value of C_w and the steady state flux, J_s, the solute concentration profile as a function of distance perpendicular to the membrane surface can be estimated using the film theory.

3.9.1.2 Data analysis for Silica

- Since silica does not exert osmotic pressure so post steady state transient flux response was not analyzed in this case. As the applied pressure and flux were known, filtration resistance or gel resistance was calculated using Darcy's law.
- The specific resistance a was calculated based on the slope of plot $1/J^2$ vs. t. from Equation 2.17. Although a is an adjustable parameter it has been commonly used as a filtration characteristic with physical basis (Equation. 2.15).
- Steady state rejection of silica was estimated based on turbidimetric analysis as described in Chapter 2.
- Concentration of gel layer formed at constant pressure was calculated based on porosity ε, of accumulated particles, which was calculated using Equation 2.15. In order to verify the calculated gel concentration, at the end of last experiment the membrane along with gel was removed from membrane cell. To determine the gel concentration and the weight of silica present in gel layer this gel was weighed before and after drying.
- Thickness of polarisation layer was also estimated using Equation 2.11 and mass of gel layer was calculated by Equation 2.12 as described in Chapter 2.

CHAPTER 4

4. Results and discussions

4.1 Ultrafiltration of polyethylene glycol (PEG)

4.1.1 Permeate flux in dead end ultrafiltration of PEG

Figure 4.1(a) and 4.1(b) show the permeate flux as a function of time for three different feed pressures (135, 270 and 405 *kPa*) for a bulk feed concentration of 1 and 5 kg/m^3. As expected, there is a sharp drop in the permeate flux from the initial value (at time t=0, corresponding to the flux of pure water) for short filtration times. At longer filtration times, the rate of flux decline gradually and eventually attains steady state value. Considering that experiments were done with out stirring, the change in the bulk feed concentration was negligible for the duration of time required for attaining steady state. Furthermore, only about 20-25 ml of the initial feed volume of 150 ml was collected as the cumulative permeate during these experiments and most of concentration polarization would take place closer to the membrane surface.

Figure 4.2 shows the steady state flux for a solute concentration of 0.2, 1 and 5 kg/m^3 as function of feed pressure. It is clear from that permeate flux becomes independent of pressure for a feed concentration of 5 kg/m^3. For a feed concentration of 1 kg/m^3,

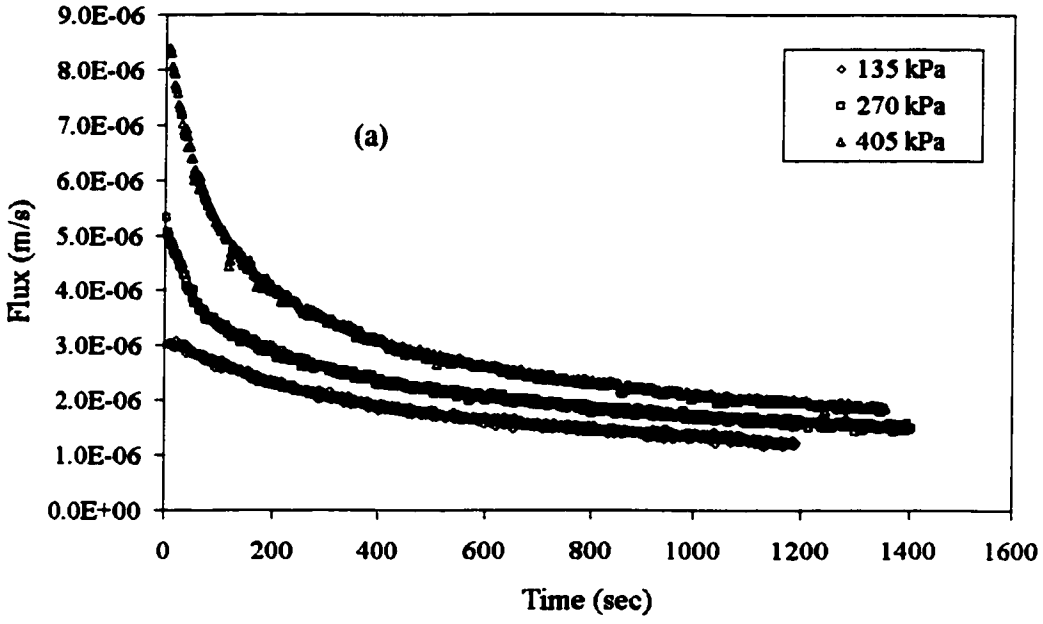

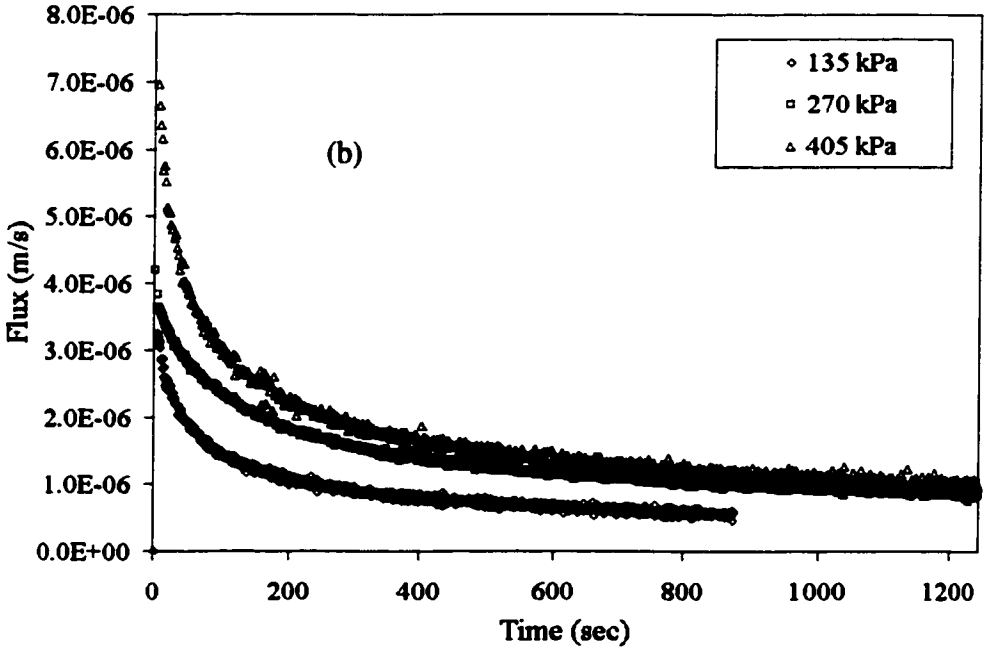

Figure 4.1 Variation of permeate flux as a function of time for various values of feed pressure. (a) *1 kg/m^3* (b) *5 kg/m^3*

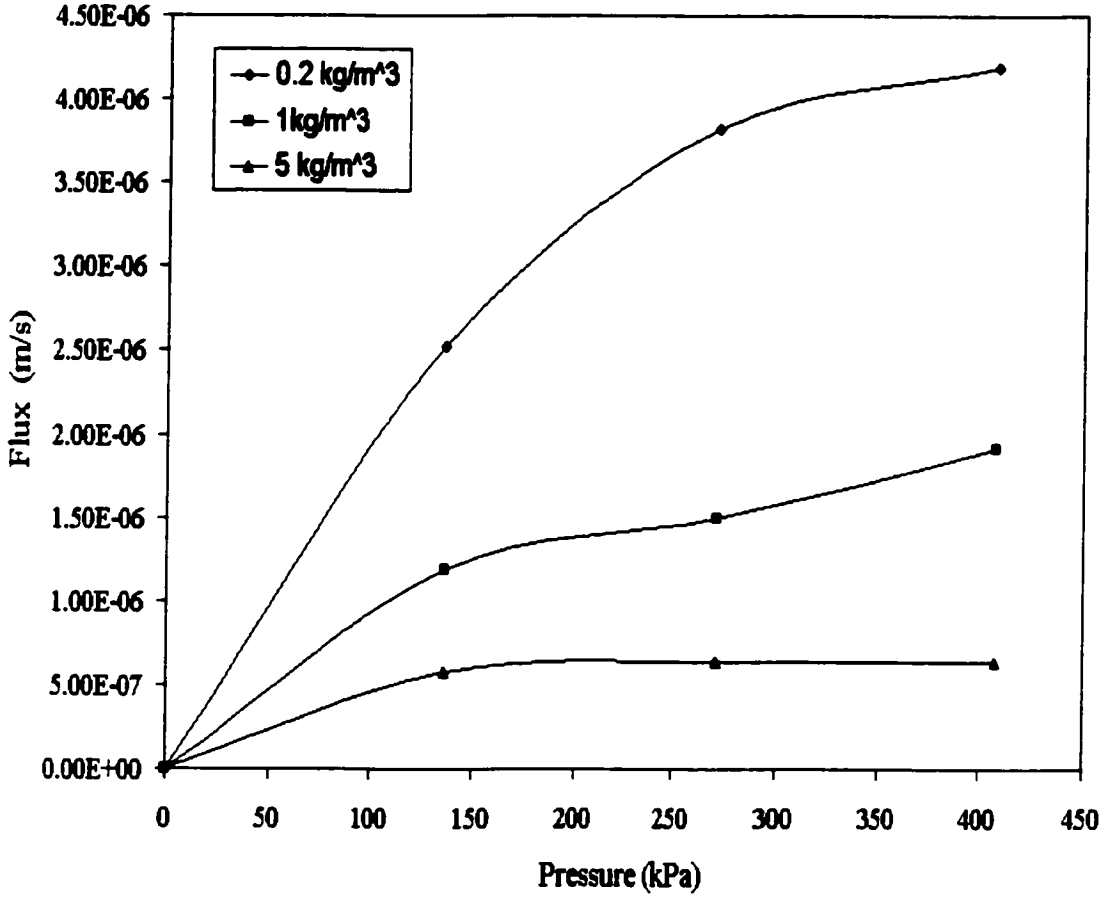

Figure 4.2 Steady state permeate flux as a function feed pressure for different feed concentrations

permeate flux is only slightly pressure dependent. The pressure range was restricted to 400 kPa due to the limitations of the test cell. After steady state was reached at a constant feed pressure, the bypass valve (see Figure. 1) was opened a crack. This resulted in a decay of the feed pressure (pressure reduction) as a function of time. The unsteady permeate flux and feed pressure was recorded automatically using data acquisition system as discussed in the experimental section.

Figure. 4.3(a) shows the variation of the unsteady state permeate flux as a function of reducing feed pressure achieved by opening the bypass valve a crack once steady state had been reached for a feed concentration of 0.2 kg/m^3. Similar plots for 1 and 5 kg/m^3 feed concentrations are shown in Figures. 4.3(b) and (c), respectively. These figures are interesting because they clearly show the contribution of the polarization layer to the overall filtration resistance. It should be noted that as the pressure decays from a higher initial value, the transient flux at any given pressure is slightly lower than the flux at the same pressure when the pressure decay is initiated from a lower initial value. For example in Figure 4.3(a), if a straight line is drawn vertically at 100 kPa, the flux resulting from a pressure decay starting from 405 kPa is slightly lower than that resulting from a pressure decay starting at 270 kPa, which in turn is lower than the flux at 100 kPa resulting from a pressure decay initiated at 135 kPa. This observation could be explained as follows:

In the case where steady state is reached at a higher pressure, the amount of solute accumulated in the polarization layer is relatively large. This has resulted in higher filtration resistance to the solvent (permeate) flow. Consequently, when the feed pressure is rapidly reduced from a high initial value, the polarization layer offers a higher

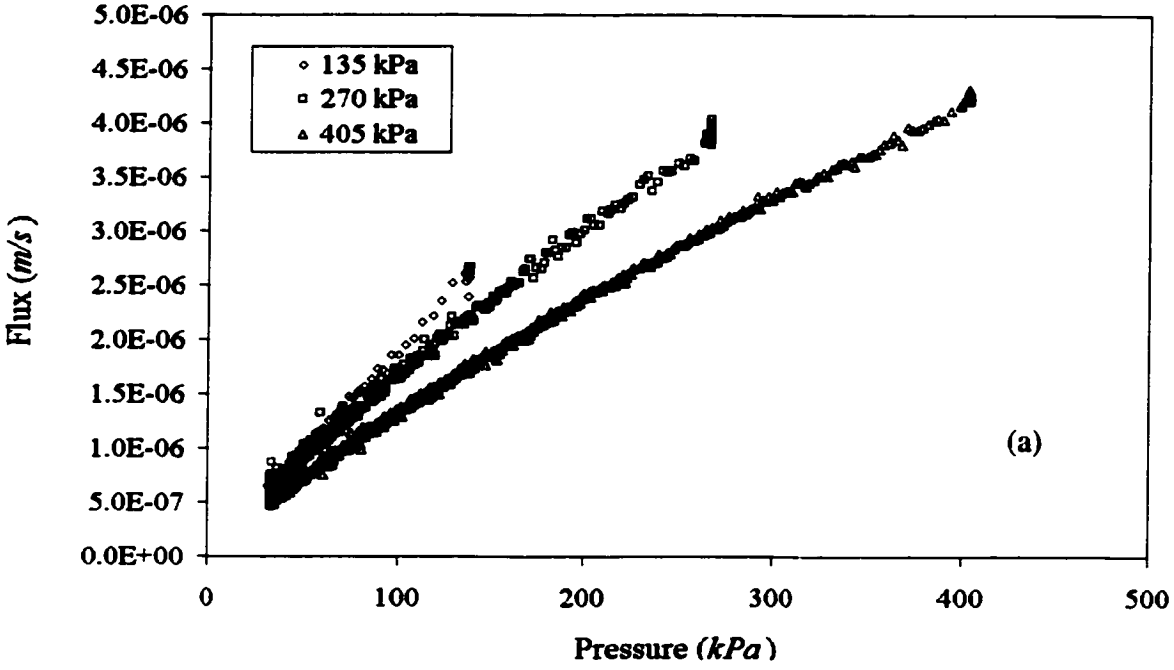

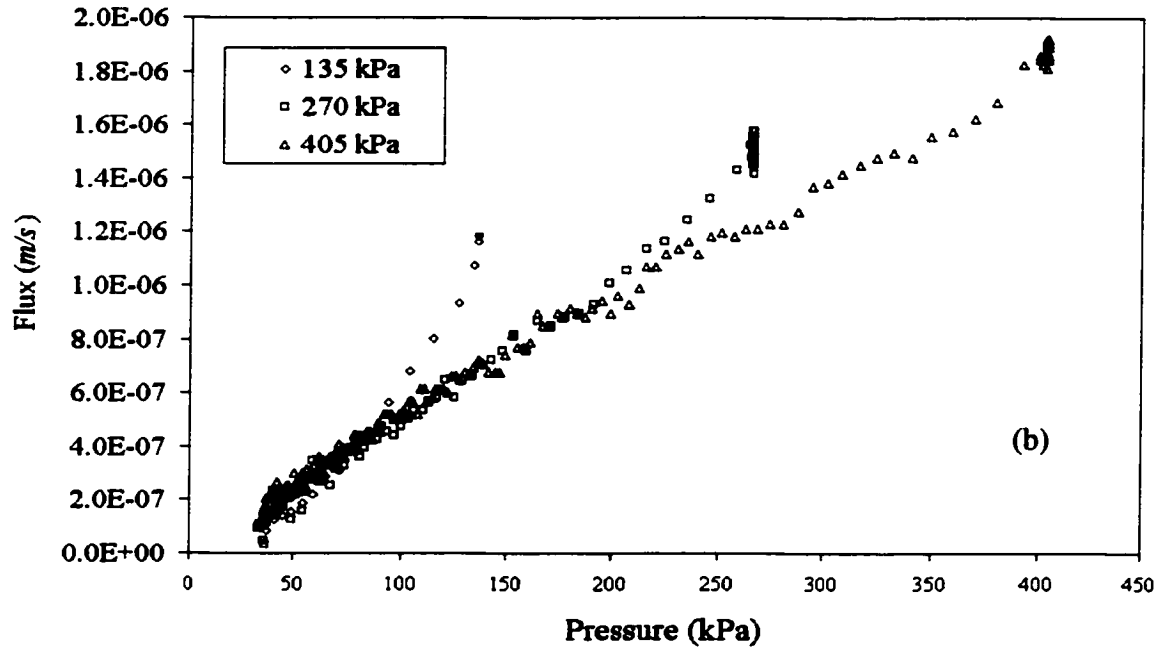

Figures 4.3 Post steady state transient variations of permeate flux as a function of reducing pressure for three different bulk feed pressures. (a) 0.2 kg/m^3 (b) 1 kg/m^3 The time scale for unsteady state UF is 120/170/190 and 100/140/170 seconds, respectively.

.

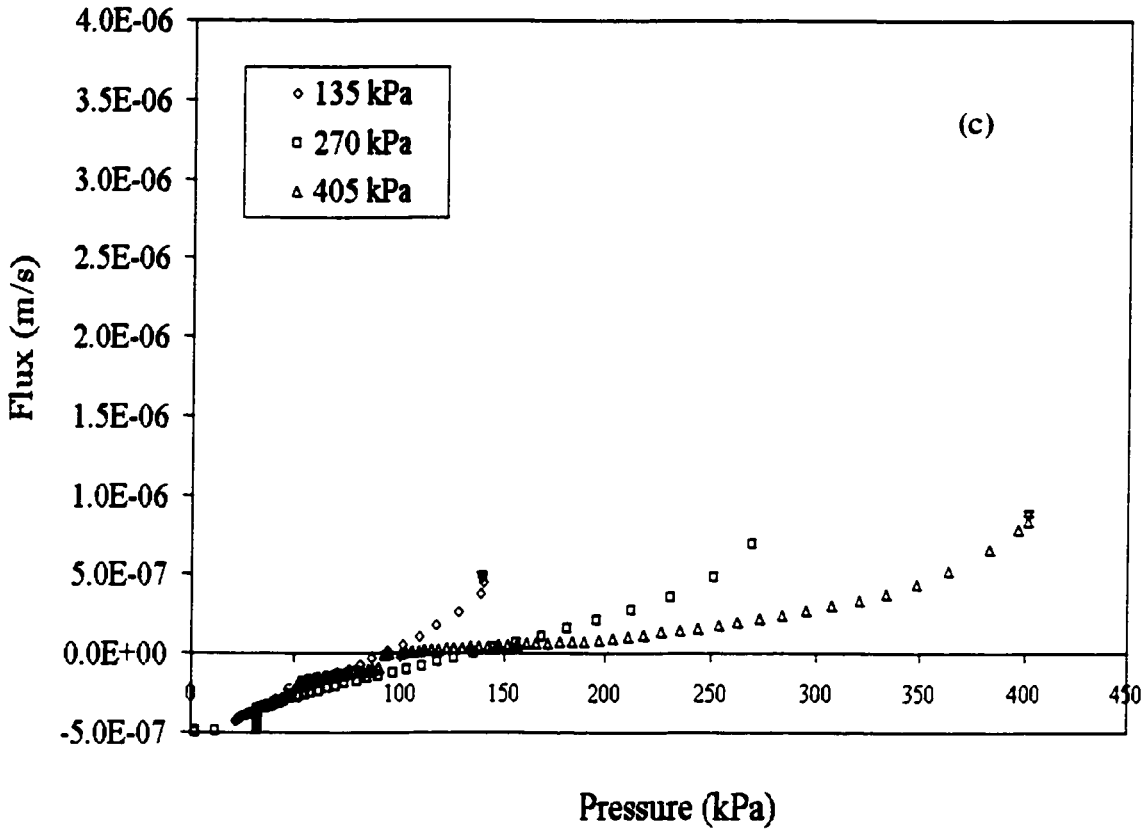

Figure 4.3(Contd.) Post steady state transient variation of permeate flux as a function of reducing pressure for three different bulk feed pressures. (c) 5 kg/m^3
The time scale for unsteady state UF is 70/100/170 seconds.

resistance to the permeate flow resulting in a slightly lower flux than the case when pressure decay was initiated from a lower initial value. Furthermore, Figure 4.3 (c) shows that irrespective of the initial pressure value, once the pressure release valve is cracked open to reduce the feed pressure, the balance registers a ***loss*** in weight as the feed pressure drops to less than about 90 kPa. The only reason the balance could register a loss in weight (a negative flux) is that feed pressure drops to a value, which is less than the osmotic pressure corresponding to accumulated solute at the membrane surface. This is indeed remarkable observation. To the best of our knowledge, this is the first time that such a phenomenon of negative flux has been demonstrated experimentally in ultrafiltration.

4.1.2 Steady state Rejection of PEG

Table 4.1 shows the steady state membrane rejection (R) based on the bulk feed concentration ($R=1-C_p/C_b$ where C_p and C_b are respectively the solute concentration in permeate and feed) for the entire concentration and pressure ranges studied in this work. As can be seen from this Table, steady state solute rejection was always greater than 97%. The membrane can therefore be treated as being completely retentive to the solute. As a consequence, the osmotic pressure of permeate can be neglected and the effective osmotic pressure difference across the membrane ($\Delta\pi$) can be set equal to π_w.

Table 4.1. Steady state PEG rejection for the entire pressure and concentration range studied in this work.

Pressure/Conc.	$0.2\,kg/m^3$	$1\,kg/m^3$	$5\,kg/m^3$
kPa	%Rejection	%Rejection	%Rejection
135	99.7	99.6	99.5
270	99.1	98.5	98.3
405	97.9	97.5	97.2

4.1.3 Total filtration resistance measurement and osmotic pressure analysis

The transient data presented in Figure. 4.3(c) can be further analyzed by plotting the time derivative of the unsteady flux (dJ/dt) v/s the time derivative of the feed pressure ($d\Delta P/dt$). This data is shown in Figure. 4.4(a). It is obvious that there is a very good linear correlation for each value of starting pressure. Using the slope values of these straight lines the filtration resistance (R_f) for each of the three starting pressures, 135, 270 and 405 kPa were found to be 1.84×10^{14}, 2.95×10^{14} and 4.30×10^{14} m^{-1}, respectively. The resistance for pure water was measured to be 3.5×10^{13} m^{-1}. Utilizing this estimated filtration resistance for all concentrations and pressures given in Table 4.2 and using Equation (2.2) (Chapter 2) the osmotic pressure (π_w) of solute accumulated at the membrane surface was calculated. This calculated π_w is plotted as a function of unsteady pressure in Figure 4.5(a). It is clear from this figure that the osmotic pressure at the membrane surface is independent of the feed pressure and clearly indicative of a gel layer dominated filtration. Considering that the osmotic pressure is independent of applied pressure and is only dependent on solute concentration, increased resistance at higher applied pressure was due to increase in gel layer thickness on the membrane surface. Furthermore, it should be noted that using Equation (2.2), the osmotic pressure of the PEG gel was found to be about 88 kPa. This is also in very good agreement with the experimental evidence of the onset of the negative flux when the feed pressure drops to values below 90 kPa (as shown in Figure. 4.3c).

A similar analysis of the data presented in Figure 4.3(b) results in Figure 4.4(b) for a PEG concentration of 1 kg/m^3. As can be seen, the graph between dJ/dt v/s $d\Delta P/dt$ is no

longer linear which clearly indicates that the solute concentration (or osmotic pressure) at the membrane surface varies as a function of the feed pressure. The filtration resistance at different feed pressure can be calculated by drawing tangents to the curves in Figure 4.4(b) or by taking the mean of various slopes at different intervals. Using these resistance values at each feed pressure, the osmotic pressure of the solute at the membrane surface (or π_w) can be calculated using Equation (2.2). The results are shown in Figure. 4.5(b). It is clear from this Figure that π_w is a function of the feed pressure and is always less than 90 kPa indicating an almost osmotically limited permeate flow. However, at higher applied pressures the contributions of gel layer towards controlling permeate flow will play a prominent role.

Table 4.2 Estimated filtration resistance for all concentrations and pressures

R_m of Pure water = 3.75E13

Pressure/ concentration	$0.2\,kg/m^3$	$1\ kg/m^3$	$5\,kg/m^3$
kPa	m^{-1}	m^{-1}	m^{-1}
135	4.09 E 13	4.166 E13	1.84 E14
270	5.34 E 13	7.92 E13	2.95 E14
405	1.29 E 14	1.35 E14	4.3 E14

4.1.4 Measurement of wall concentration (C_w)

A correlation between the solute osmotic pressure and its concentration has been provided by Bhattacharjee et al. (1996). They demonstrated that Flory's equation for the change in chemical potential (the osmotic pressure) of PEG, as a function of volume fraction was an accurate correlation for osmotic pressure and concentration of PEG.

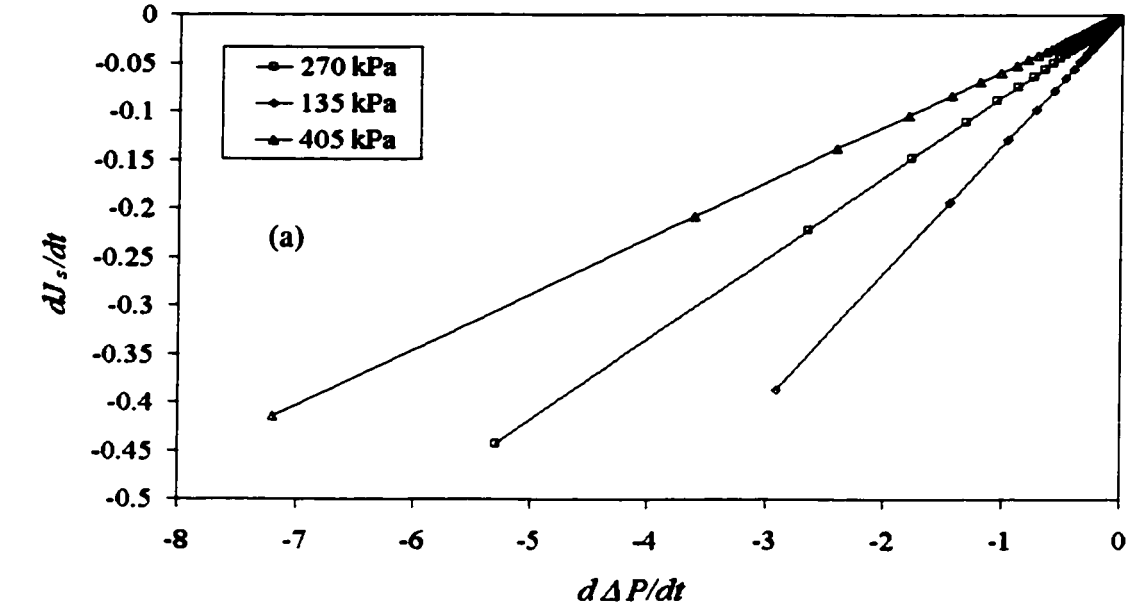

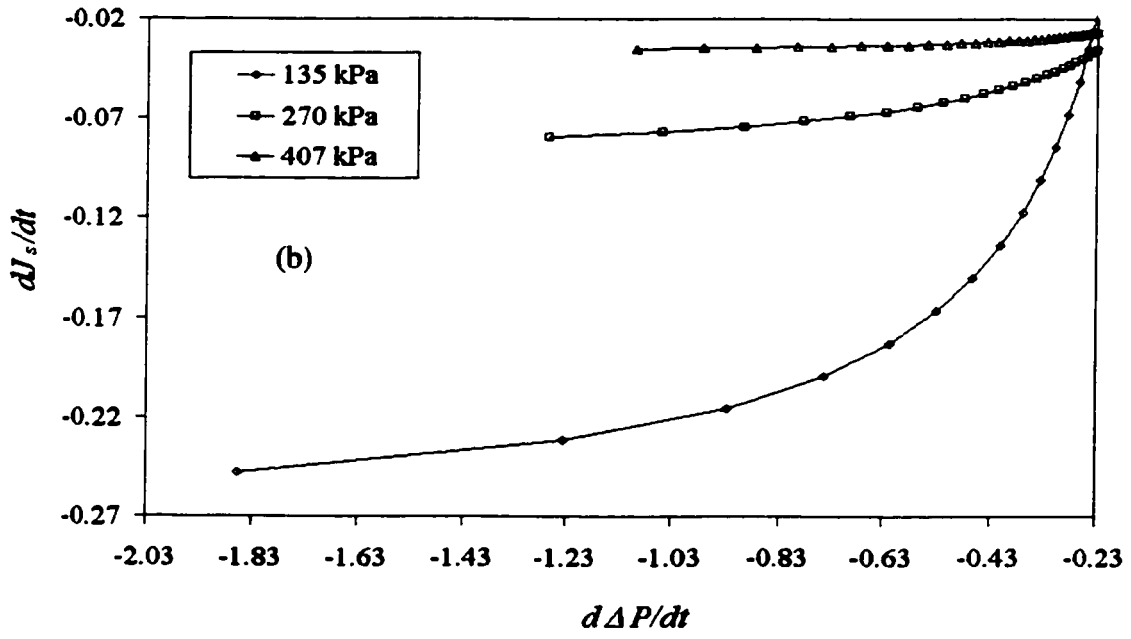

Figure 4.4 *dJs/dt* v/s *dP/dt* (a) for data presented in Figure 4.3c. (b) for data presented in Figure 4.3b.

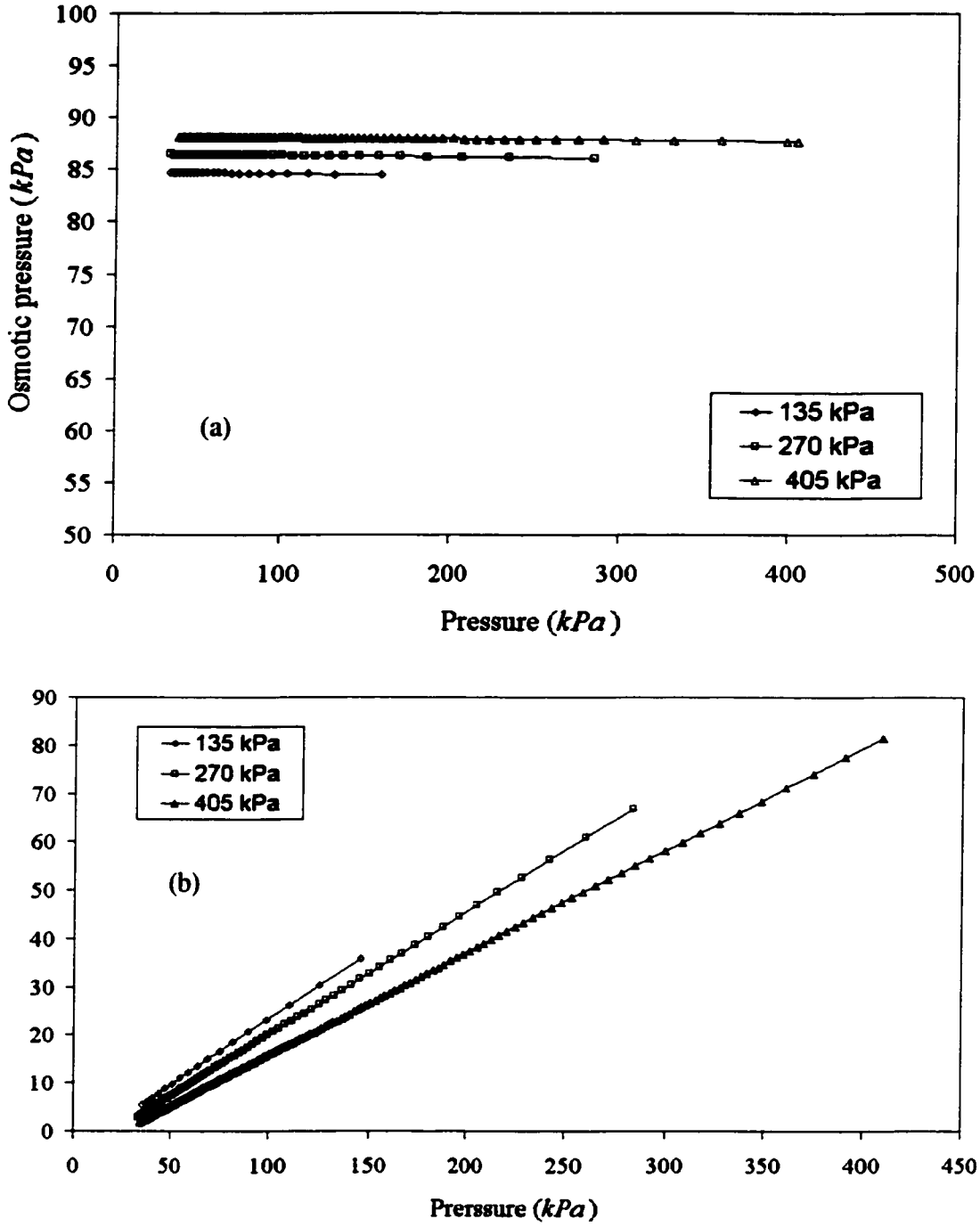

Figure 4.5 PEG osmotic pressure at membrane surface π_w (a) for PEG bulk concentration of 5 kg/m^3 (b) for PEG bulk concentration of 1 kg/m^3

Flory's equation relates the osmotic pressure with solute volume fraction as

$$\pi = -\frac{RT}{V_1}\left[\ln(1-\gamma_p) + (1-\frac{1}{n})\gamma_p + \chi_{12}\gamma_p\right] \tag{2.4}$$

where, $\gamma_p = c/\rho_p$ is volume fraction of polymer, c is the polymer concentration, ρ_p is polymer density and n is the number of monomer sub units in the polymer chain. The Flory-Huggins interaction parameter χ_{12} is a linear function of solute concentration for linear chain polymers and the concentration dependence is best expressed as

$$\ln|\chi_{12}| = p + qc \tag{2.5}$$

where p and q are constants having values –0.604 and 1.7452 m^3/kg respectively. Equation (2.4) can be used to calculate C_w (the solute wall concentration) from the estimated π_w values from experimental data (Figures. 4.5a and 4.5b). Calculated values of wall concentration are given in Table 4.3.

Table 4.3 Solute wall concentration for all bulk feed concentration and feed pressures

Pressure/ Concentration	C_b at 0.2 kg/m^3	C_b at 1 kg/m^3	C_b at 5 kg/m^3
	C_w kg/m^3	C_w kg/m^3	C_w kg/m^3
135	102	116	124
270	113	118	124
405	121	122	124

4.1.5 Steady state solute concentration profile in the polarization layer

It is instructive to calculate the steady state solute concentration profile in the polarization layer using this value of C_w and the steady state flux, J_s, the solute concentration profile as a function of distance perpendicular to the membrane surface can be estimated using

the film theory (Zydney, 1996; van den Berg et al., 1989; Bhattacharjee and Datta, 2001) and the following equation:

$$C_x = C_b + (C_w - C_b)\exp(\frac{-J_s x}{D}) \tag{2.6}$$

where D is diffusivity and is calculated using literature correlation [Bhattacharjee and Datta, 2001). The boundary layer thickness (δ) can then be estimated as that value of x at which the solute concentration becomes almost equal to the bulk solute concentration. Figure 4.6(a) to 4.6(c) show the steady state solute concentration profile within the polarization layer for three different steady feed pressures and bulk feed concentration of 0.2, 1 and 5 kg/m^3 respectively. As can be seen from the inserted smaller figures in Figure 4.6(b)-(c) that for higher bulk feed concentration the membrane concentration is constant initially and than later decreased as thickness increases while for the lower bulk feed concentration the decrease in concentration is instantaneous verifying the existence of gel layer. It is also clear from these figures that for a given bulk feed concentration, the extent of the polarization layer is independent of the feed pressure.

4.1.6 Thickness of polarization layer

The extent of the polarization layer for each value of bulk feed concentration is plotted in Figure. 4.7. This figure clearly shows that the extent of the polarization layer is a function of the bulk solute concentration and that make-up of the polarization layer could be such as to provide significant hydraulic resistance compared to the membrane resistance. It is therefore necessary to account for the additional filtration resistance of polarization layer when calculating the overall filtration resistance. Application of this

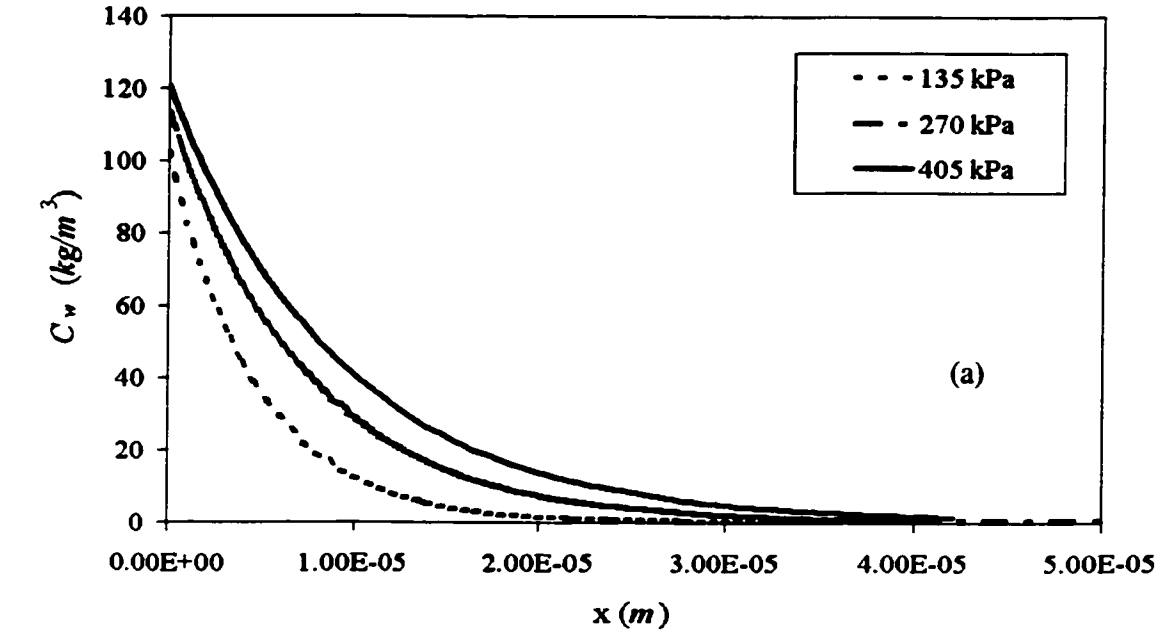

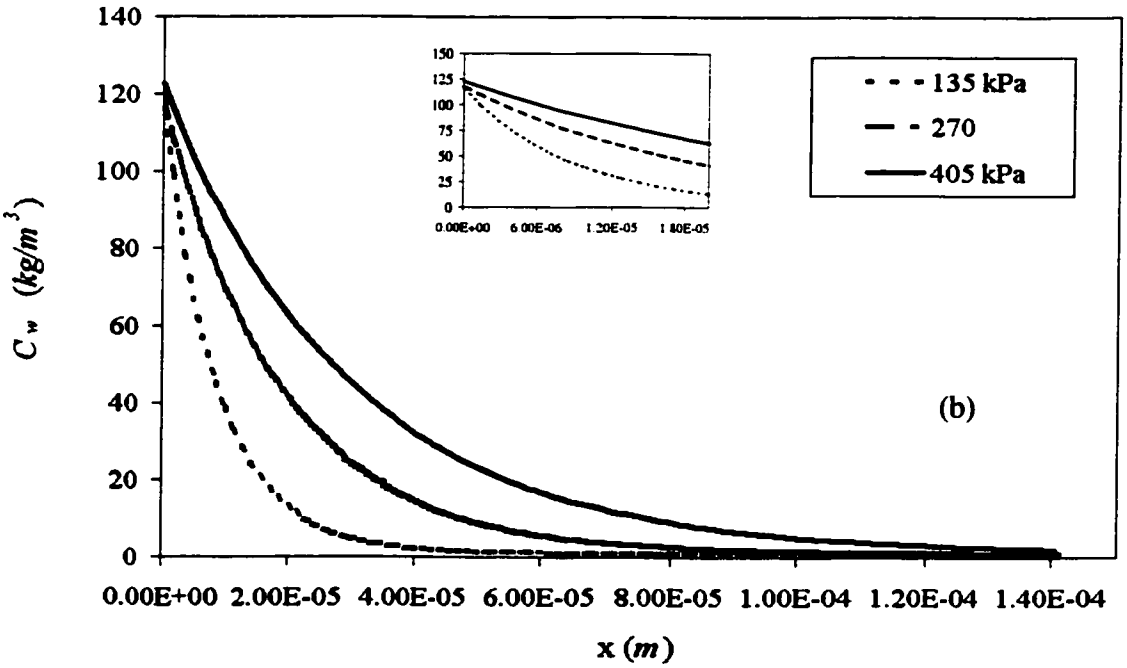

Figure 4.6 Variation of steady state PEG concentration as a function of distance from the membrane surface for three different feed pressures (a) for bulk PEG concentration of 0.2 kg/m^3 (b) for bulk PEG concentration of 1 kg/m^3

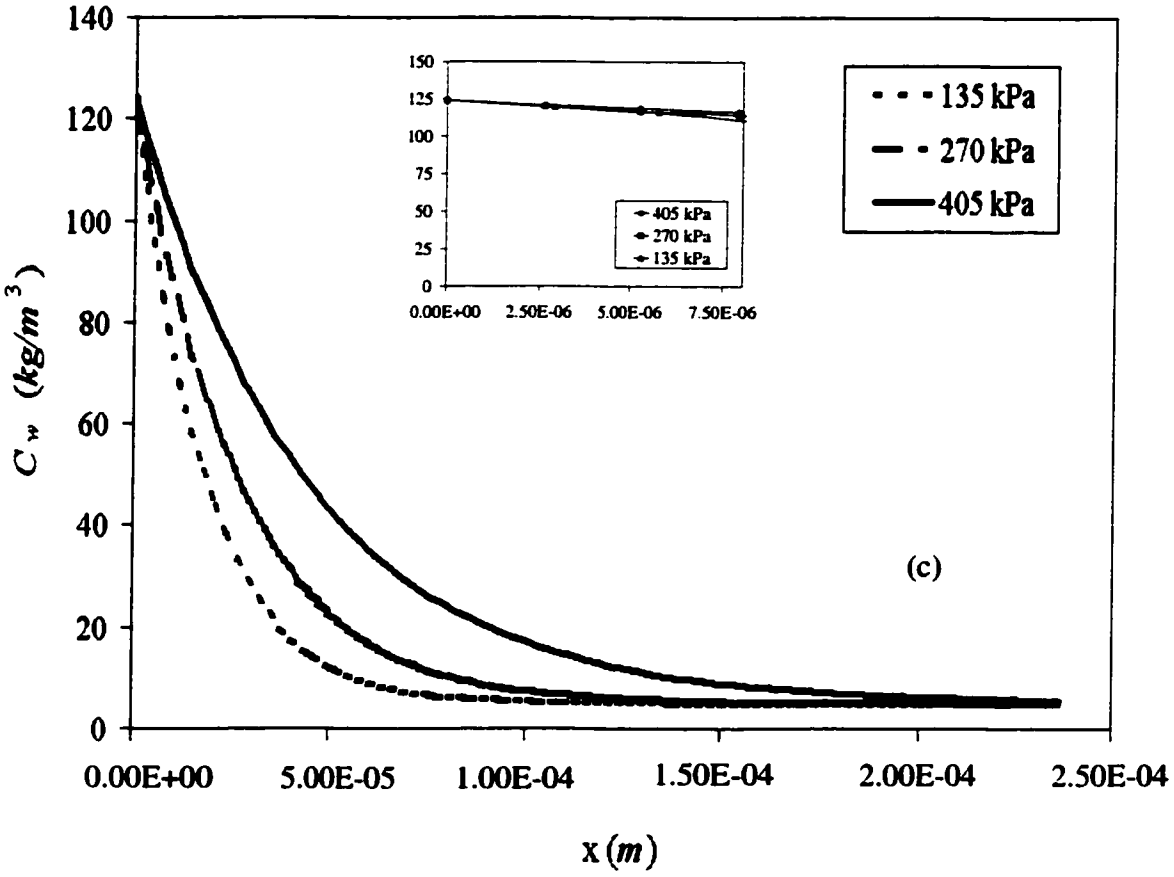

Figure 4.6 (Contd.) Variation of steady state PEG concentration as a function of distance from the membrane surface for three different feed pressures (c) for bulk PEG concentration of 5 kg/m^3. Inset Figure shows variation in C_w at small distances from membrane.

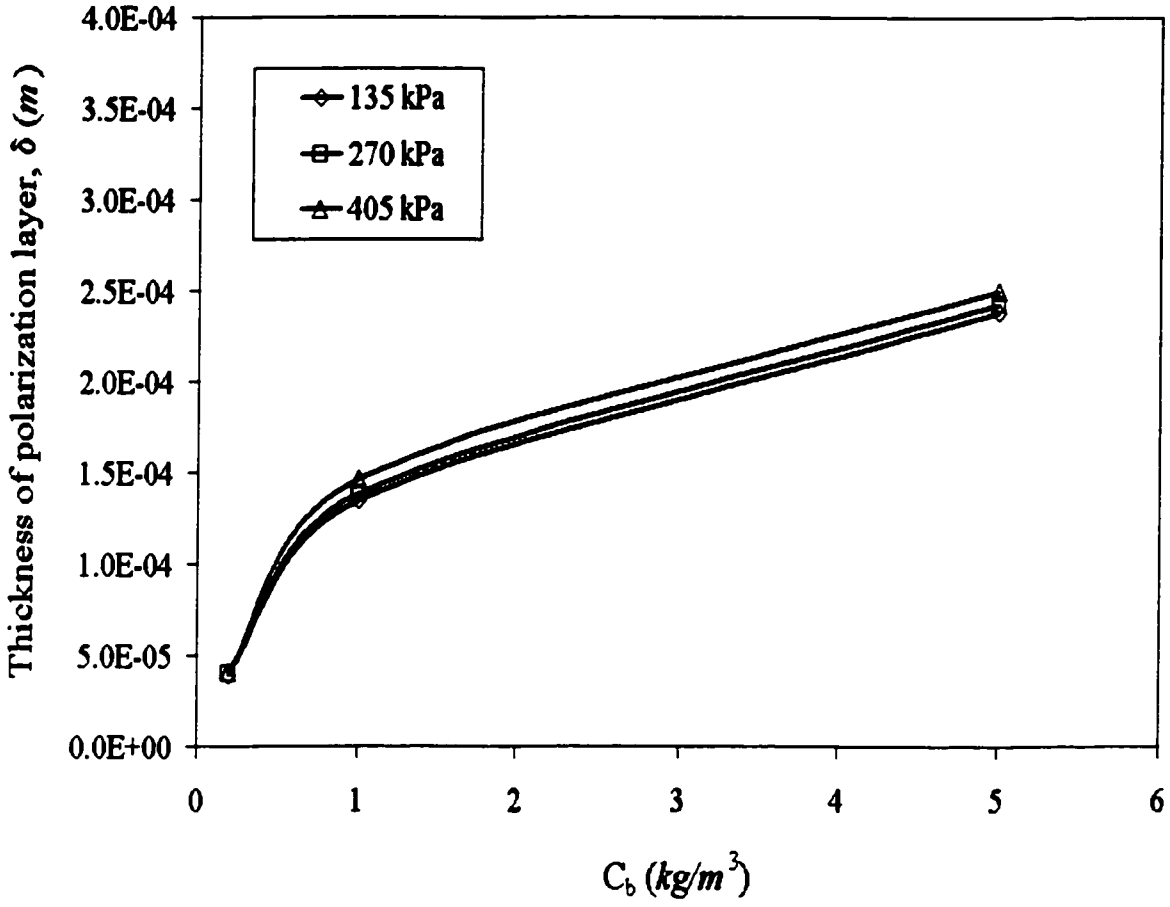

Figure 4.7 Calculated thickness of polarization layer as a function of bulk PEG concentration.

analysis will be limited to those gel layers that are not sufficiently diffused and offer significant resistance to flow of solvent.

4.2 Ultrafiltration of dextran

4.2.1 Permeate flux during dead end ultrafiltration of dextran

Permeate flux as a function of time for dextran T40 solution are shown in Figures 4.8(a) to 4.8(c) for a feed concentration of 0.2 to 5 kg/m^3 for different applied pressure of 135, 270 and 405 *kPa*. It is clear from these figures that permeate flux initially drops rapidly whereas the decrease is gradual at a later stage. This sudden drop in flux in the beginning of experiment is well explained by the osmotic pressure model where a build up of polarization layer at membrane surface, which leads to increase of the solute concentration at membrane surface. The osmotic pressure rises rapidly resulting in the decrease of net driving force. This high concentration at membrane surface is due to the high rejection and low diffusion coefficient of dextran that considerably reduces the rate of back transport leading to further increase in concentration on the surface.

Figure 4.8(c) shows the flux as a function of time for 5 kg/m^3 dextran solution. It is clear from this figure that compared to other two cases with lower concentration of dextran, the steady state value of fluxes are almost independent of applied pressure. This phenomenon is more clearly shown in Figure 4.9 where flux is plotted as a function of applied pressure for different bulk feed concentration. It is interesting to note that in UF of PEG solution, the pressure independent flux was gel layer controlled but in the case of UF of dextran it appears to be osmotic pressure limited flux.

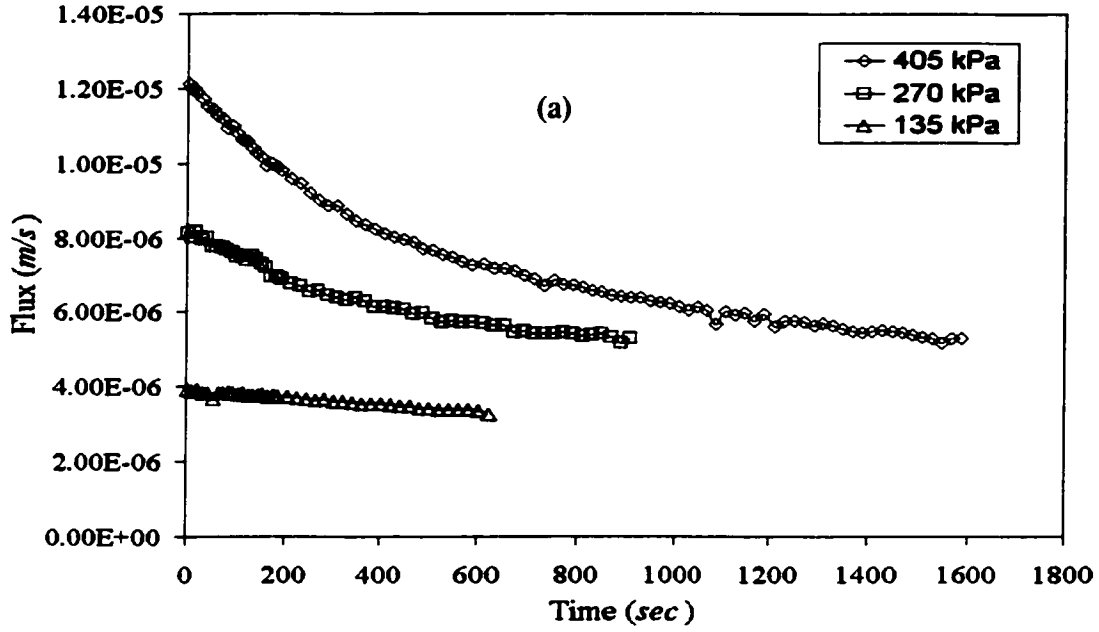

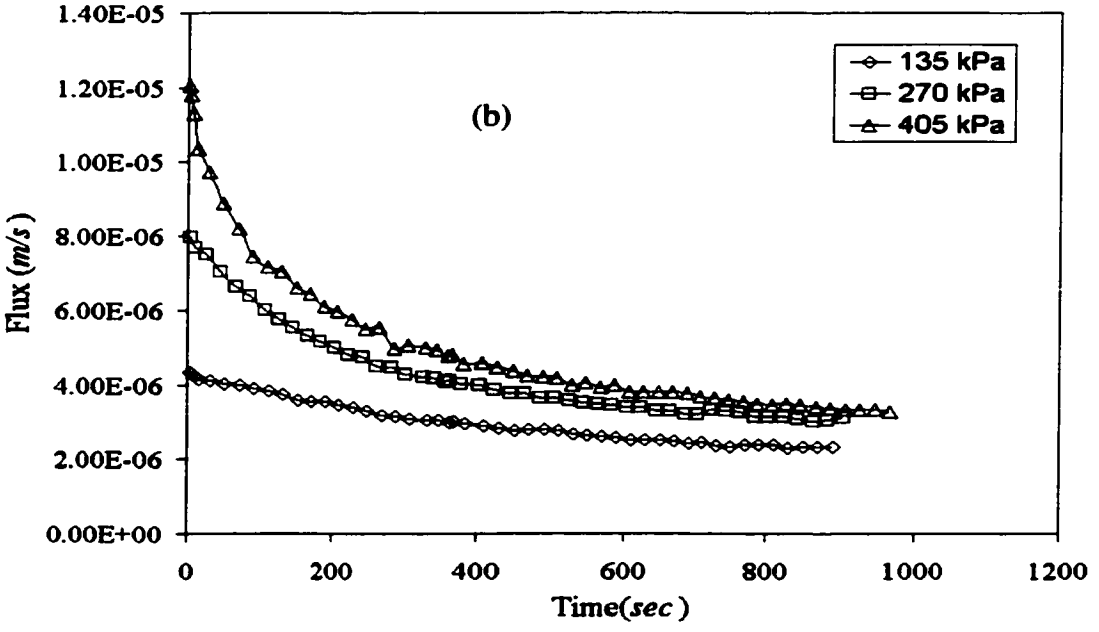

Figure 4.8 Variation of permeate flux as a function of time for various values of feed pressure. (a) 0.2 kg/m^3 (b) 1 kg/m^3

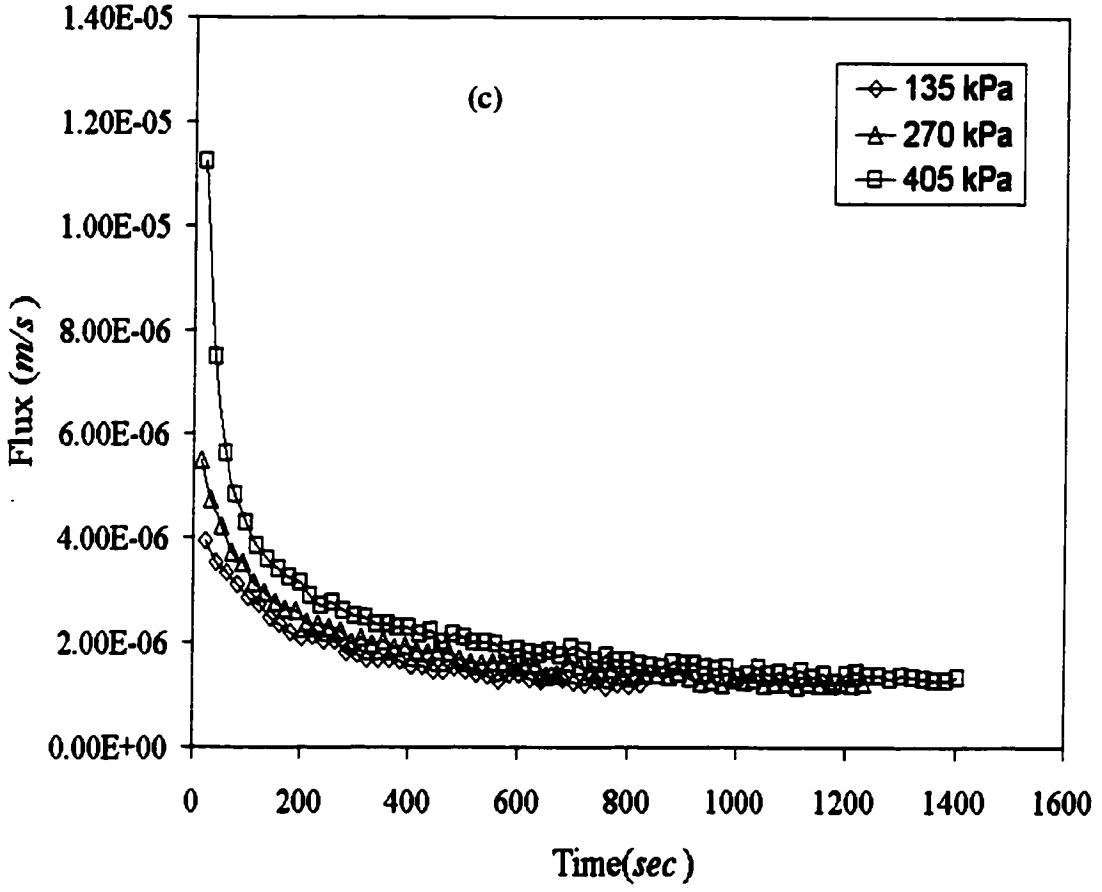

Figure 4.8 (Contd.) Variation of permeate flux as a function of time for various values of feed pressure. (c) 5 kg/m^3

These observations are similar to many reported in the literature (Jonsson, 1984, van Oers 1992). At lower applied pressure and lower bulk feed concentration the flux indeed changes with change in applied pressure but at higher pressure and higher concentration the flux is almost pressure independent. This is probably due to higher osmotic pressure build up which led to the almost constant driving force for different applied pressures. The steady state flux values are given in Table 4.4. Effect of bulk concentration was also shown in Figure 4.9. It is well known that an increase in bulk concentration of the solution decreases permeates flux. Higher feed concentration leads to higher osmotic pressure, and hence lower flux is observed. Further, higher concentration may be giving higher polarized layer resistance, which is inversely proportional to flux. However, the trends of the curves are identical as bulk concentration increases at a fixed pressure, which can be seen in Figures 4.8(a) to 4.8(c).

Table 4.4 Steady state flux of dextran T40 at different applied pressure and concentrations.

ΔP (*kPa*)	J_s (*m/s*) at various bulk concentrations (C_b) and pressures		
	0.2 kg/m^3	**1** kg/m^3	**5** kg/m^3
135	3.25×10^{-6}	2.31×10^{-6}	1.18×10^{-6}
270	5.22×10^{-6}	3.02×10^{-6}	1.25×10^{-6}
405	5.30×10^{-6}	3.40×10^{-6}	1.35×10^{-6}

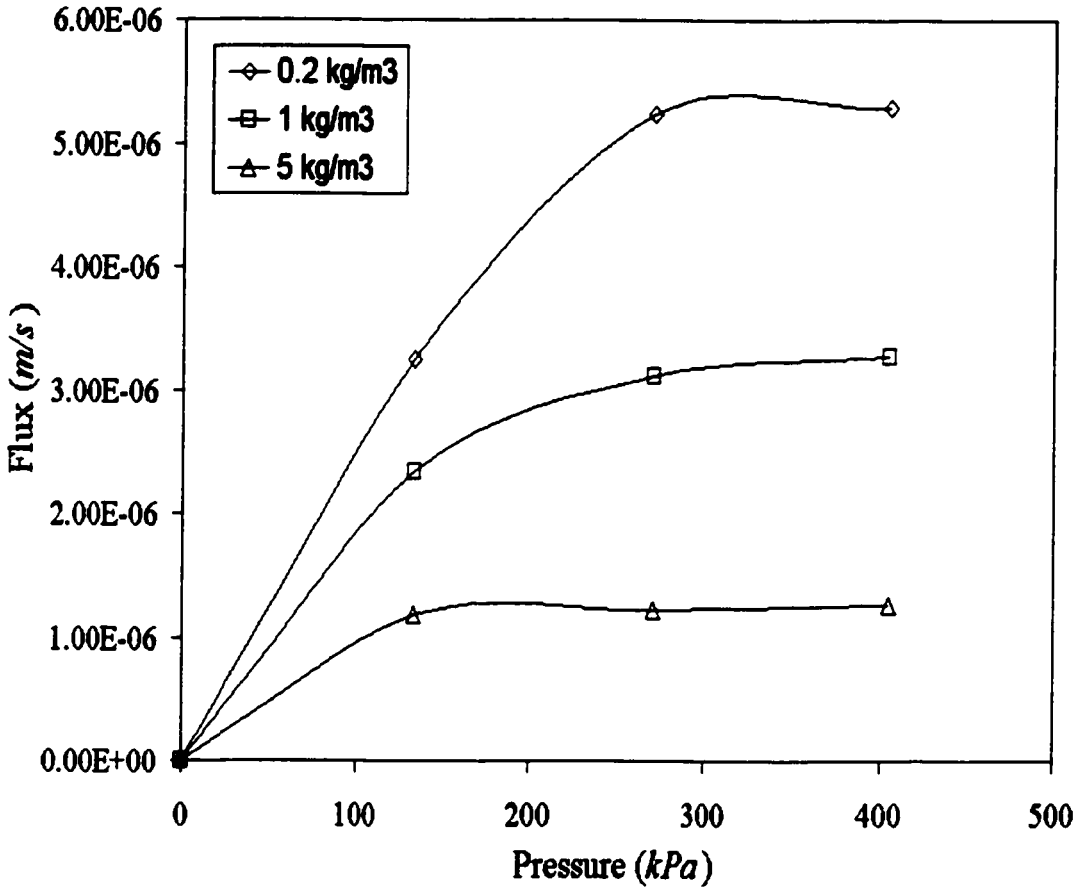

Figure 4.9 Steady state permeate flux as a function feed pressure for different feed concentrations

Figure 4.10(a) and (b) show the variation of unsteady state permeate flux as a function of reducing feed pressure for initial feed concentration of 1 and 5 kg/m^3 (as explained in experimental part of Chapter 3). These figures clearly explain the concept of polarization layer build up and their dependence on applied pressure and feed concentration. It is clearly noted from these figures that in the case of pressure decay from any higher value, transient decay of flux at any given pressure at particular time is slightly lower than the flux at same pressure when pressure decay started from a lower initial value. This is due to accumulation of more solute at membrane surface when ultrafiltration was carried out with higher initial feed concentration thereby explaining the pressure independent flux concept. However, unlike the case of PEG, a negative flux was not observed. It simply means that at no point the osmotic pressure is higher than the applied pressure. These transient data were used to calculate the actual filtration resistance as it has been described in the case of PEG. Actual Filtration resistance was found to be a function of applied pressure and solute concentration. The experimental and estimated values of actual filtration resistance, membrane resistance and polarization resistance are given in Table 4.5 (a to c). Detailed filtration data is also listed in these tables for different applied pressures and initial bulk feed concentrations. It is clear from these Tables that the membrane resistance remained same while the percentage of resistance offered due to polarization in ultrafiltration of dextran (R_p) which accounts for the total filtration resistance (R_f) was found to be dependant on applied pressures and initial bulk feed concentrations. Considering that 95-98% of PWP was recovered, it was assumed that there was no pore plugging and adsorption of solute on membrane and therefore resistance due to pore plugging and adsorption has been ignored.

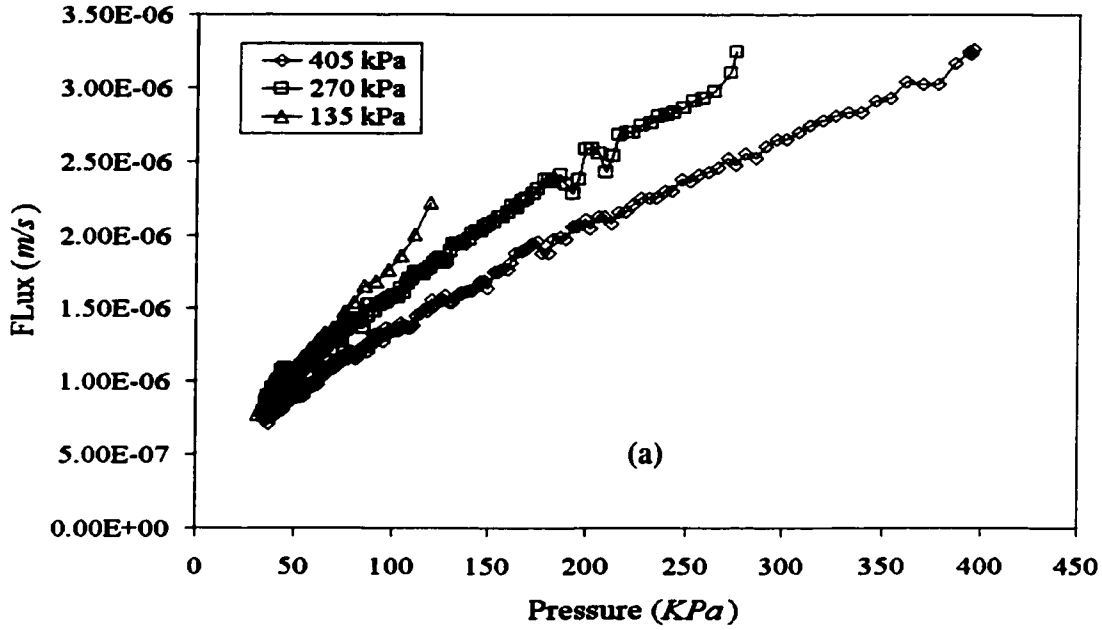

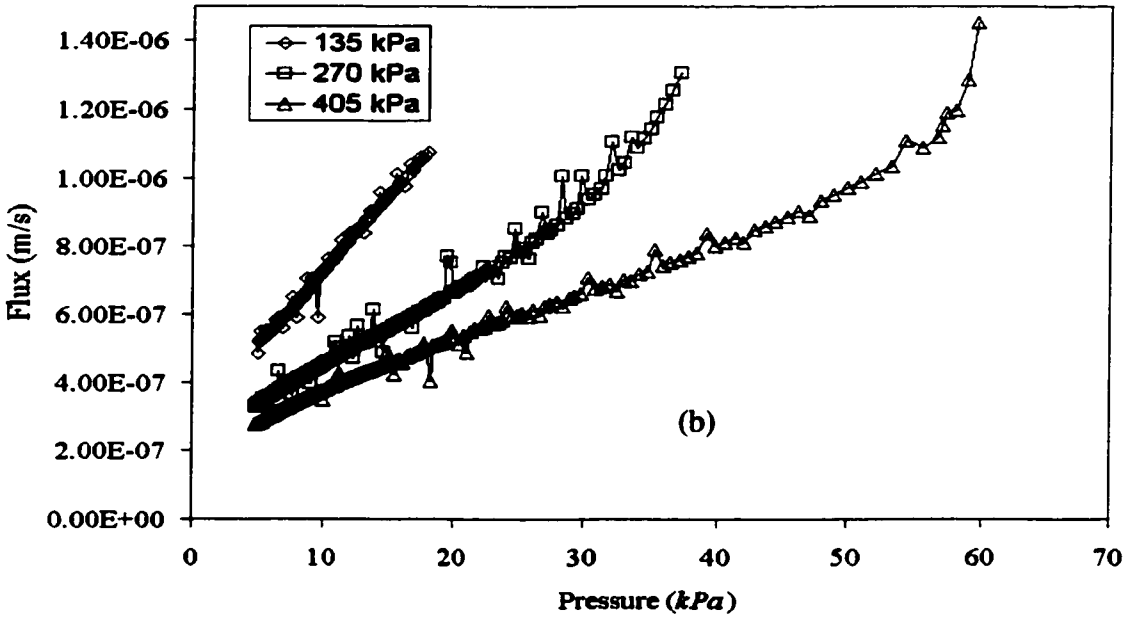

Figure 4.10 Post steady state transient variation of permeate flux as a function of reducing pressure for three different bulk feed pressures. (a) 1 kg/m^3 (b) 5 kg/m^3 The time scale for unsteady state UF is 80/130/160 and 100/140/170 sec. for the above two cases

Table 4.5 Filtration resistance analysis of dextran T40 at different initial bulk concentration and applied pressures.

4.5 a

Dextran 5 kg/m^3				
ΔP **(kPa)**	$R_f = R_m + R_p$	R_m	R_p	Percentage due to R_p
135	1.37×10^{14}	3.51×10^{13}	1.01×10^{14}	74.3
270	1.83×10^{14}	3.51×10^{13}	1.48×10^{14}	80.8
405	3.06×10^{14}	3.51×10^{13}	2.71×10^{14}	88.5

4.5 b

Dextran 1 kg/m^3				
ΔP **(kPa)**	$R_f = R_m + R_p$	R_m	R_p	Percentage due to R_p
135	5.12×10^{13}	3.51×10^{13}	1.61×10^{13}	31.5
270	1.02×10^{14}	3.51×10^{13}	6.73×10^{13}	65.7
405	1.50×10^{14}	3.51×10^{13}	1.15×10^{14}	76.6

4.5 c

Dextran 0.2 kg/m^3				
ΔP **(kPa)**	$R_f = R_m + R_p$	R_m	R_p	Percentage due to R_p
135	3.83×10^{13}	3.51×10^{13}	2.16×10^{11}	8.36
270	4.55×10^{13}	3.51×10^{13}	1.04×10^{13}	22.9
405	7.06×10^{13}	3.51×10^{13}	3.55×10^{13}	50.3

4.2.2 Dextran rejection

Table 4.6 shows the observed steady state membrane rejection (R) for the entire range of pressure and concentration studied in this work. As can be seen from this Table, the steady state solute rejection was always greater than 90% and it was found to be the function of applied pressure and feed concentration. As shown in Figure 4.11 the steady state dextran rejection decreased with increase in flux and the maximum observed rejection at flux for lowest concentration and pressure was observed, this means that in entire evaluated flux region the rejection is influenced by concentration polarization. This is confirmed by higher observed rejection for 0.2 kg/m^3 feed concentration at 135 kPa compared to 5 kg/m^3 feed concentration at 405 kPa applied pressure.

Table 4.6 Steady state rejection of dextran T40 at different applied pressures and concentrations.

ΔP (kPa)	**Dextran rejection (%) at various bulk concentrations (C_b) and pressures**		
	0.2 kg/m^3	**1 kg/m^3**	**5 kg/m^3**
135	97.0	95.9	95.1
270	94.3	93.4	91.2
405	92.1	90.9	90.1

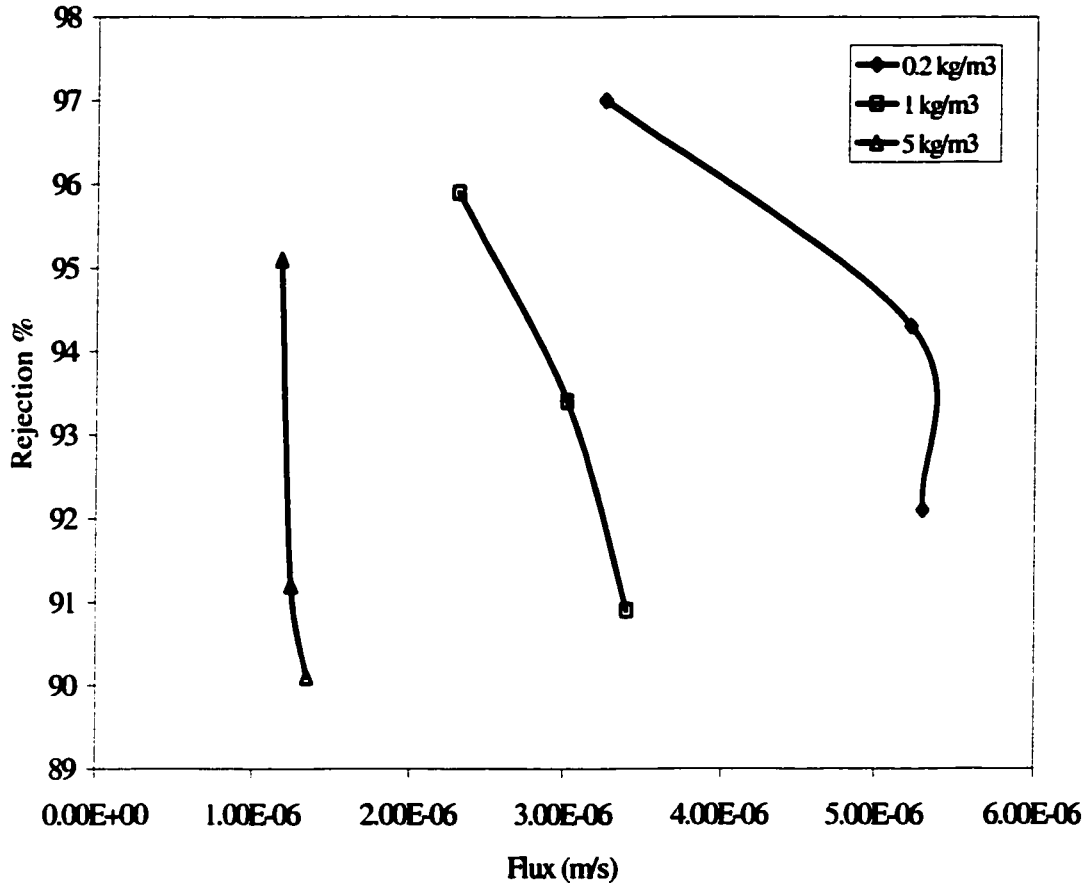

Figure 4.11 Steady state dextran rejection as a function of permeate flux.

4.2.3 Response of permeate flux to sudden pressure change (Pressure cycle)

Figure 4.12(a)- 4.12(c) show unsteady-state permeate flux as function of time in response to a sudden pressure change for Dextran T40 with different initial bulk feed concentrations. The sudden change of pressure was classified as pressure cycle in which pressure was changed according to the following sequence.

135 kPa -270 kPa -135 kPa -270 kPa-405 kPa -135 kPa.

A starting trans-membrane pressure (t =0) was set to 135 kPa for all three cases. After steady state was reached, ΔP was increased to 270 kPa; once steady state was achieved again pressure was dropped to 135 kPa and this procedure was repeated according to the defined pressure cycle above. This procedure was used to predict the unsteady-state flux response. As can be seen from Figures 4.12(a) -4.12(c) for all three concentrations, an increase in ΔP result in corresponding increase in steady state permeate flux. However, at the same time an unsteady behavior was observed, for example when pressure was increased from 135 kPa to 270 kPa and after some time changed back to lower pressure. For the lower feed concentration (0.2 kg/m^3 to 1 kg/m^3) it was found that with 100% increase in applied pressure the steady state permeate flux increased by 35- 50% only. Moreover this increment in steady state flux was further decreased by 2-5 % when pressure was increased by additional 50% from 270 kPa to 405 kPa. In this cycle a decrease in pressure back to 135 kPa resulted in reversible decrease in permeate flux to a slightly lower than the steady state value obtained by starting at 135 kPa. This flux behavior is well predicted by the osmotic pressure model. The doubling of applied pressure does not lead to the doubling of permeate flux, because an increase in

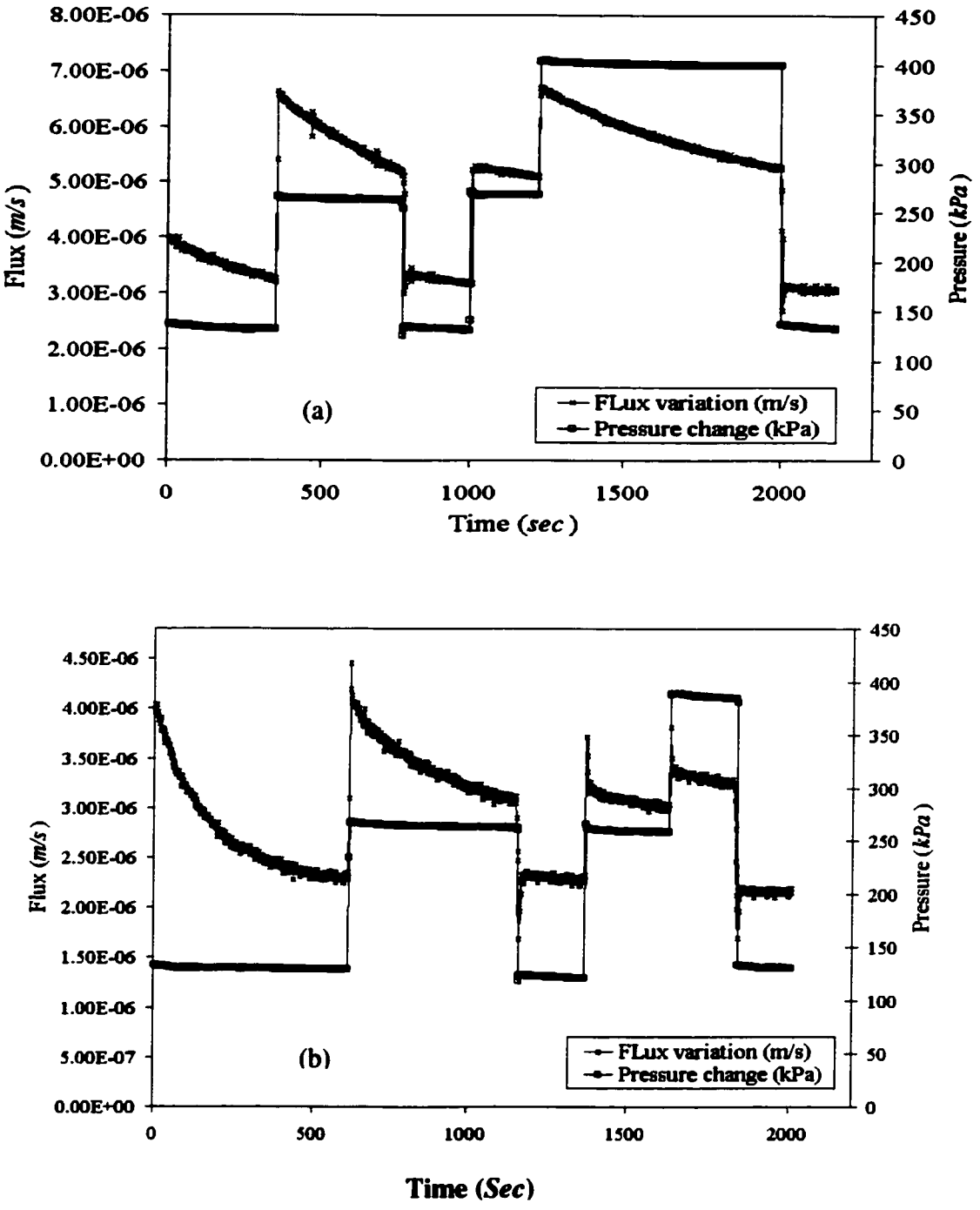

Figure 4.12 Unsteady-state permeate flux as function of time in response to a sudden pressure change for Dextran (a) 0.2 kg/m^3 (b) 1 kg/m^3

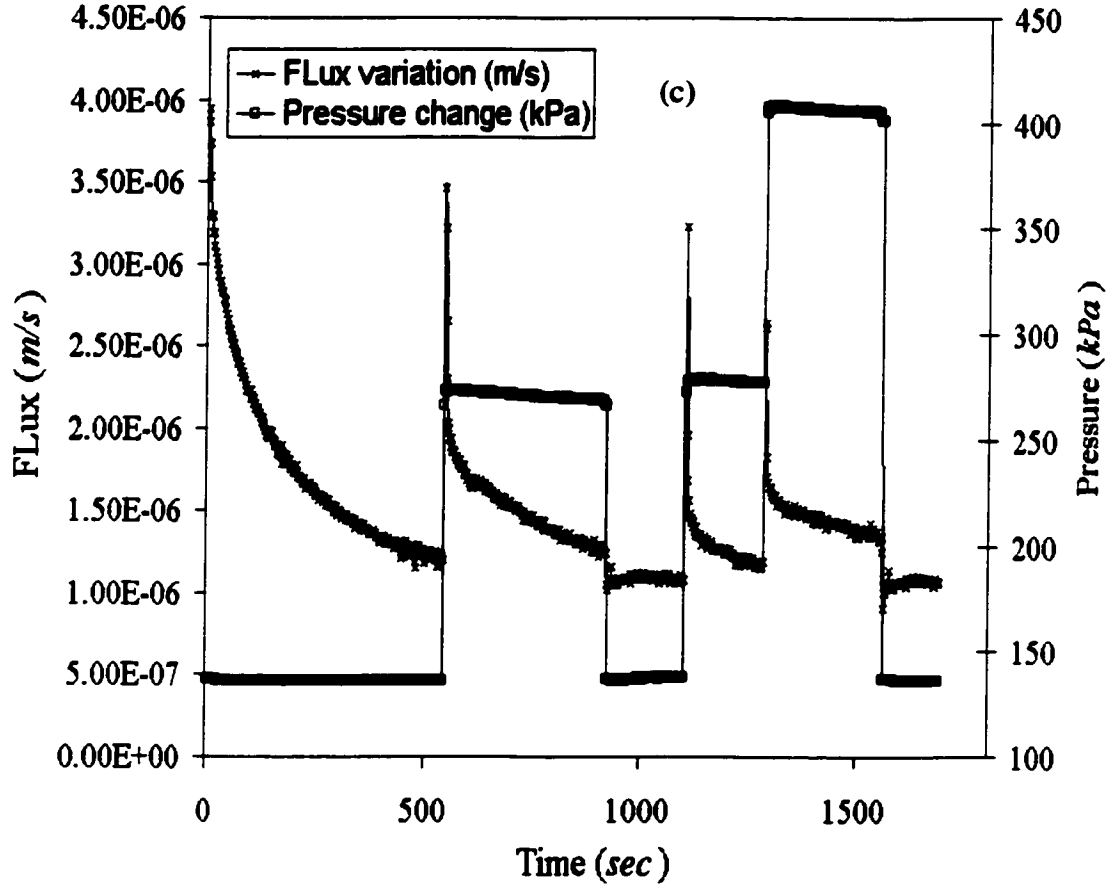

Figure 4.12(Contd.) Unsteady-state permeate flux as function of time in response to a sudden pressure change for Dextran (c) 5 kg/m^3

pressure is partly compensated by an increase in osmotic pressure and similarly the 50-100% decrease in applied pressure does not result in the same decrease in permeate flux, as evidenced from figure 4.12. At both pressure changes the concentration gradient at the membrane surface varied quickly however, there was a gradual decrease in flux during entire experiment which is again due to increase of the bulk concentration with time. Our experimental observations are in agreement with theoretical studies reported earlier (Karode, 2000). The response of the flux to the sudden pressure changes can provide additional information, which is indicative of sole presence of a polarization layer. The measurement shows that the steady state flux varies due to change in pressure, which clearly indicates that only polarization layer is present. However, for the higher feed concentration of 5 kg/m^3, where flux has an almost equal value for both pressures or flux change is not very high like the previous two cases, does not provide proof of the presence of a gel layer. In order to show this one needs additional verifications, which we have discussed in Chapter 4 (Section 4.1).

4.2.4 Osmotic pressure (π_w) as a function of unsteady pressure.

Using experimentally measured permeate flux at given bulk solute concentration and applied pressure, followed by the determination of total filtration resistance as defined in Tables 4.5(a to c), osmotic pressure of accumulated solute at membrane surface can be calculated using Equation (2.7) as defined in Chapter 2. This calculated π_w is plotted as a function of unsteady pressure for bulk solute in Figures 4.13(a) and 4.13(b) for

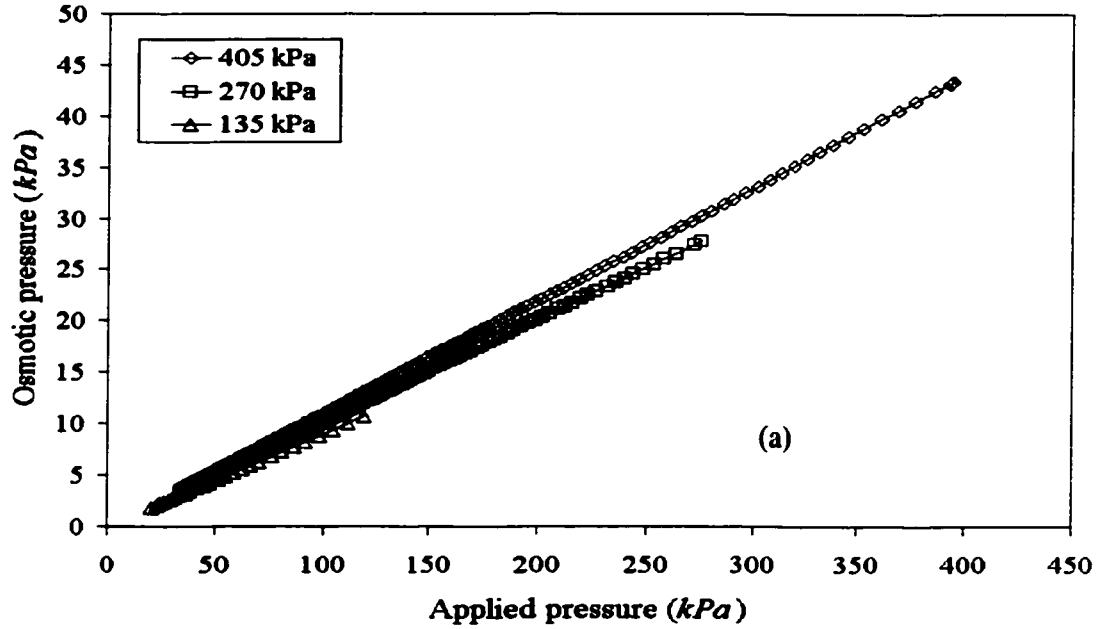

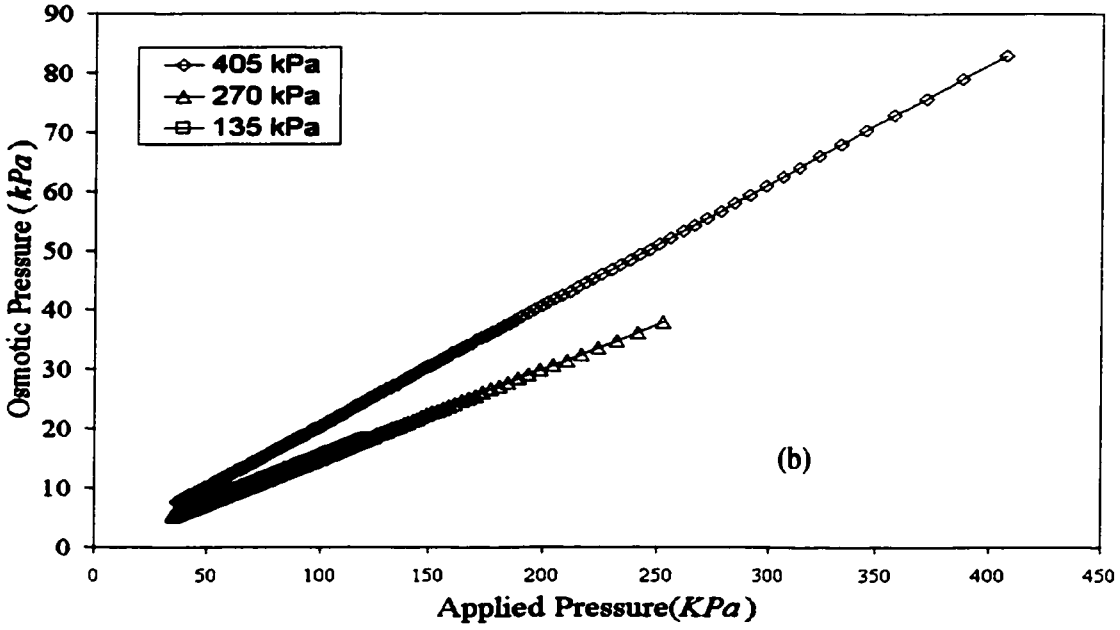

Figure 4.13 osmotic pressure at membrane surface π_w (a) for dextran bulk concentration of 1 kg/m^3 (b) for dextran bulk concentration of 5 kg/m^3

concentrations of 1-5 kg/m^3 and different initial applied pressures. This analysis shows that for all bulk feed concentrations and feed pressures, the osmotic pressure of Dextran at membrane surface was a function of feed pressure, which is clearly indicative of osmotic limited ultrafiltration.

4.2.5 Concentration profile in the polarization layer

It is assumed that an increase in concentration in the polarization layer at membrane surface and its variation as a function of distance perpendicular to membrane surface can be calculated according to the film theory as described in the case of PEG using concentration value C_m and the steady state flux, J_s. Figures 4.14(a) - 4.14(c) show the development of steady state solute concentration profile within the polarization layer for three different bulk feed concentrations (0.2, 1 and 5 kg/m^3) and applied pressures, respectively. These concentration profiles were plotted as a function of distance perpendicular to the membrane surface. It is clear from these figures that the concentration increases sharply at the initial stage of UF. The flux drop is also drastic during this stage. As can be seen from these figures that the concentration adjacent to the membrane is depend on applied pressure and bulk feed concentration. Further, it can be noted from these figures that the extent of polarization layer is almost independent of feed pressure.

The boundary layer thickness was plotted as a function of bulk feed concentration for different applied pressures in Figure 4.15. It is evident from these figures that boundary layer thickness is independent of applied pressure but varies with bulk feed

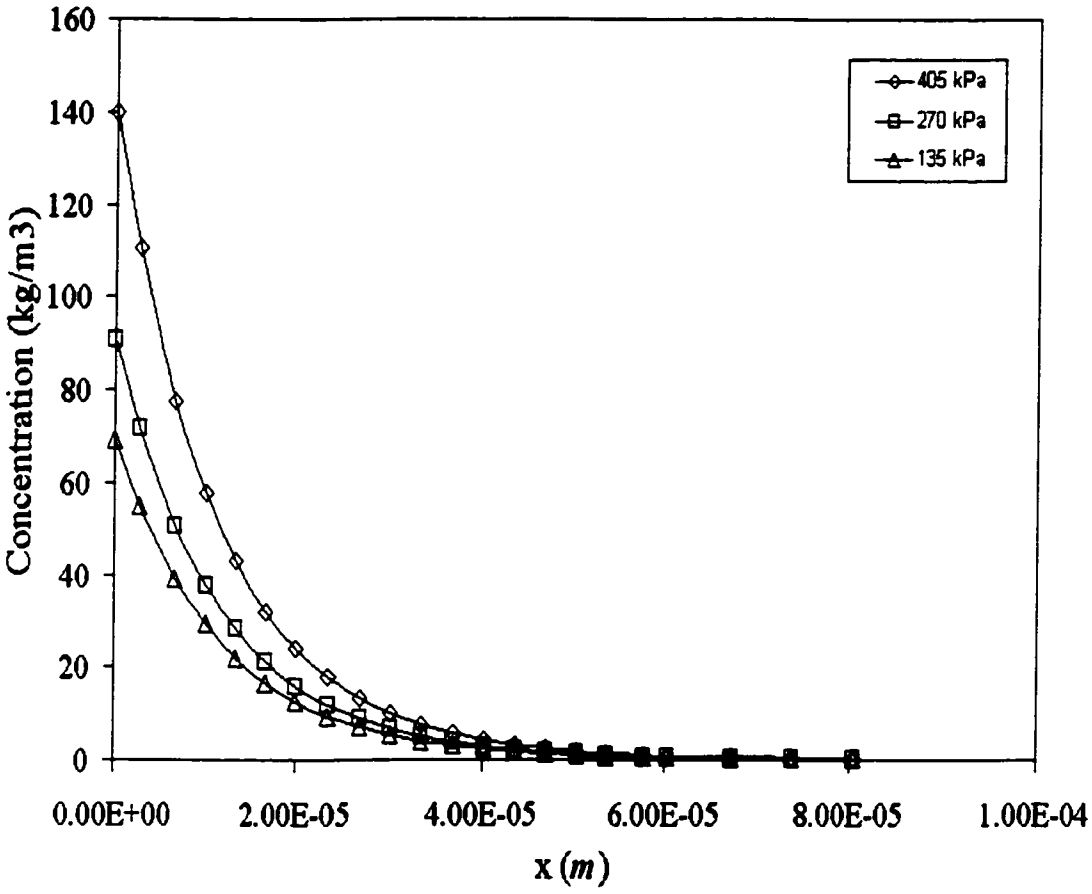

Figure 4.14(a) Variation of steady state concentration as a function of distance from the membrane surface for three different feed pressures for bulk dextran concentration of 0.2 kg/m^3

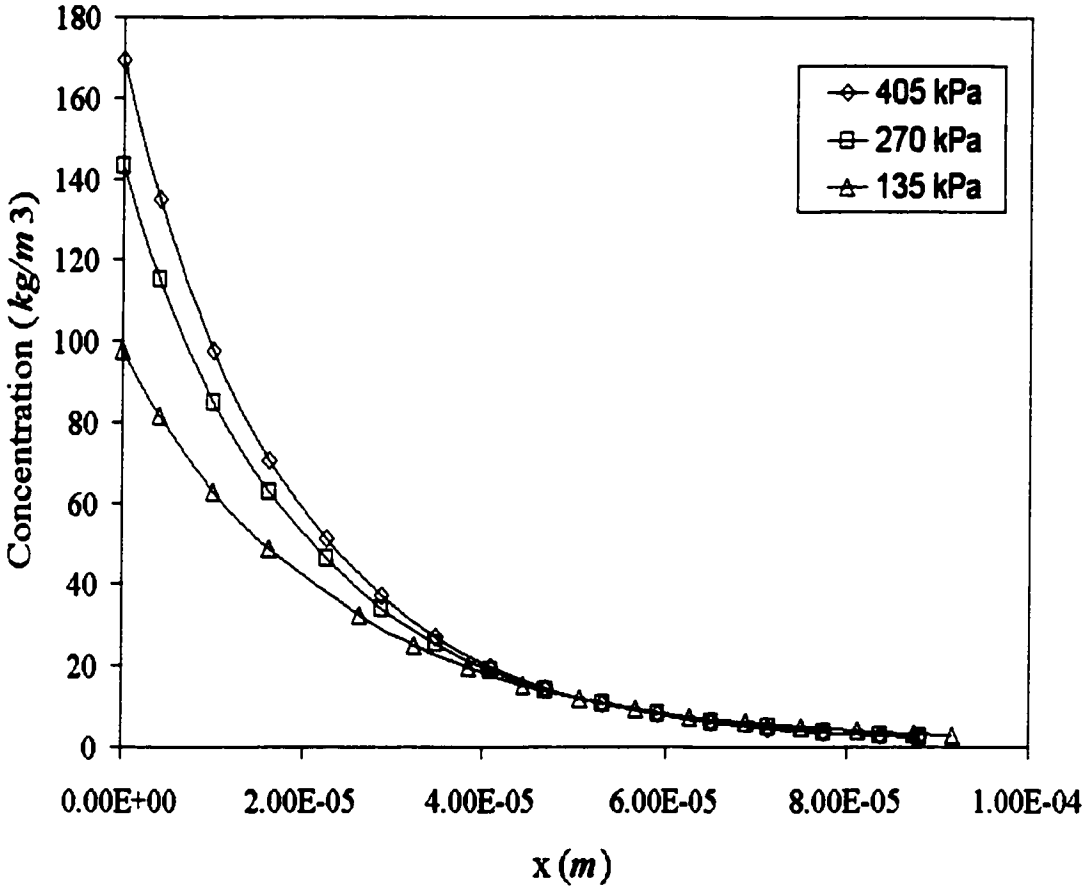

Figure 4.14(b) Variation of steady state concentration as a function of distance from the membrane surface for three different feed pressures for bulk dextran concentration of 1 kg/m^3

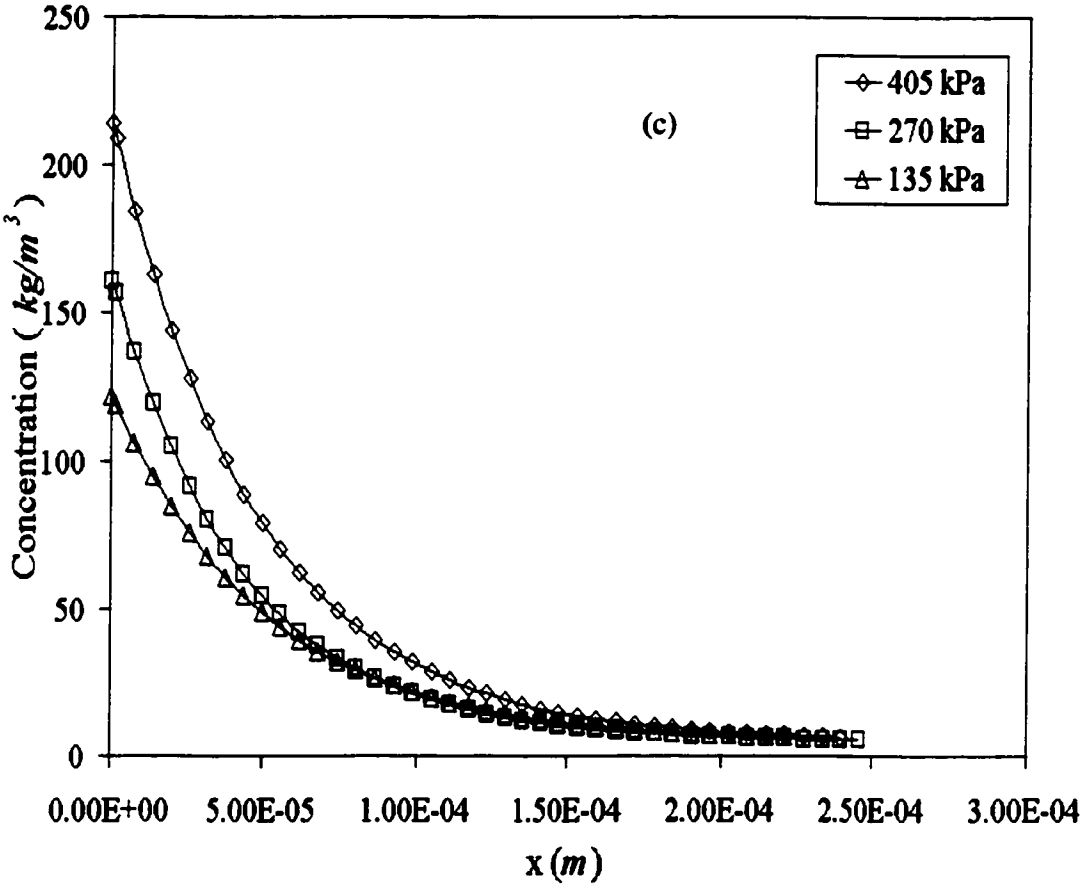

Figure 4.14(c) Variation of steady state concentration as a function of distance from the membrane surface for three different feed pressures for bulk dextran concentration of 5 kg/m^3

concentration; the polarization thickness is that value of x where boundary layer concentration is equal to bulk concentration (Section 4.1.5 PEG). Figure 4.16 and 4.17 show the variation of steady state membrane surface concentration and osmotic pressure exerted by the solute present in polarization layer as a function of bulk feed concentration and applied pressure. It is clear from these figures that at higher applied pressure and bulk feed concentration, the membrane surface concentration is higher. As the osmotic pressure is a function of concentration it also varies with bulk concentration accordingly.

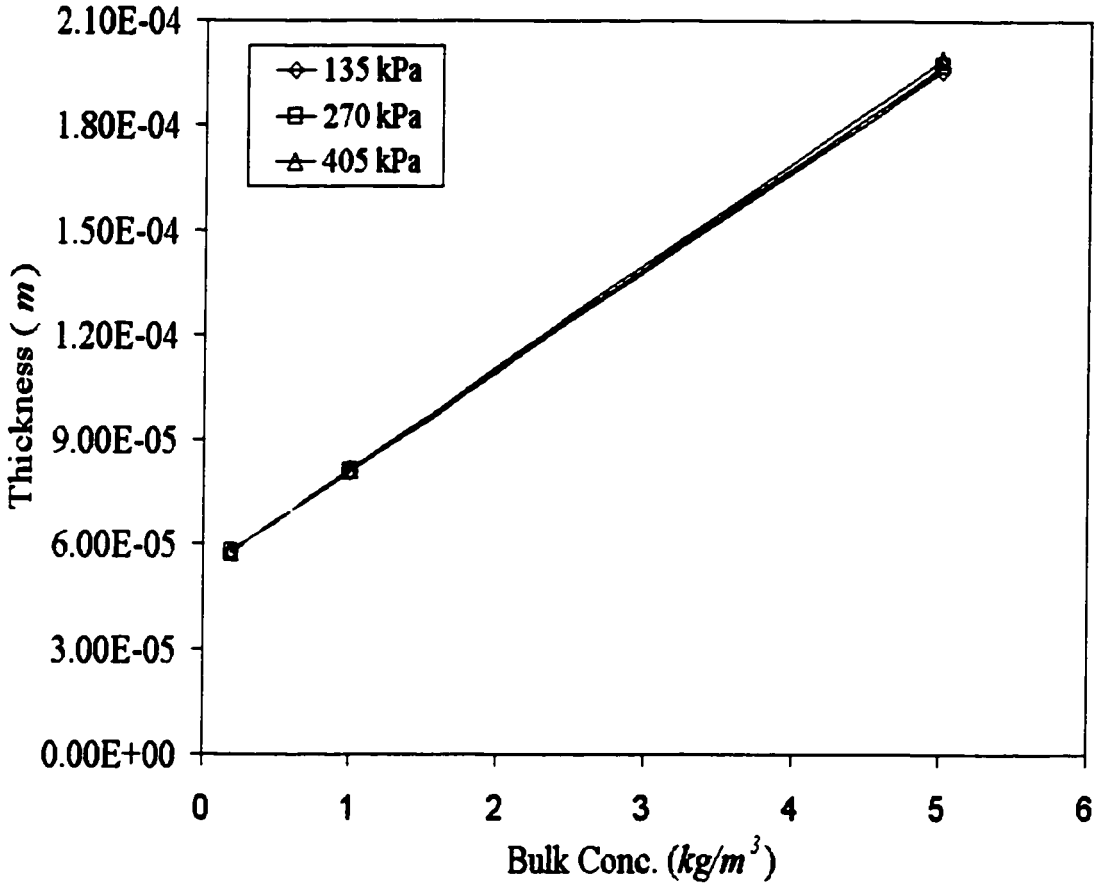

Figure 4.15 Boundary layer thickness as a function for bulk feed concentration of dextran for different applied pressures.

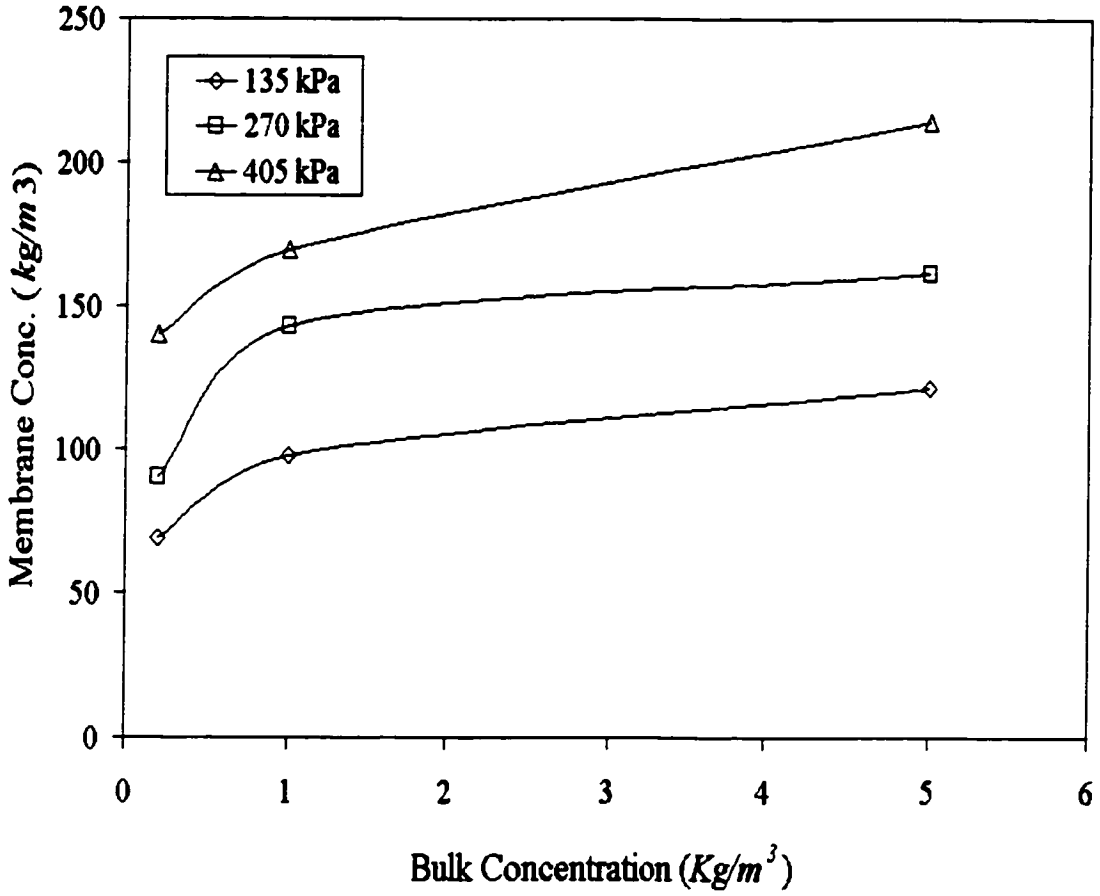

Figure 4.16 Concentration at membrane surface as a function of bulk feed concentration for dextran for different applied pressures

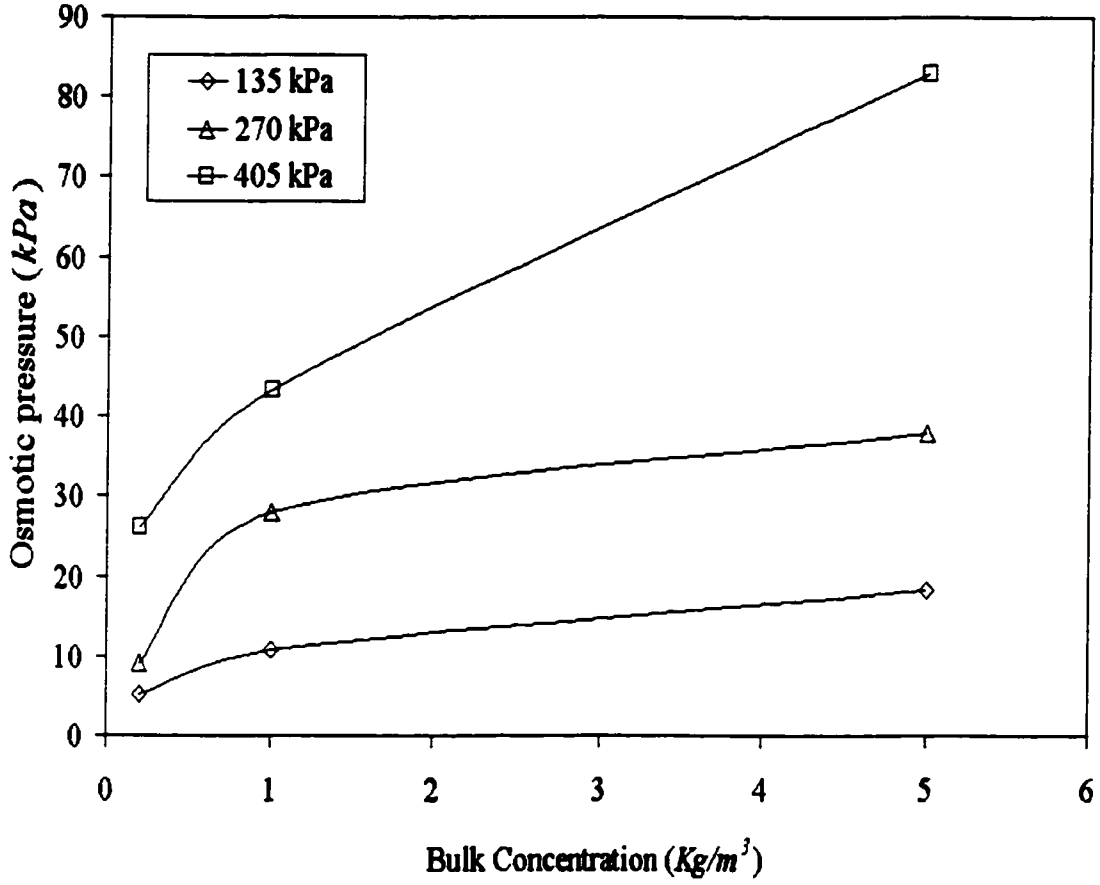

Figure 4.17 Osmotic pressure exerted by solute accumulated at membrane surface as a function of bulk feed concentration for dextran for different applied pressures

4.3. Ultrafiltration of Silica

4.3.1 Permeate flux during dead end ultrafiltration of silica and formation of gel

Experiments on ultrafiltration of silica suspensions involved measuring the flux as a function of time for three silica concentrations; these data are depicted for different applied pressures of 135, 270 and 405 *kPa* in Figures 4.18(a) and 4.18(b). It is clear from these figures that flux decreases rapidly until steady state is reached. This phenomenon can be explained by the formation of gel layer at membrane surface. The decrease in flux is the result of increase in gel layer thickness and increased resistance of deposited layer, more details will be discussed later in this section. The flux behavior in unstirred filtration of silica has been modelled using Darcy's law where solvent flux is directly proportional to the effective pressure difference and inversely proportional to the filtration resistance. The osmotic pressure of silica is considered to be negligible. A detailed description of various models has been given in Chapter 2 (Section 2.2 to 2.6). As can be seen from inserted figures in Figure 4.18(a) and 4.18(b) experiment, flux was time invariant in the beginning of the experiment and after few seconds a sudden drop in flux compared to pure water permeation (PWP) was observed. Subsequent to this observation flux decreased gradually. Duration for which flux was time invariant is called characteristic time. After this characteristic time, a 'gel layer' forms on the membrane surface and permeate flux decreases with time till a steady state is reached. This characteristic time of time invariant flux decreases as bulk feed concentration increases as shown in Figure 4.19. This sudden drop in the flux after this

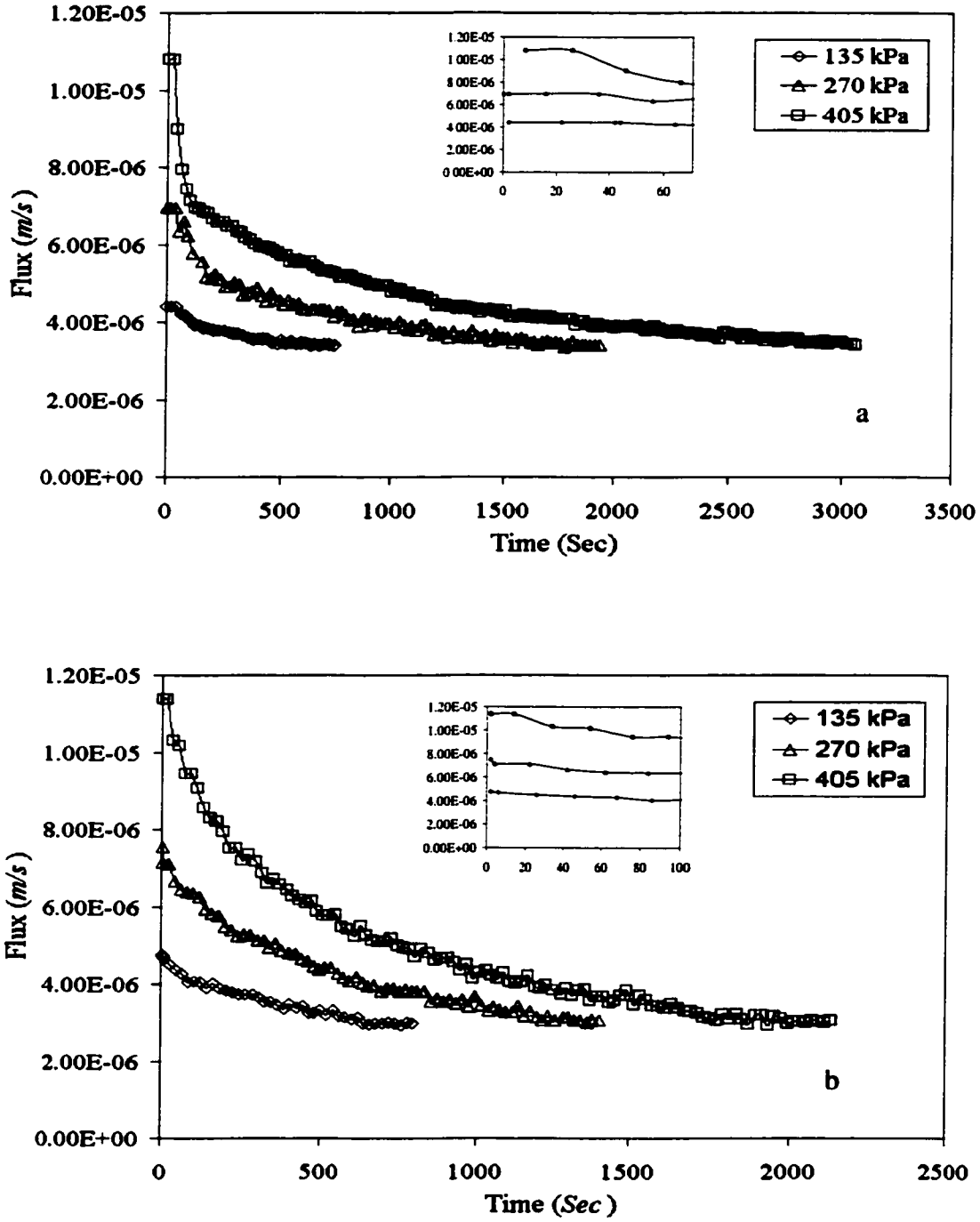

Figure 4.18 Variation of permeate flux as a function of time for various values of feed pressure. (a) 21 kg/m^3 (b) 28 kg/m^3

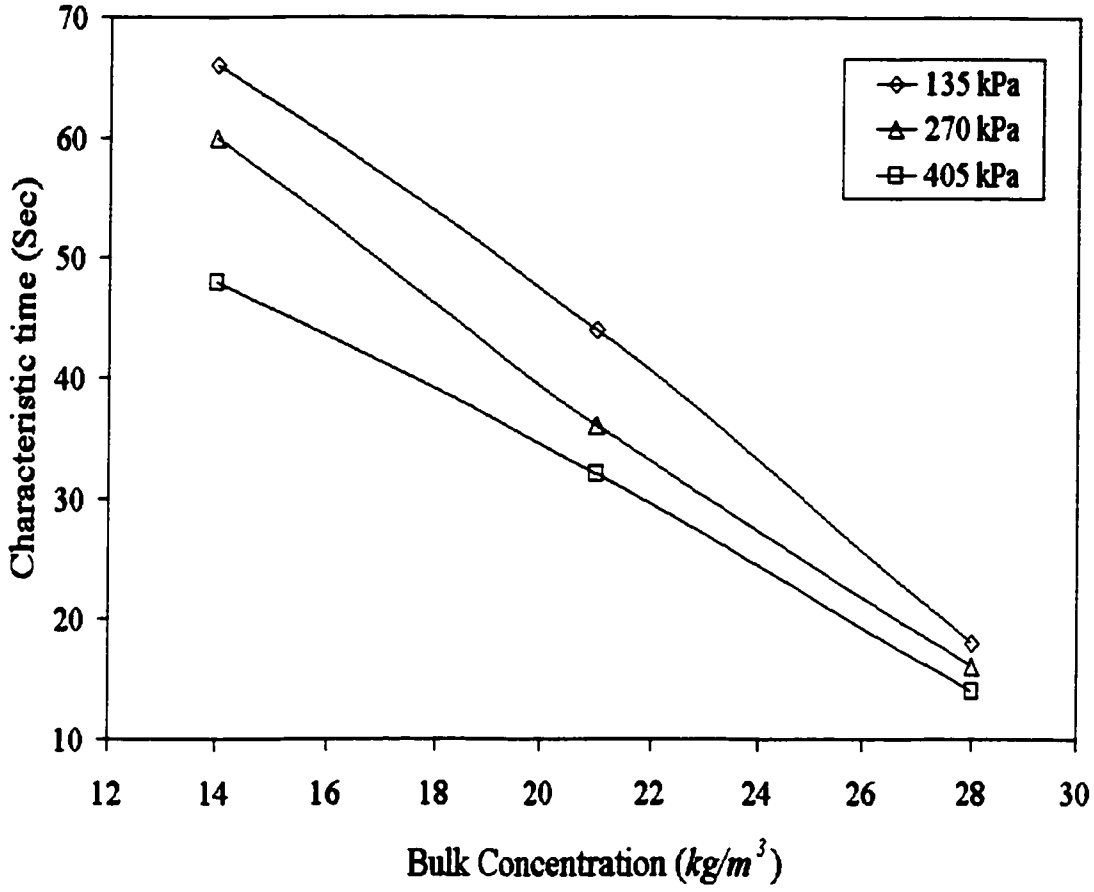

Figure 4.19 Variation of characteristic time as a function bulk feed concentration of silica

time invariant flux in the beginning of experiment is due to the build up of polarization layer at membrane surface that leads to increase of the concentration at membrane surface. This high concentration at membrane surface is due to the high rejection of silica almost 100% and considerably low rate of back transport due to low diffusion coefficient of silica in water. This also means that gel formation is rapid and almost instantaneous at the beginning of filtration particularly when the initial feed concentration is high. The steady state rejection of silica was also found to be almost 100%. This rejection was calculated based on turbidimetric analysis as described in Chapter 2. Turbidimeter allows us to measure the concentration of suspensions based on NTU (Nephelometric Turbidity Unit) an ISO-designated unit of turbidimetric measurement. Silica rejection data listed in Table 4.7 clearly shows that rejection is nearly 100%. Figure 4.18(a) and 4.18(b) show that the steady state values of flux are almost independent of applied pressure. This phenomenon is more clearly shown in Figure 4.21 where flux is plotted as a function of applied pressure for different bulk feed concentrations.

Table 4.7 Silica rejection for different bulk feed concentrations and applied pressures.

Pressure/ Feed Concentration.	14 kg/m^3	21 kg/m^3	28 kg/m^3
kPa	%Rejection	%Rejection	%Rejection
135	99.9	99.9	99.9
270	99.9	99.9	99.9
405	99.9	98.9	99.8

It is obvious that there is no osmotic pressure built up in case of silica therefore this pressure independent flux was only gel layer controlled. Effect of bulk concentration was also shown in Figure 4.20. It is well known that as bulk concentration of solution increases permeate flux decreases. Higher initial bulk concentration leads to more deposition of solute at membrane surface since membrane is fully retentive. Consequently, higher resistance would be offered by deposited solute that would lead to lowering of flux. Further, higher concentration might be offering higher polarized layer resistance, which is inversely proportional to flux. However, the trend of the curves in Figures 4.18(a) and 4.18(b) are identical as bulk concentration is increased at a fixed pressure. The polarization time, t_p, defined as time of flux decay necessary to reach 1.05 time the steady state flux, J_s, is compared for the various bulk solute concentrations and pressures used in Figure 4.21. Since unstirred filtration of silica takes long time the value of t_p ranged from about 450 to 2800 seconds for the conditions of our experiments. As can be seen from Figure 4.21 that polarization time increases with increase in applied pressure and decreases with increase in bulk solute concentration for the same applied pressure.

4.3.2 Specific resistance of silica gel.

Unstirred ultrafiltration data are plotted as $1/J^2$ versus t in Figure 4.22(a) and 4.22(b) for silica concentration of 21 and 28 kg/m^3 at different pressures. The slope of $1/J^2$ versus t plot was used to calculate the specific resistance, a, using Equation 2.17 described in Chapter 2. The values of slope and J were those obtained at the end of each experiment when almost steady state was reached. These 'a' values are listed in Table 4.8 and are

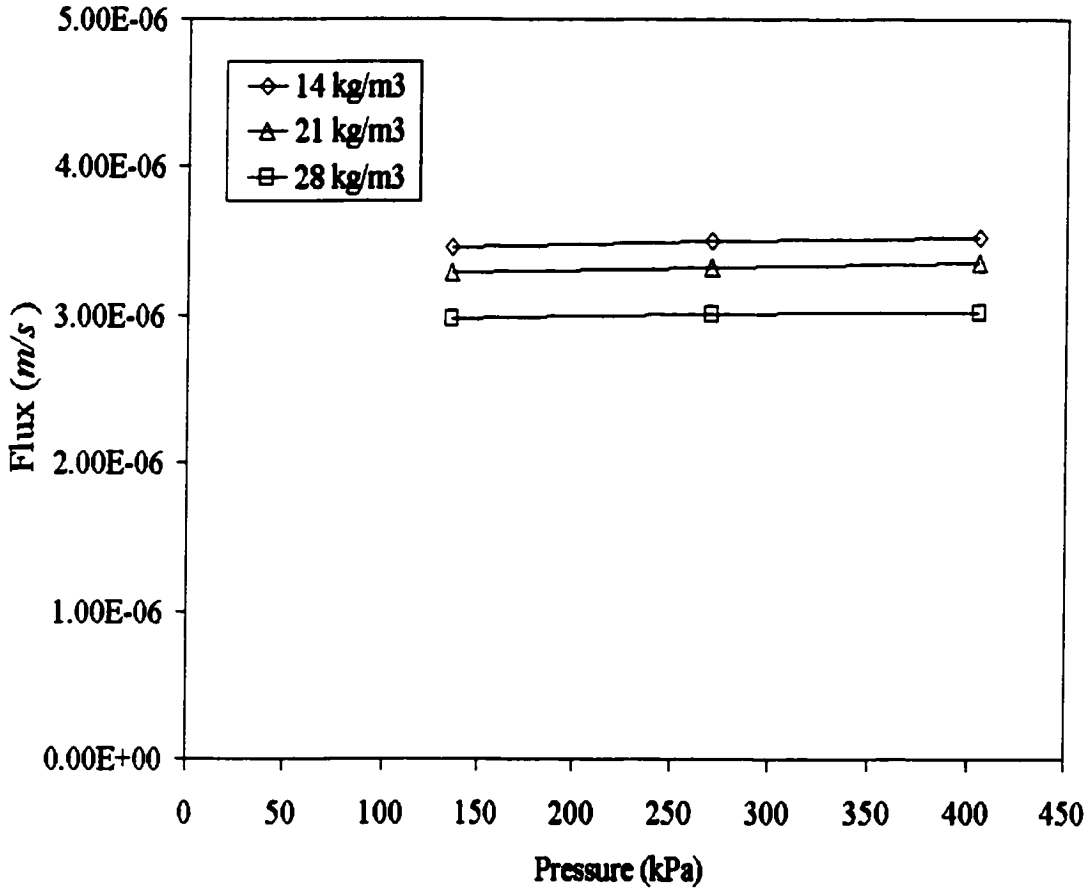

Figure 4.20 Steady state permeate flux of silica as a function feed pressure for different feed concentrations

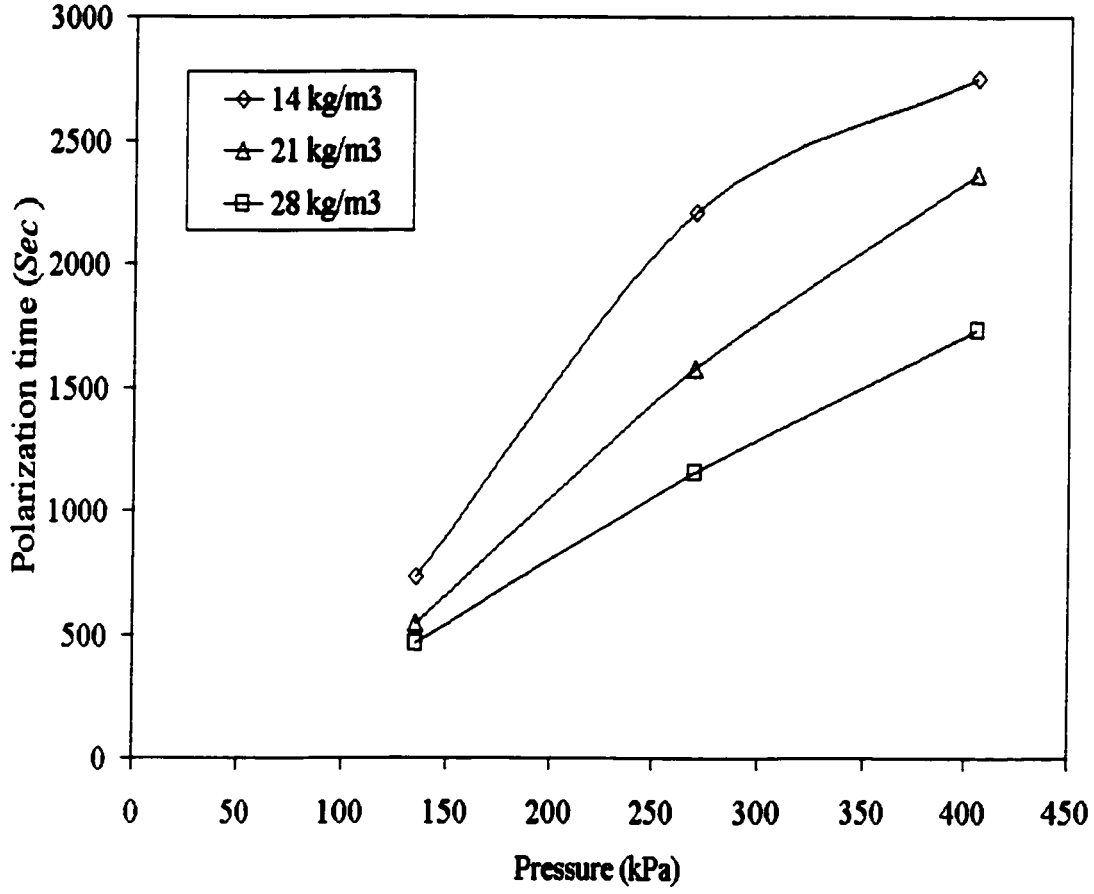

Figure 4.21 Polarization time as a function of applied pressure for different bulk feed concentrations of silica.

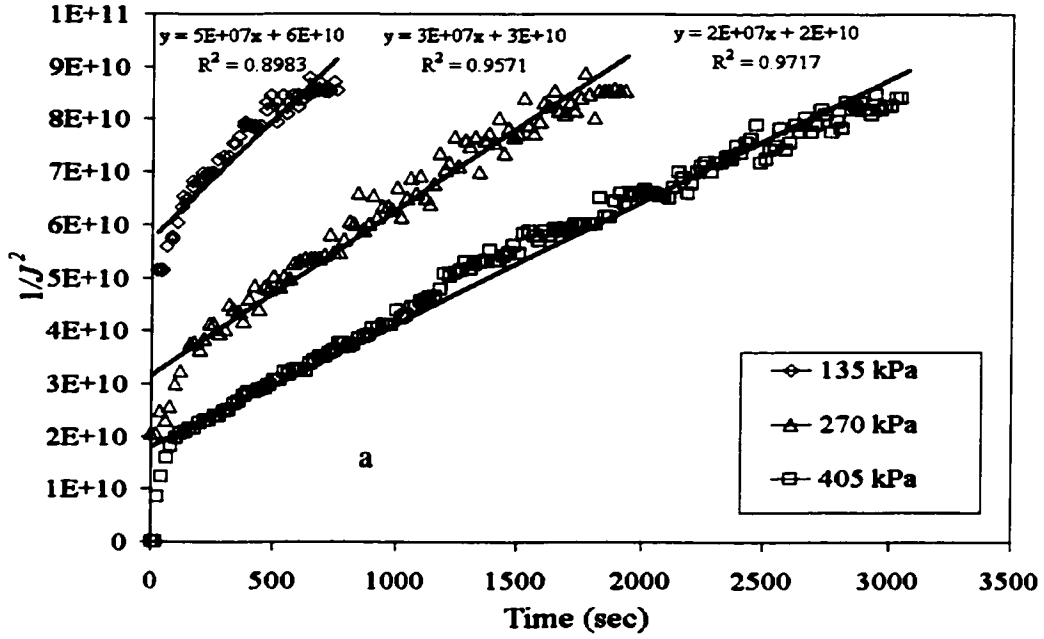

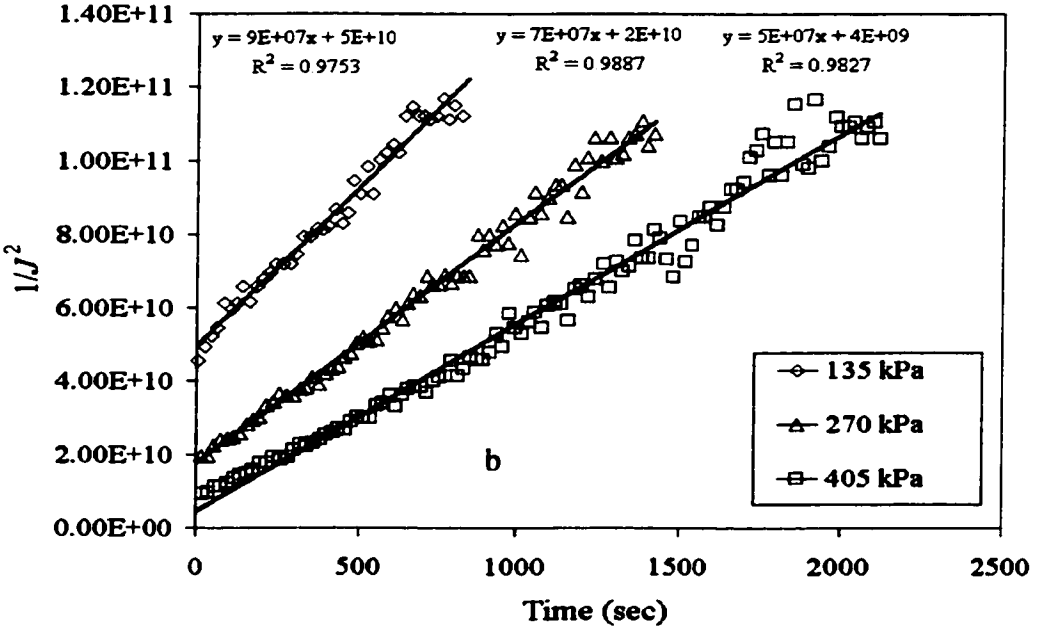

Figure 4.22 Typical inverse flux ($1/J^2$) versus time plot for silica in unstirred UF. (a) 21 kg/m^3 (b) 28 kg/m^3

Table 4.8 Specific resistance's at different silica concentrations.

Pressure/ Feed Concentration.	14 kg/m^3	21 kg/m^3	28 kg/m^3
KPa	*m/kg*	*m/kg*	*m/kg*
135	1.08 E 14	1.47 E14	2.1 E14
270	1.22 E 14	1.65 E14	2.65 E14
405	1.32 E 14	1.76 E14	2.98 E14

Figure 4.23 shows the plot of specific resistance versus applied pressure for different concentrations. Our results support the previously reported data by Stakic (1989) Vladisavljevic et al. (1992); Chudacek and Fane (1984) by showing that specific resistance of silica gel depends on bulk solution physiochemical properties and operating conditions. The specific resistance of this gel was found to be dependent on applied feed pressure as well as bulk feed concentration. In more general terms, any parameter that increases the incipient convective flux of particles towards the membrane will increase specific resistance. The pressure dependence of '*a*' particularly in the beginning of the experiment could account for non-linearity in $1/J^2$ versus t plot (e.g. Figure 4.22a).

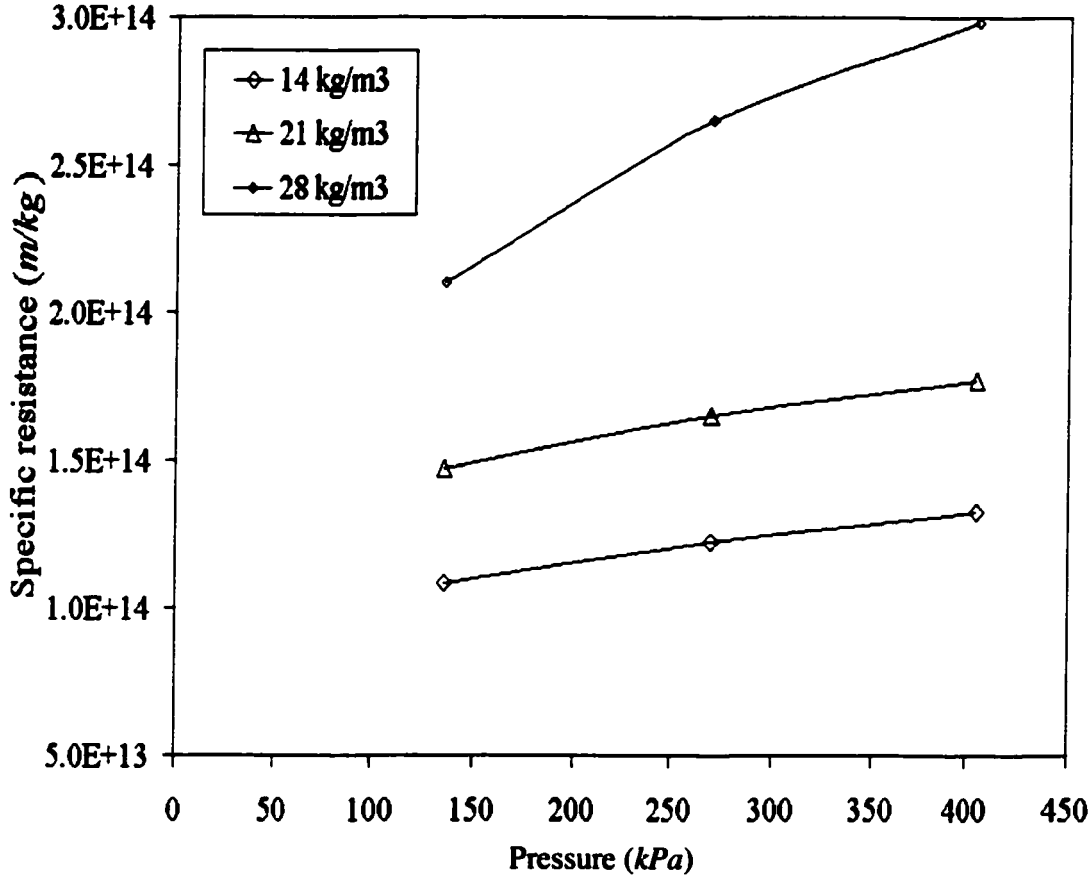

Figure 4.23 Specific resistance as a function of applied pressure for various silica concentrations.

4.3.3 Effect of different operating condition on deposit thickness

A linear relation between increase of deposited layer thickness and filtered volume in unstirred silica filtration was observed. Effect of concentration on deposited thickness at fixed pressure can be seen in Figure 4.24 where deposited thickness of layer was found to be a function of bulk feed concentration. Also it can be noted that for same deposited thickness the volume filtered is more for lower bulk feed concentration. Deposited thickness as a function of time was plotted in Figures 4.25(a) to 4.25(c) for different bulk feed concentration and applied pressures. This aspect becomes even more apparent when filtration time is increased. It was also found that at same applied pressure the growth of deposit thickness was more for higher concentration solution. Steady state permeate flux values corresponding to the deposit thickness for different concentrations at same applied pressure are listed in Table 4.9. The steady state flux decreases while deposit thickness increases with significantly with increase in concentration. Figure 4.26 shows that for same deposit thickness permeate flux is greater with higher concentrations.

Table 4.9 Steady state permeate flux and deposit thickness for various feed concentrations of silica

Feed Pressure (kPa)	Feed Concentration, (kg/m^3)	Permeate Flux (m/s)	Deposit Thickness (m)
135	14	3.46×10^{-6}	3.42×10^{-5}
	21	3.29×10^{-6}	3.86×10^{-5}
	28	2.97×10^{-6}	5.13×10^{-5}
270	14	3.50×10^{-6}	1.15×10^{-4}
	21	3.32×10^{-6}	1.28×10^{-4}
	28	3.01×10^{-6}	1.31×10^{-4}
405	14	3.52×10^{-6}	2.08×10^{-4}
	21	3.36×10^{-6}	2.21×10^{-4}
	28	3.02×10^{-6}	2.37×10^{-4}

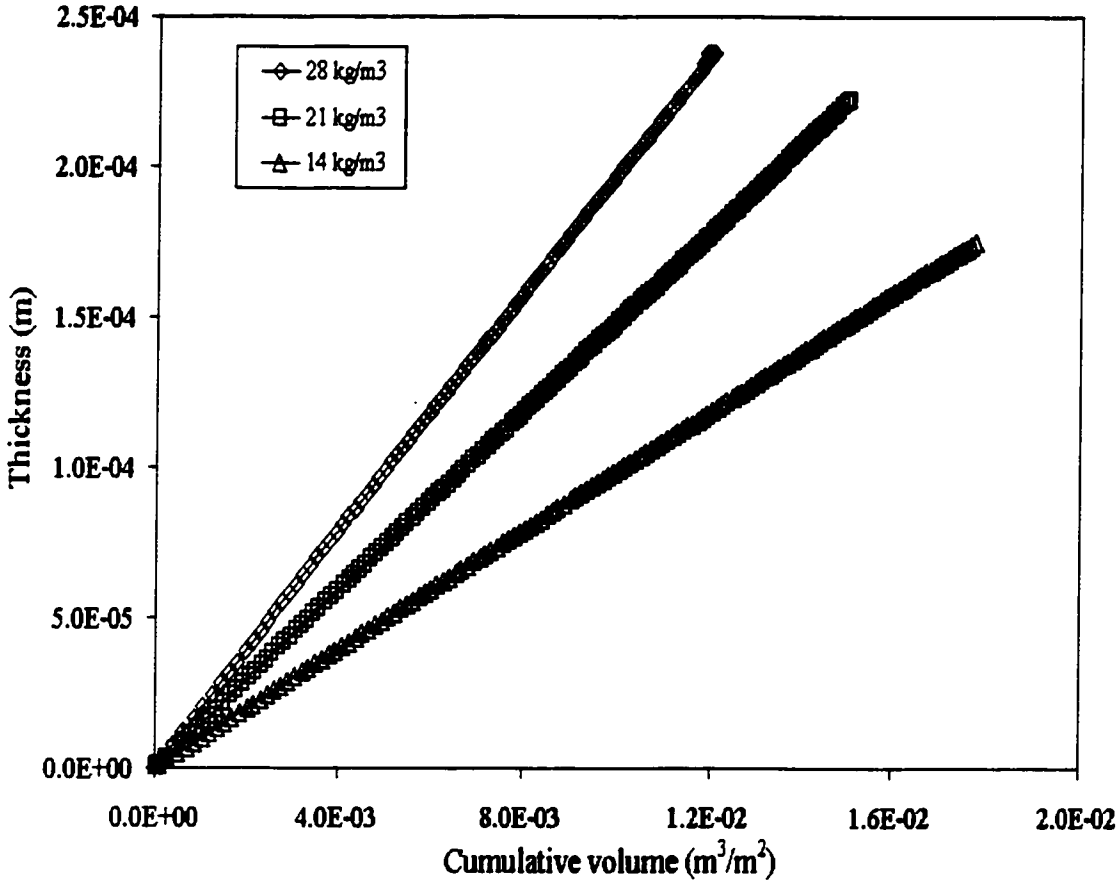

Figure 4.24 Effect of concentration on deposit build-up as a function of cumulative volume at constant pressure of 405 *kPa*

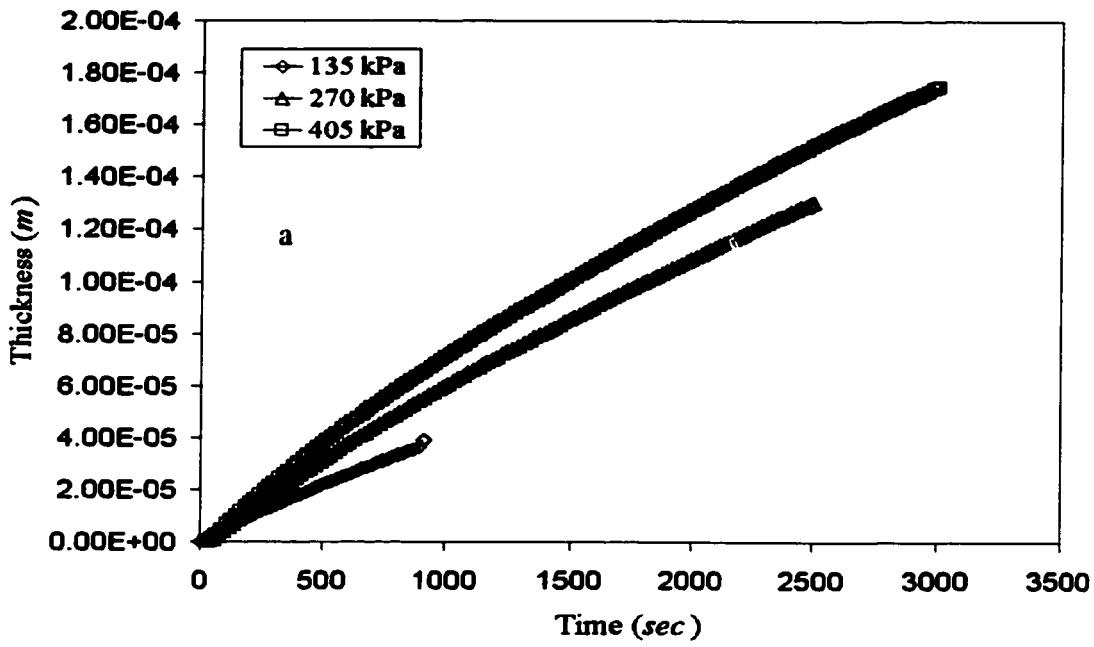

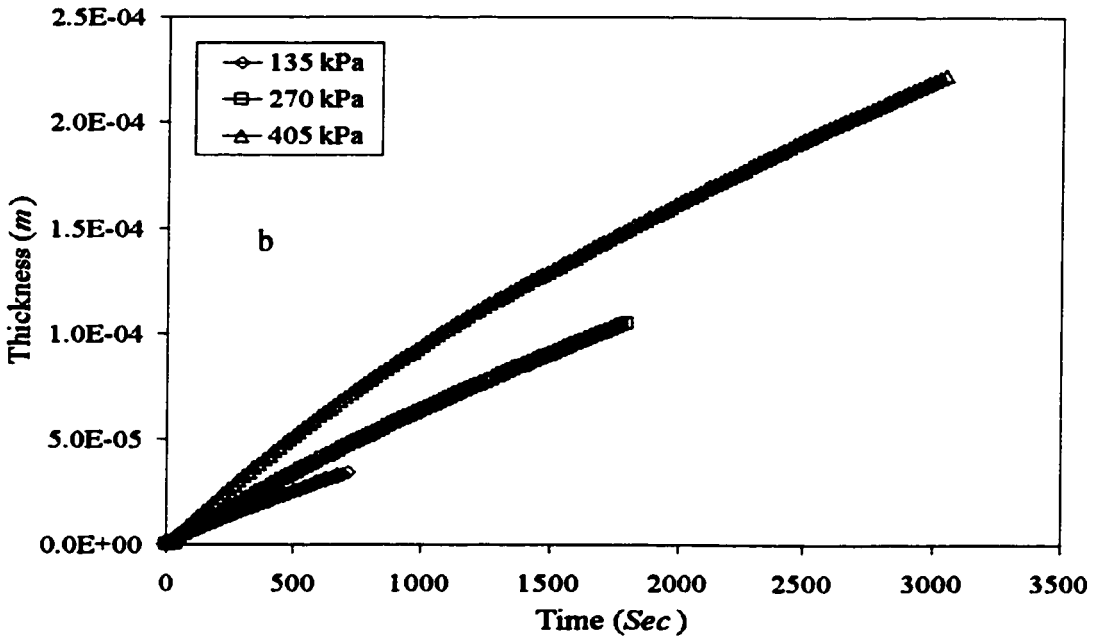

Figure 4.25 Deposited thickness as a function for different bulk feed concentration and applied pressures (a) 14 kg/m^3 (b) 21 kg/m^3

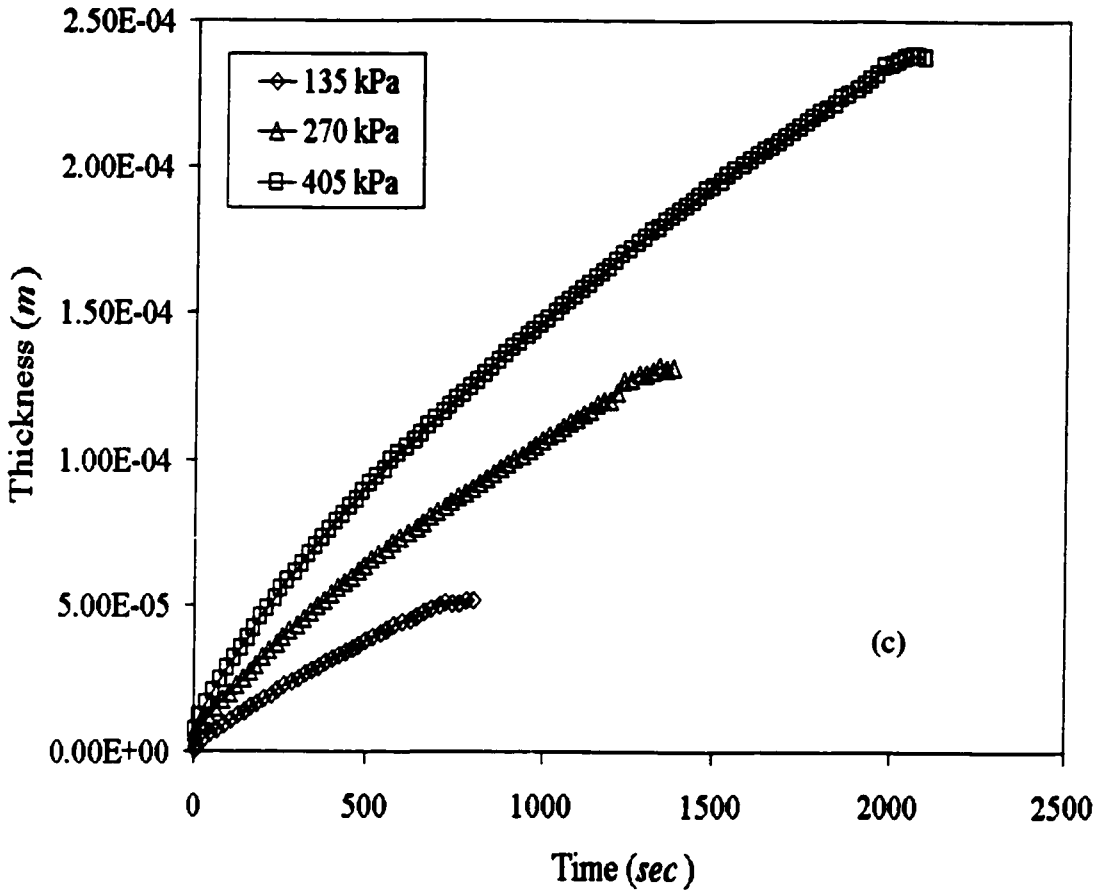

Figure 4.25(Contd.) Deposited thickness as a function for different bulk feed concentration and applied pressures (c) 28 kg/m^3

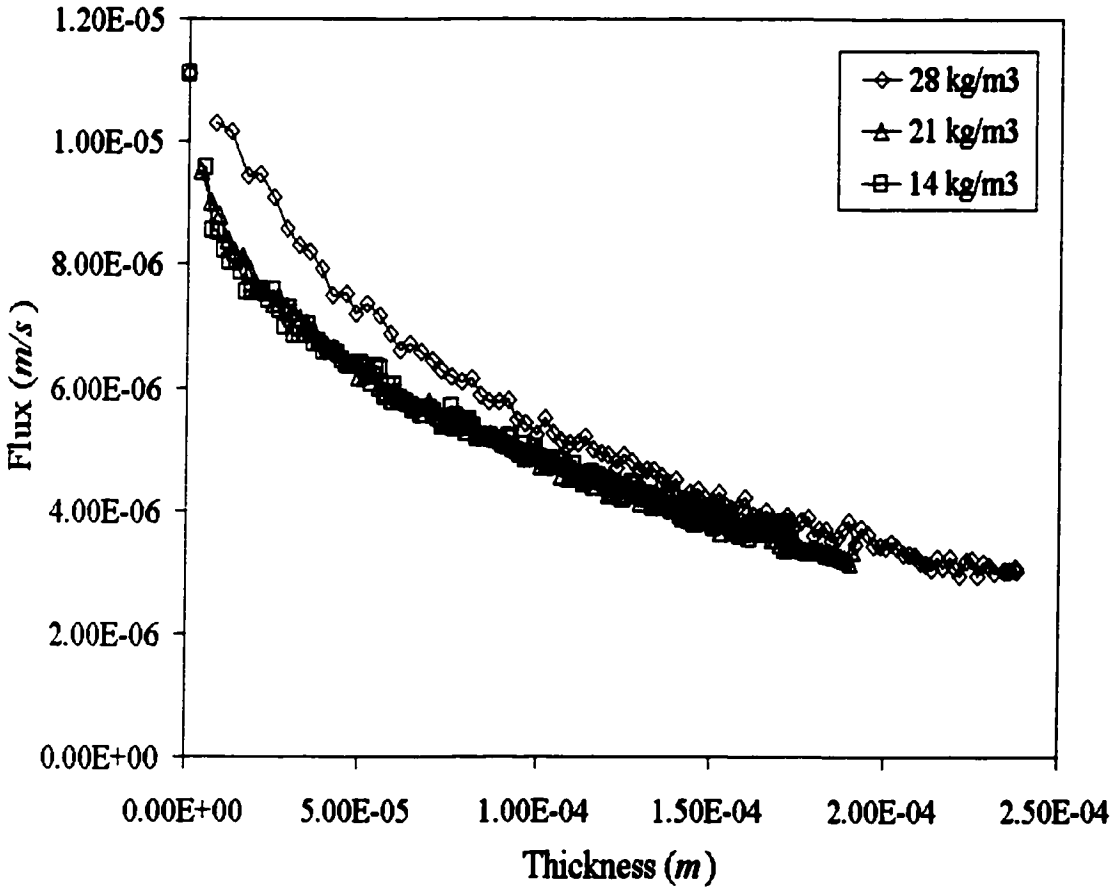

Figure 4.26 Permeate flux as a function of deposit thickness for various concentrations and identical pressure of 405 *kPa*

This may be due to the fact that suspensions at lower concentration contain fewer large particles and thus deposited layer may be less permeable. Once the gel was formed and flux reached to its steady state value, the deposit thickness at that steady state flux was found to be a function of applied pressure and concentration as shown in Figure 4.27.

4.3.4 Filtration resistance during filtration.

Knowledge of steady state flux and other experimental parameters allows the calculation of the total filtration resistance ($R_m + R_g$) for deposited layers of different thicknesses. Following Darcy's law as described in Equation (2.1) total filtration resistance is the sum of membrane resistance (R_m) and that of deposits (R_g) and can be calculated from steady state data. The total filtration resistance gradually increases, and reaches maximum value at the end of filtration for all unstirred filtration of silica suspension. Total filtration resistance was determined at the end of experiment. Figure 4.28 shows the variation of deposit resistance as a function of deposit thickness at various concentrations and applied pressures. The filtration resistance was found to be directly proportional to deposit thickness. Figure 4.29 shows the variation of filtration resistance with applied pressure and concentrations. It is clear from this figure that for a given feed concentration filtration resistance grows more significantly with pressure and similarly for a given pressure it varies directly with feed concentration. The increase of filtration resistance with increase in pressure at same concentration is due to increase of rate of gel formation. The increase of filtration resistance, influenced by the increase of silica concentration at constant pressure, is the result of the increase of gel mass and of its specific resistance.

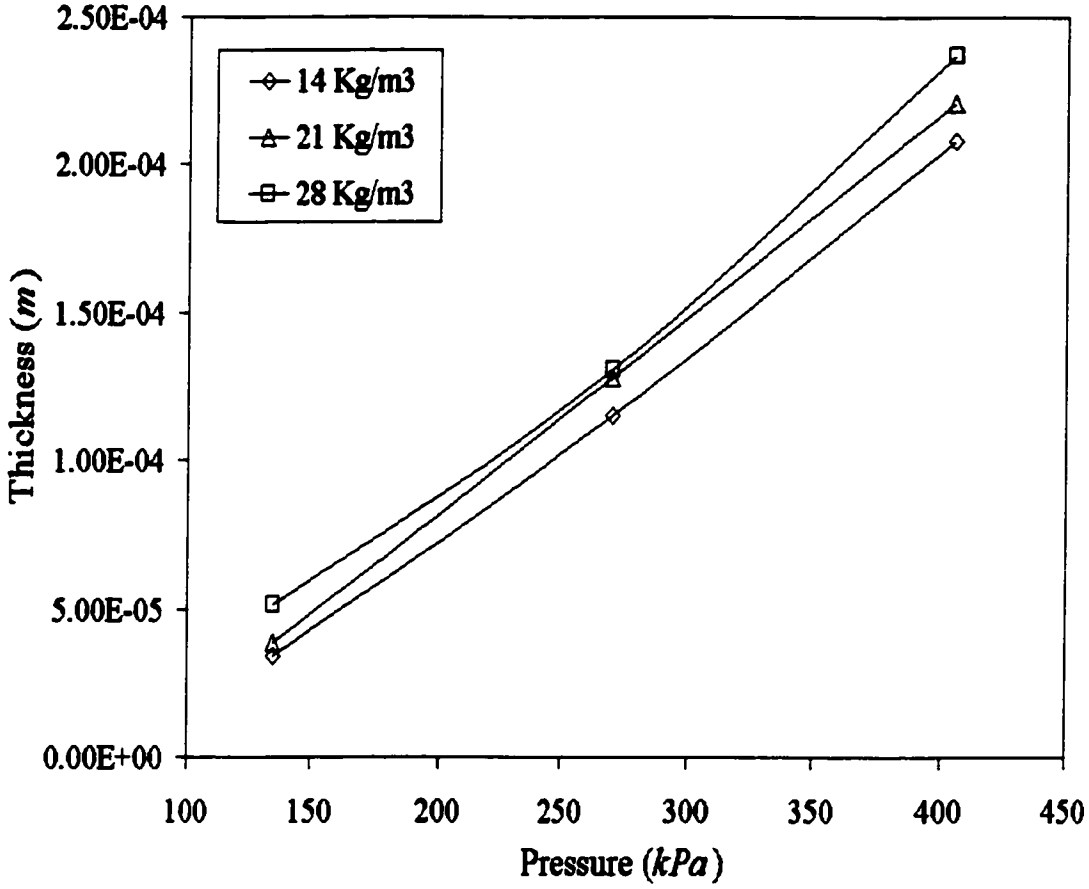

Figure 4.27 Deposit thickness as a function of applied pressure for various concentrations

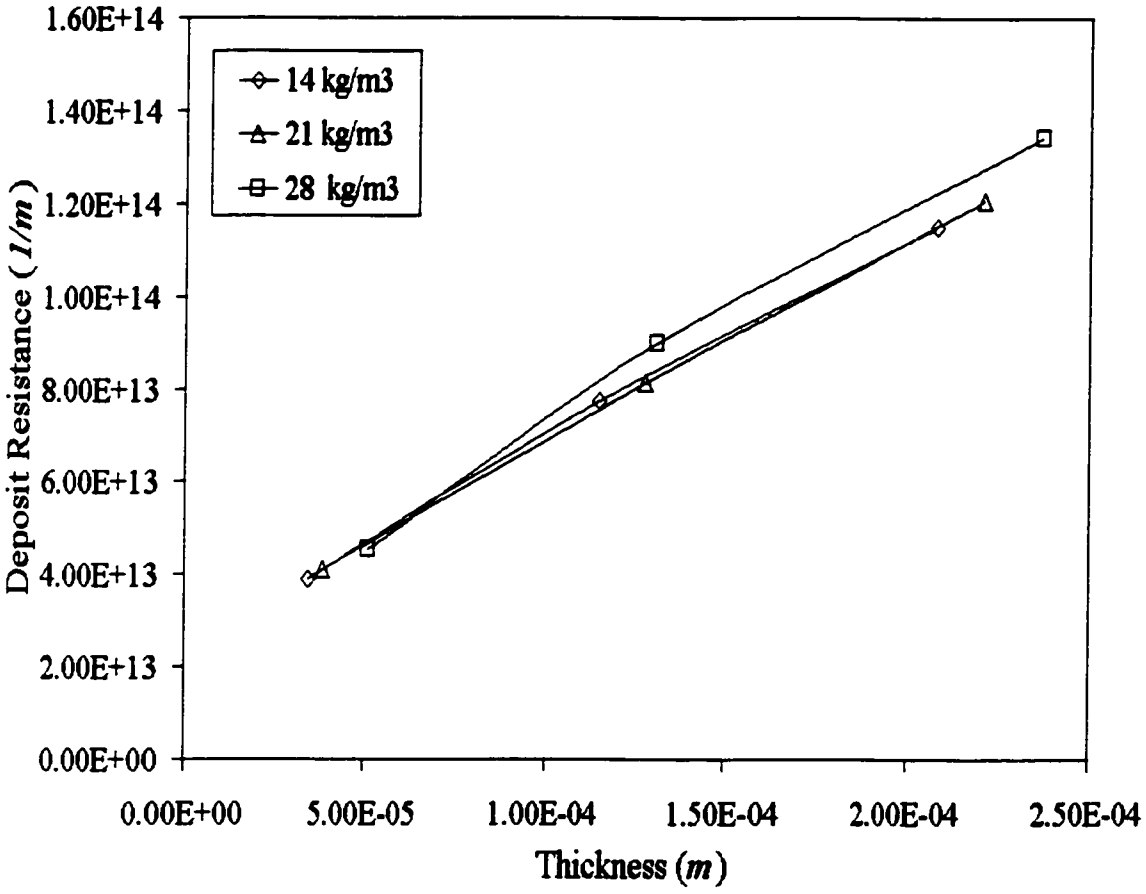

Figure 4.28 Deposit resistance as a function of deposit thickness for various concentrations

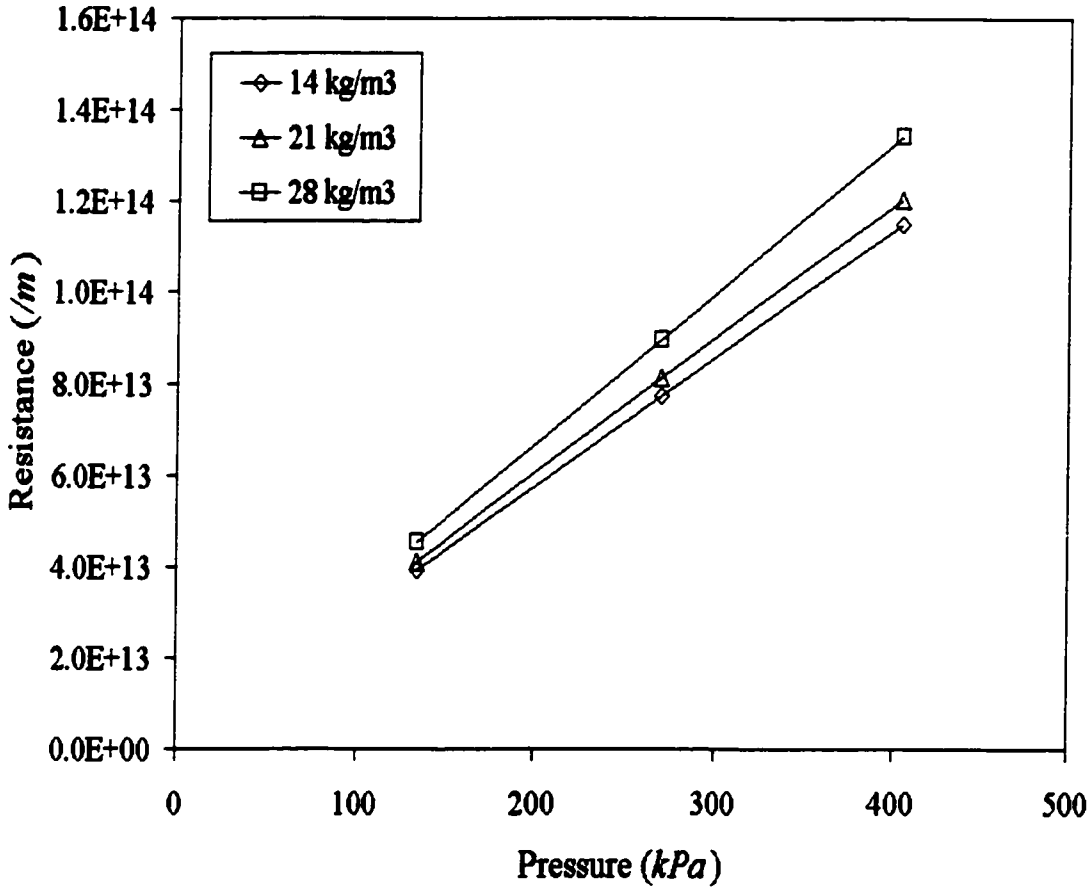

Figure 4.29 Deposit Resistance as a function of applied pressure for various concentrations of silica

It has been reported in literature that increase of resistance observed is mainly due to the compressibility of deposited layer (Hamachi and Peuchot, 1999).

4.3.5 Deposit porosity

One can use, Equation (2.15) described in Chapter 2 to determine the porosity of the deposit, provided average particle size, particle density and the calculated value of specific resistance are known. The porosity of the deposited gel as shown in Figure 4.30 was found to be decreasing with increase in bulk concentration of suspensions for identical pressure. Hamachi and Peuchot (1999) reported that generally porosity of bentonite tends to increase with increase in deposited thickness in case of cross flow filtration. However, in our study of dead end filtration of silica suspension it was observed that the porosity of deposited layer invariably decreased with increased in thickness of this layer. One possible explanation of this observation could be that in our study the deposition of particle is not selective. Further for identical bulk feed concentration of suspension, Figure. 4.30 also show a decrease in porosity as transmembrane pressure increases. This could be due to the compression of deposited layer as reporter earlier (Hamachi and Peuchot, 1999)

4.3.6 Gel concentration

The concentration of silica was calculated based on porosity, following the equation reported by van Oers (1992) and Karode (2000).

$$\varepsilon_g = 1 - \frac{C_g}{\rho} \tag{6.2}$$

Where ε_g is porosity of gel, ρ is solute density.

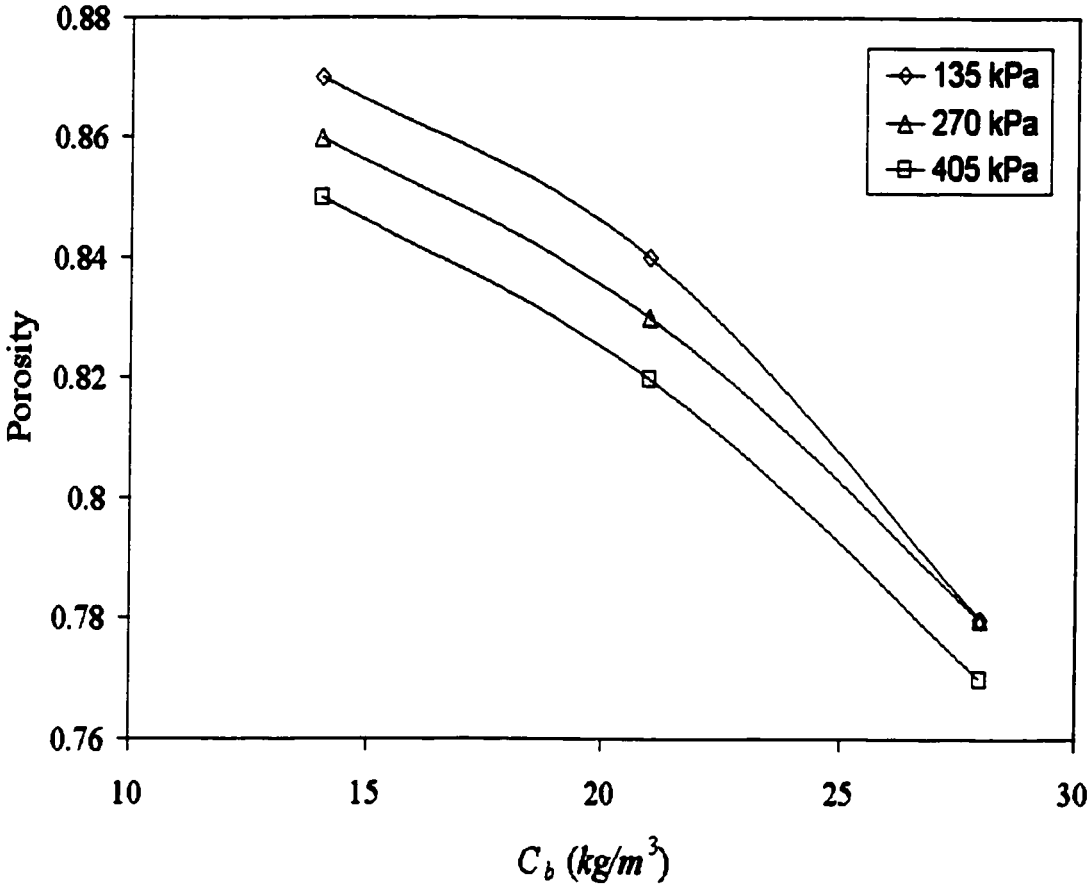

Figure 4.30 Deposit porosity variation as a function of bulk feed concentrations of silica.

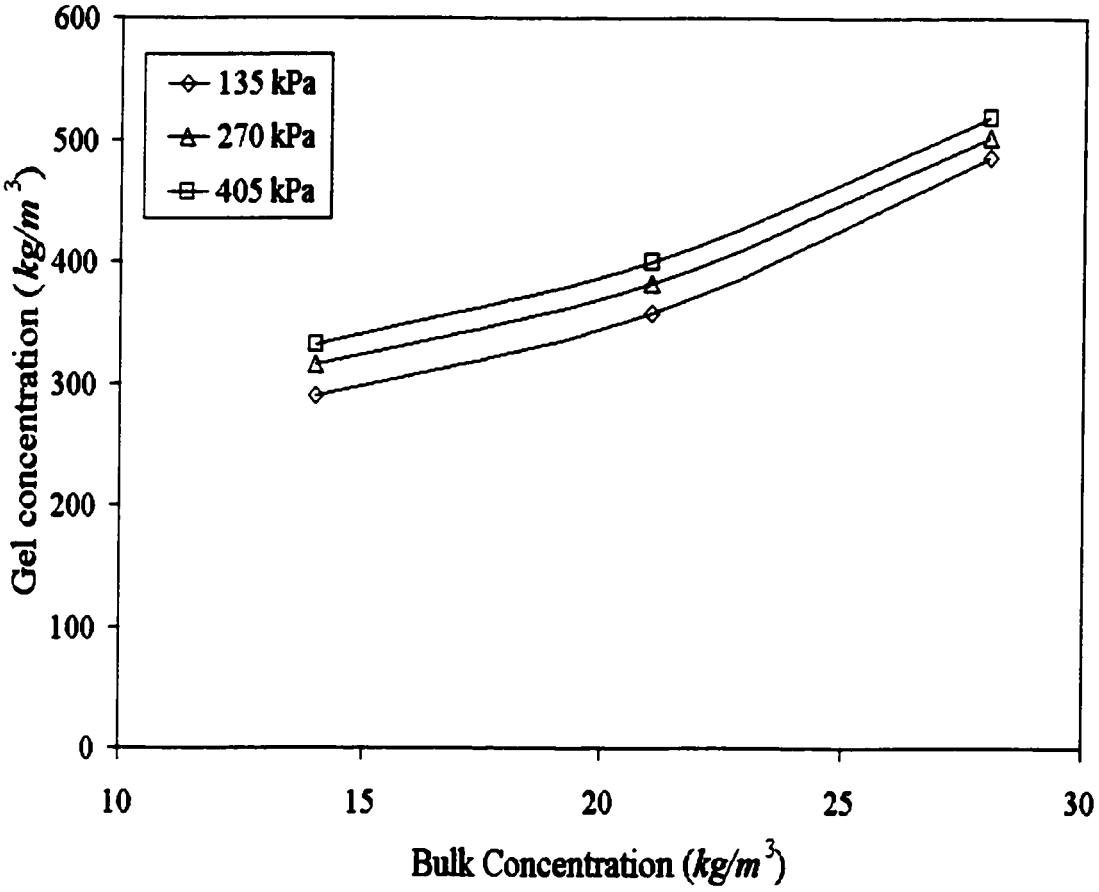

Figure 4.31 Gel concentration as a function of bulk feed concentration.

In case of unstirred filtration, the silica gel concentration increases with increase in feed concentration and trans-membrane pressure as shown in Figure 4.31. This also implies that greater the thickness, lesser the porosity and higher the gel concentration. The actual concentration of deposit was also determined at the end of experiment.

The membrane with silica deposited over it was removed from the membrane cell and was weighed before and after drying. It was found that the experimental concentration differed by only 10-12% with the calculated one. These experimental and estimated gel concentrations at feed pressure of 405 kPa are listed in Table 4.9.

Table 4.9 Estimated and experimental gel concentration for various bulk feed concentrations of silica

Feed Pressure (kPa)	Feed Concentration C_o (kg/m^3)	Estimated Gel Concentration, C_g (kg/m^3)	Experimental Gel Concentration, C_g (kg/m^3)
405	14	331	299
405	21	400	353
405	28	518	460

CHAPTER 5

5. Conclusions and Recommendations

5.1 Conclusions

- Experimental set-up reported in this work could be used satisfactorily for recording steady state as well as post steady state transient filtration data.
- Post steady state filtration regimes such as gel layer or osmotic pressure were clearly identified using the analysis reported in this work.
- The experimental work verified the existence of theoretically predicted negative flux under certain conditions i.e. when applied pressure is less than the osmotic pressure of solute.
- Using the method proposed in this work, it was possible to estimate the filtration resistance offered by the polarization layer in ultrafiltration of macromolecular solutions.
- It was further demonstrated that the thickness of the polarization layer in ultrafiltration of macromolecular solutions could be significantly large. It was also concluded that the thickness of the polarization layer is a function of the bulk solute concentration and a higher bulk concentration led to thicker polarization layer.

- Ultrafiltration of dextran exhibits gradual flux decline with time followed by reversible steady state flux for a sudden increase followed by a decrease to an initial value of trans-membrane pressure.
- A fundamental analysis of deposited gel layer could be applied to the solute, which only forms a gel layer (Silica). Initially, there was a critical or characteristic time for which permeate flux was time invariant, during which time the concentration at the membrane surface increased that led to gel formation. The steady state rejection was found to be 100%. It was concluded that the steady state permeate flux was independent of the change in applied pressure.
- It appeared that the evolution of deposit thickness is a function of cumulative volume. It was shown that deposit is directly linked to convective flux while back diffusion was almost negligible. Kozeny-Carman equation could be used to determine the silica gel porosity for subsequent calculation of concentration of silica deposits.
- The calculated average concentration for gel formation was found within 10-12% of the experimentally determined concentration.

5.2 Recommendations

1. Present study reports post steady state filtration for a concentration range of 0.2-5 kg/m^3 solutes in water where gel layer and osmotic controlled regimes could be identified. Further investigation should include studies using other macromolecules as well as feeds with higher than 5 kg/m^3 solute concentrations for investigating a wider concentration range.
2. The concept of gel layer formation and osmotic pressure controlled filtration should be explored in blends of water and solvents.
3. In order to verify general applicability of the analysis developed in this work, additional studies in ultrafiltration of suspensions such as bentonite, alumina, titania and zirconia should be undertaken.

CHAPTER 6

6. References

Balmann, H. de. and R. Nobrega, " The deformation of dextran molecules: causes and consequences in ultrafiltration", J. Membr. Sci., 40, 311(1989)

Bhattaacharjee, C. and P.K. Bhattacharya, " Prediction of limiting flux in ultrafiltration of kraft liquor", J. Membr. Sci., 72, 137 (1992)

Bhattaacharjee, S. and P.K. Bhattacharya, " Flux decline behaviour with low molecular weight solutes during ultrafiltration in an unstirred batch cell", J. Membr. Sci., 72, 149(1992)

Bhattacharjee, S., A. Sharma and P.K. Bhattacharya, "A unified model for flux prediction during batch cell Ultrafiltration" J. Membr. Sci., 111, 243(1996)

Bhattacharjee, C. and S. Datta, "A numerical simulation for the prediction of flux and rejection during ultrafiltration in unstirred batch cell using variable diffusivity concept", Sep Purif. Tech., 24, 13(2001)

Blatt, W.F., A. Dravid, A.S. Michaels and L.M. Nelson, " Solute polarization and cake formation in membrane ultrafiltration: causes, consequences and control techniques", in Memb. Sci. and Tech., ed. J.E. Flinn, Plenum Press, NY, 74(1970)

Bowen, W. R. and Frank Jenner, " Theoretical descriptions of membrane filtration of colloids and fine particles: an assessment and review", Adv. In Coll. and interface Sci., 56, 141(1995)

Cheryan, M., " Ultrafiltration Handbook", Technomic Publishing Company, Inc., Lancaster, (1986)

Choe, T.B., P. Masse, A. Verdier and M.J. Clifton,"Flux Decline in Batch Ultrafiltration: Concentration Polarization and cake Formation", J. Membr. Sci., 26, 1(1986)

Chudacek, M.W. and A.G. Fane, " The dynamics of polarization in unstirred and stirred ultrafiltration", J. Membr. Sci. 21, 145(1984).

Clifton, M.J., N. Abidine, P. Aptel and V. Sanchez, " Growth of the polarization layer in ultrafiltration with hollow fibre membranes", J. Membr. Sci. 21, 233(1984).

Dal-Cin, M. M., C. M. Tam and M.D. Guiver, "Polysulfone Membranes V. Polyphenylsulfone (Radel R)-Polyvinylpyrrolidone Membranes" J. Appl. Polym. Sci., 54, 783(1994)

Doshi, M. R. and Daniel R. Trettin, " Ultrafiltration of colloidal suspensions and macromolecular solutions in an unstirred batch cell", Ind. Eng. Chem. Fundam., 20, 221(1981)

Elimelech, M. and S. Bhattacharjee "A Novel Approach for Modeling Concentration Polarization in Cross Flow Membrane Filtration Based on the Equivalence of Osmotic Pressure Model and Filtration theory" J. Membr. Sci., 145, 223(1998)

Fane, A.G., C.J.D. Fell and A.G. Waters, " The relationship between membrane surface pore characteristics and flux for ultrafiltration membranes", J. Membr. Sci., 9, 245(1981)

Fane, A.G., C.J.D. Fell and A.G. Waters, " Ultrafiltration of protein solutions through permeable membranes. The effect of adsorption and solution enviroment", J. Membr. Sci., 16, 211(1983a)

Fane, A.G., " Factors affecting flux and rejection in ultrafiltration", J. Sep. Proc. Technol., 4, 15(1983b)

Fane, A.G. " Ultrafiltration of suspensions", J. Membr. Sci., 20, 249(1984)

Franken, A.C.M. and Fane A.G. Fane, " Environmental management using membranes" in CHEMECA. 90, Australasian Chemical Engineering Conference, Univ. of Aukland School of engineering,Aukland, NZ, 754(1990)

Gekas, V. and B. Hallstrom, " Mass transfer in the concentration polarization under turbulant crossflow. I. Critical literature review and adaptation of existing sherwood correlation to membrane operations", J. Membr. Sci., 30, 153(1987)

Glater, J., " The early history of reverse osmosis membrane development", Desalination, 117, 297(1998)

Kesting, R.E. and A.K. Fritzche, " Polymeric gas separation membranes", John Wiley & Sons, Inc., New York, NY, 1993

Goldsmith, R.L., "Macromolecular Ultrafiltration with Microporous Membrane" Ind. Eng. Chem., Fundam., 10, 13(1971)

Granath, K.A. and B.E. Kvist, " Molecular weight distribution analysis by gel chromatograhy on sephadex", J. Chromatogr., 28, 69(1967)

Hamachi and M., M. Mietton-Peuchot, " Experimental investigations of cake characteristics in cross flow microfiltration", Chem. Eng. Sci., 54, 4023(1999)

Henry, J.D., Jr., " Crossflow filtration", In: N.N. Li (Ed.), Recent development in separation science, Vol. 2, CRC Press, Cleveland, OH, 205(1972)

Ho, W.S.W and K.K. Sirkar, " Overview" in " Membrane Handbook", W.S. Winston Ho and K. K. Sirkar, Chapman & Hall, New York, NY(1992), pp3-5.

Jackson, G.W. and D.F. James, " the hydrodynamic resistance of hyaluronic acid and its contribution to tissure permeability", Biorheology, 19, 317(1982)

Jonsson, A.-S, " Fundamental principles of ultrafiltration", Chem. Eng. Process, 27, 67(1990)

Jonsson, G., " Boundary layer phenomena during ultrafiltration of dextran and whey protein solutionss", Desalination, 51, 61(1984)

Karode, S.K., " A method for prediction of the gel concentration in macromolecular ultrafiltration", J. Membr. Sci., 171, 131(2000).

Karode, S.K., " A new unsteady state model for macromolecular ultrafiltration", Chem. Eng. Sci., 55, 1769(2000).

Karode, S.K., " Unsteady state flux response: a method to determine the nature of the solute and gel layer in membrane filtration", J. Membr. Sci., 188, 9(2001).

Kozinski, A.A. and E. N. Lightfoot, " Protein ultrafiltration: a general example of boundary layer filtration", AIChE J., 18, 1030(1972)

Kulkarni, S.S., W. Funk and Norman N. Li, " Ultrafiltration" in " Membrane Handbook", W.S. Winston Ho and K. K. Sirkar, Chapman & Hall, New York, NY(1992), p391.

Lonsdale, H.K., "The growth of membrane technology", J. Membr. Sci., 10, 81(1982)

Madson, R.F., " Hyperfiltration and ultrafiltration in plate and frams systems", Elsvier, New York, (1977)

Matsuura, T., " Synthetic membranes and membrane separation processes", CRC Press Inc., Boca Raton, Florida (1994)

Michaels, A.S., " New separation technique for CPI", Chem. Eng. Prog., 64, 31(1968)

Mulder, M., " Basic principles of membrane technology", 2nd Ed., Kluwer Academics, Dordocht, Boston, (1996)

Nakao, S., J.G. Wijmans, and C.A. Smolders, " Resistance to the permeate flux in unstirred ultrafiltration of dissolved macromolecular solutions", J. Membr. Sci., 26, 165(1986)

Nicolas, S., I. Boulanouar and B. Bariou, " Unstirred dead end ultrafiltration: a method to determine diffusion coefficient or osmotic pressure for non charged macromolecular solutions", J. Membr. Sci., 103, 19(1995)

Nilsson, J.L., " Protein fouling of UF membranes: causes and consequences", J. Membr. Sci., 52, 121(1990)

Ogston, A.G and N. Preston, " Macromolecular compression of dextran", Biochem. J., 183, 1(1979)

Paradanos, P., J.I. Arribas and A. Hernandez, " Mass transfer coefficient and retention of PEG in low pressure cross flow ultrafiltration through asymmetric membranes", J. Membr. Sci., 99, 1(1995)

Paradanos, P., J.de Abajo, J.G. de la Campa and A. Hernandez, " A comparative analysis of flux limit models for ultrafiltration membranes", J. Membr. Sci., 108, 129(1995)

Peppin, S.L. and Janet A.W. Elliott, " Non equilibrium thermodynamics of concentration polarization", Adv. In Coll. and interface Sci., 92, 1(2001)

Porter, M.C., "Ultrafiltration of colloidal dispersions",AIChE Symp. Ser., 68, 21(1972b)

Porter, M.C., " Concentration polarization with membrane ultrafiltration", Ind. Eng. Chem. Prod. Res. Dev., 11, 234(1972a)

Reihanian, H., C.R. Robertson and A.S. Michaels, " Mechanism of polarization and flouling of ultrafiltration membranes by proteins, J. Membr. Sci. 16, 237 (1983).

Rene, F. and M. Lalande, " Momentum and mass transfer during ultrafiltration of dextran with tubular mineral membranes in turbulent regime", J. Membr. Sci., 56, 29(1991)

Shen, J.J. and R.F. Probstein, " On the prediction of limiting flux in laminar ultrafiltration of macromolecular solutions", Ind. Eng. Chem. Fundam., 16, 459(1977)

Stakic, M., Slobodan Milonjic, Vladeta Pavasovic and Zoja Ilic, " Ultrafiltration of Silica Sols", Collect. Czech. Chem. Commun., 54, 91(1989)

Trettin, D. R. and M. R. Doshi, "Pressure Independent Ultrafiltration- Is it Gel Limited or Osmotic Pressure Limited?" in A.F. Turbak (Ed.), Synthetic membranes: Hyper filtration and ultrafiltration uses,Vol. 154, 373-407 (1981).

vanden Berg, G. B., I.G. Racz and C.A. Smolders, "Mass transfer coefficient in cross flow UF" J. Membr. Sci. 47, 25 (1989).

Van Oers, C.W., M.A.G. Vorstman, W.G.H.M Muijselaar and. P.J.A.M Kerkhof, "Unsteady – state flux behavior in relation to the presence of a gel layer", J. Membr. Sci., 73, 231-246 (1992)

Vladisaviljevic, G.T., S.K. Milonjic, D. Nikolic and V.Lj. Pavasovic, " Influence of temperature on the ultrafiltration of silica sol in a stirred cell" J. Membr. Sci. 66, 9(1992).

Ward, A.S., " Liquid filtration theory", in " Filtration: Principle and practices", M.J. Matteson and C. Orr, Marcel Dekkar, Inc., New York, NY(1987), 135

Wijmans, J.G., S. Nakao, and C.A. Smolders, "Flux Limitation In Ultrafiltration: Osmotic Pressure Model And Gel Layer Model, J. Membr. Sci., 20, 115-124 (1984)

Wijmans, J.G., S. Nakao, J.W.A. van den Berg, F.R. Tolestra and C.A. Smolders, "hydrodynamic resistance of concentration polarization boundary layer in ultrafiltration, J. Membr. Sci., 22, 117(1985)

Zydney, Andrew L. "Stagnant film model for concentration polarization in membrane systems" J. Membr. Sci., 130, 275-281 (1997)

Appendix

Sample Calculations

(a) Calculation for Steady state Rejection (*R*) of PEG

Using following equation Steady state Rejection (*R*) of PEG can be calculated.

$$R = 1 - \frac{C_P}{C_b}$$

Where C_p and C_b are the solute concentration in permeate and feed respectively.

For bulk feed concentration of 5 kg/m^3 and applied pressure of 405 kPa

C_b=5000 ppm

C_p=245 ppm

R= 1- 245/5000 = 0.951, i.e 95.1%

(b) Calculation for actual filtration resistance (R_f) using slope method.

Using the values of slope from the graphs of dJ_v/dt v/s $d\Delta P/dt$ Figure 4.4 and by equating with the slope of following equation we can calculate the actual filtration resistance

$$\frac{dJ_v}{dt} = \frac{1}{\mu R_f}\left[\frac{d\Delta P}{dt} - \frac{d\Delta \pi}{dt}\right]$$

for bulk feed concentration of 5 kg/m^3 and applied pressure of 135 kPa

Slope = 0.133

μ = 0.001 Pa.s

$$\text{Slope} = \frac{1}{\mu R_f}$$

$R_f = 1/(\mu \times \text{Slope}) = 1 \times 6808.721/(\mu \times 0.133) \times 2.77 \times 10^{-7} = 1.84 \times 10^{14}$

Note: Here 6808.721 is conversion factor to change pressure from *psi* to *kPa* and 2.77E-7 is conversion factor to change flux from lmh to m^3/m^2s.

(c) Estimation of Osmotic pressure using actual filtration resistance

Once the filtration resistance is calculated the osmotic pressure near wall can be estimated using following equation.

$$J_s = \frac{\Delta P - \Delta \pi}{\mu R_f}$$

Where, J_s is the solute flux, ΔP is the applied pressure, R_f is the total filtration resistance and $\Delta \pi$ the osmotic pressure difference across the membrane

for bulk feed concentration of 5 kg/m^3 and applied pressure of 135 *kPa*

$J_s = 2.77 \times 10^{-7}$ m/s

$\mu = 0.001$ Pa-s

$R_f = 1.84 \times 10^{14}$ m^{-1}

$\Delta P = 135000$ Pa

$\Delta \pi = \Delta P - (J_s \cdot \mu \times R_f) = 135000 - (0.001 \times 2.77 \times 10^{-7} \times 1.84 \times 10^{14}) = 85{,}320$ Pa

$\Delta \pi = 85.5$ kPa

(d) Measurement of wall concentration (C_w)

For PEG, Flory's equation relates the osmotic pressure with solute volume fraction as

$$\pi = -\frac{RT}{V_1}\left[\ln(1-\gamma_p) + (1-\frac{1}{n})\gamma_p + \chi_{12}\gamma_p^{\,2}\right]$$

where,

$\Delta\pi$ is estimated osmotic pressure at membrane surface = 85.5 kPa

$\gamma_p = c/\rho_p$ is volume fraction of polymer

c is the polymer concentration to be calculated

ρ_p is polymer density = 1200 kg/m^3

n is the number of monomer sub units in the polymer chain = 35000

The Flory-Huggins interaction parameter χ_{12} is a linear function of solute concentration for linear chain polymers and the concentration dependence is best expressed as

$$\ln|\chi_{12}| = p + qc$$

where p and q are constants having values –0.604 and 1.7452 respectively.

R = 8.31 $J/mol\ K$

T = 298 K

V_1 = molar volume of solvent = 1.8×10^{-5}

From the estimated osmotic pressure and using above correlation and defined values, wall concentration can be estimated as follows.

for bulk feed concentration of 5 kg/m^3 and applied pressure of 135 kPa

$$85500 = -\frac{8.31*298}{1.8\times10^{-5}}\left[\ln(1-\frac{c}{1200}) + (1-\frac{1}{35000})(\frac{c}{1200}) + (\exp(-0.604+1.7452c))(\frac{c}{1200})^2\right]$$

C_w= 124 kg/m^3

For Dextran, following correlation has been used to estimate the wall concentration from osmotic pressure.

$$\Delta\pi = 35.5C_m + 0.752C_m^{\ 2} + 76.4\times10^{-4}C_m^{\ 3}$$

For bulk feed concentration of 5 kg/m^3 and applied pressure of 135 kPa

$\Delta\pi = 18.37\ kPa = 18370\ Pa$

Putting this value in above equation we get,

$$18370 = 35.5C_m + 0.752C_m^{\ 2} + 76.4\times10^{-4}C_m^{\ 3}$$

$C_m = 121.8\ kg/m^3$

(e) Calculation of specific resistance for Silica

The specific resistance 'a' was calculated based on the slope of plot $1/J^2$ vs. t.

(Figure 6.5) of the following equation.

$$\frac{1}{J^2} = \frac{(R_m\mu)^2}{(\Delta P)^2} + \frac{2C_b a\mu}{\Delta P}t$$

For bulk feed concentration of 21 kg/m^3 and applied pressure of 135 kPa

Equating the slope with the slope expression in thef above equation, we get.

$$\text{Slope} = \frac{2C_b a\mu}{\Delta P}$$

Slope = 5×10^7 (from Figure 6.5)

$R_m = 3.5\times10^{13}$

$\mu = 1.1\times10^{-3}$ Pa.s

$\Delta P = 135000$ Pa

$C_b = 21\ kg/m^3$

Substituting the values in above equation we get

$$5\times10^7 = \frac{2\times21\times a\times0.0011}{135000}$$

$$a = \frac{5\times10^7\times135000}{2\times21\times0.0011}$$

$a = 1.47 \times 10^{14}$

(f) Calculation of porosity of Silica gel.

Once the specific resistance was calculated, the porosity can be calculated from the following equation.

$$a = \frac{180(1-\varepsilon_g)}{d_p^{\,2}\varepsilon_g^{\,3}\rho}$$

where 'a' is specific resistance, d_p is diameter of silica particle and ε_g is porosity of gel.

For bulk feed concentration of 21 kg/m^3 and applied pressure of 135 kPa

$a = 1.47 \times 10^{14}$

$d_p = 12 \times 10^{-9} m$

$\rho = 2250\ kg/m^3$

$$1.47 \times 10^{14} = \frac{180(1-\varepsilon_g)}{(12\times10^{-9})^2\varepsilon_g^{\,3}\times12\times10^{-9}}$$

$\varepsilon_g = 0.84$

(f) Calculation of Silica gel concentration

The concentration of silica was calculated based on porosity using following equation

$$\varepsilon_g = 1 - \frac{C_g}{\rho}$$

$\varepsilon_g = 0.84$

$C_g = \rho \times (1-\varepsilon_g) = 2250 \times (1-0.84)$

$C_g = 357.1\ kg/m^3$